AD-A130 359 GENERAL 3D AIRBORNE ANTENNA RADIATION PATTERN CODE USERS MANUAL(U) OHIO STATE UNIV COLUMBUS ELECTROSCIENCE LAB H H CHUNG ET AL. FEB 83 RADC-TR-83-39 1/2

UNCLASSIFIED F30602-79-C-0068 F/G 9/2 NL

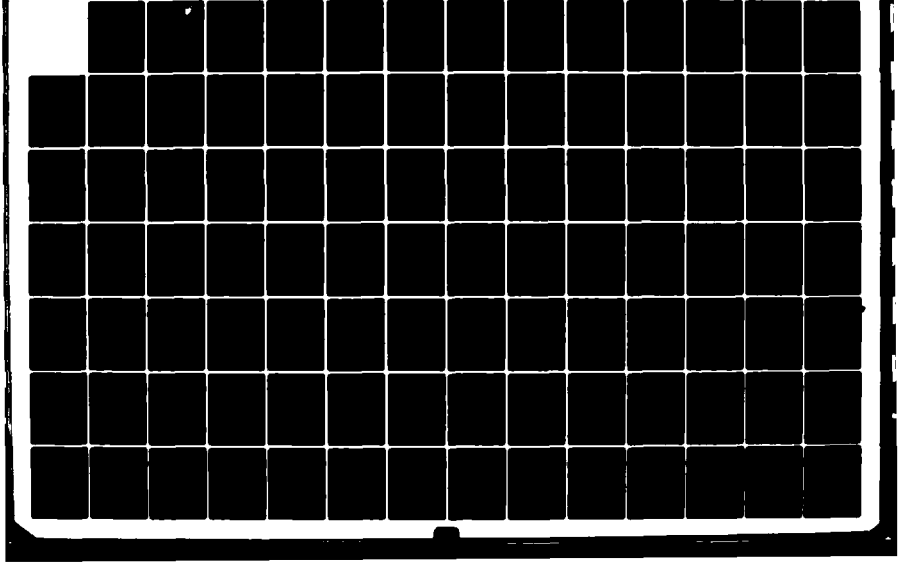

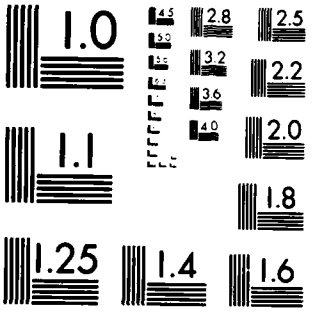

MICROCOPY RESOLUTION TEST CHART
NATIONAL BUREAU OF STANDARDS 1963-A

RADC-TR-83-39
Interim Report
February 1983

12

GENERAL 3D AIRBORNE ANTENNA RADIATION PATTERN CODE USERS MANUAL

The Ohio State University

Hsin H. Chung and W. D. Burnside

APPROVED FOR PUBLIC RELEASE; DISTRIBUTION UNLIMITED

ROME AIR DEVELOPMENT CENTER
Air Force Systems Command
Griffiss Air Force Base, NY 13441

This report has been reviewed by the RADC Public Affairs Office (PA) and is releasable to the National Technical Information Service (NTIS). At NTIS it will be releasable to the general public, including foreign nations.

RADC-TR-83-39 has been reviewed and is approved for publication.

APPROVED: Stuart H. Talbot

STUART H. TALBOT
Project Engineer

APPROVED: B. Beek

BRUNO BEEK
Technical Director
Communications Division

FOR THE COMMANDER: John P. Huss

JOHN P. HUSS
Acting Chief, Plans Office

If your address has changed or if you wish to be removed from the RADC mailing list, or if the addressee is no longer employed by your organization, please notify RADC (DCCR), Griffiss AFB NY 13441. This will assist us in maintaining a current mailing list.

Do not return copies of this report unless contractual obligations or notices on a specific document requires that it be returned.

UNCLASSIFIED

SECURITY CLASSIFICATION OF THIS PAGE (When Data Entered)

REPORT DOCUMENTATION PAGE		READ INSTRUCTIONS BEFORE COMPLETING FORM
1. REPORT NUMBER RADC-TR-83-39	2. GOVT ACCESSION NO. A130359	3. RECIPIENT'S CATALOG NUMBER
4. TITLE (and Subtitle) GENERAL 3D AIRBORNE ANTENNA RADIATION PATTERN CODE USERS MANUAL		5. TYPE OF REPORT & PERIOD COVERED Interim Report Apr 81 - Jul 82
		6. PERFORMING ORG. REPORT NUMBER ESL 711679-10
7. AUTHOR(s) Hsin H. Chung W. D. Burnside		8. CONTRACT OR GRANT NUMBER(s) F30602-79-C-0068
9. PERFORMING ORGANIZATION NAME AND ADDRESS The Ohio State University Electroscience Lab Dept of Electrical Engineering Columbus OH 43212		10. PROGRAM ELEMENT, PROJECT, TASK AREA & WORK UNIT NUMBERS 62702F 45196308
11. CONTROLLING OFFICE NAME AND ADDRESS Rome Air Development Center (DCCR) Griffiss AFB NY 13441		12. REPORT DATE February 1983
		13. NUMBER OF PAGES 144
14. MONITORING AGENCY NAME & ADDRESS(if different from Controlling Office) Same		15. SECURITY CLASS. (of this report) UNCLASSIFIED
		15a. DECLASSIFICATION/DOWNGRADING SCHEDULE N/A

16. DISTRIBUTION STATEMENT (of this Report)

Approved for public release; distribution unlimited.

17. DISTRIBUTION STATEMENT (of the abstract entered in Block 20, if different from Report)

Same

18. SUPPLEMENTARY NOTES

RADC Project Engineer: Stuart H. Talbot (DCCR)

19. KEY WORDS (Continue on reverse side if necessary and identify by block number)

Uniform Geometric Theory of Diffraction
Electromagnetic Radiation and Scattering
Aircraft Mounted Antennas
Aircraft Antenna Radiation Performance
Computer Program

20. ABSTRACT (Continue on reverse side if necessary and identify by block number)

This report describes a computer program and how it may be used to analyze the performance antennas mounted on aircraft. The computer program may also be used to simulate a wide variety of complex electromagnetic radiation problems using the spheroid/plates model. The computer program is based upon the uniform Geometric Theory of Diffraction (GTD) and various computed patterns are compared with experimental results in the report. The organization of the computer program code, definition of input and

DD FORM 1 JAN 73 1473 EDITION OF 1 NOV 65 IS OBSOLETE

UNCLASSIFIED

SECURITY CLASSIFICATION OF THIS PAGE (When Data Entered)

output data, and examples for simulating antenna performance on different airframes are also presented.

TABLE OF CONTENTS

LIST OF TABLES

LIST OF FIGURES

I. INTRODUCTION

In order to investigate the radiation patterns of antennas in a complex environment such as on an aircraft fuselage which was modeled by a composite prolate spheroid the following Fortran IV computer code has been developed. The computer code is used to compute the near zone and far zone radiated fields for antennas mounted on a composite prolate spheroid and in the presence of a set of finite flat plates. The analysis applied in the development of this code is based on the uniform geometrical theory of diffraction (UTD) 1,2,3.

The code allows the user to simulate a wide variety of complex electromagnetic radiation problems using the speheroid/plates model. For example, the composite prolate spheroid can be used to simulate the fuselage of an aircraft; whereas, the plates are used to represent the wings, stabilizers, stores, etc. Alternatively, the antenna could be mounted directly on a ship mast. In this case the mast could be approximated by the composite prolate spheroid with the other ship structures simulated by flat plates. Note that the plates can be attached to the composite prolate spheroid and/or to other plates. In fact, the plates can be connected together to form a box. In terms of special sections in the input data set, this code is specifically designed to analyze the radiation characteristics of antennas mounted on aircraft configurations.

As with any ray optical solution such as this UTD code, there is a limit to the number of interactions included in the field computation. In this case, the code includes the source, reflected, diffracted, and

higher order terms such as the reflected/reflected, reflected/diffracted, diffracted/reflected, and diffracted/diffracted fields. The higher order terms are due to the multiple field interactions between plates. It assumes that the higher-order diffracted and reflected fields from the composite prolate spheroid surface are small in which case they can be neglected. The user may request the code (by using the "TO:" COMMAND) to compute the higher order terms when he thinks they have a significant effect on the results otherwise the code will compute first order terms only. This implies that the code can handle structures for which the energy does not significantly bounce back-and-forth across the target. In any event, the code automatically shadows all terms, such that if a higher-order interaction should have been included the resulting pattern will contain a discontinuity. These higher-order terms are normally negligible and can only affect the pattern in rather small sectors. However, if they are significant in some region, the amplitude of the jump is associated with the radiation level of the missing higher-order term. Consequently when the solution fails because of a lack of higher-order terms, it tends to indicate its failure.

The code has the flexibility to handle arbitrary pattern cuts. In addition, an arbitrary antenna type can be analyzed provided the current distribution across the aperture is known. This is done by approximating the distribution by a set of magnetic current elements mounted on the composite prolate spheroid surface. The magnetic current elements have a cosine distribution along the magnetic current direction and a

uniform distribution in the orthogonal direction. The code can, also, treat a monopole; however, its length cannot exceed a quarter wavelength.

The mutual coupling effect for monopole arrays mounted on fuselage can be handled by thin-wire theory (4), if the region near the array is nearly flat. For engineering purposes, image theory can be applied to calculate the relative current distributions as equivalent dipole arrays. The relative current value on each dipole is then taken to be part of the input data for each monopole source specification. The final pattern is the superposition of the contributions from each individual monopole.

The limitations associated with the computer code result from the basic nature of the analyses. The solution is derived using the UTD, which is a high frequency approach. In terms of the scattering from plate structures this means that each plate should have edges at least a wavelength long. In terms of the composite prolate spheroid structure its major and minor radii should be at least a wavelength in extent. In addition, each antenna element should be at least a wavelength from all edges. In some cases, the wavelength limit can be reduced to a quarter wavelength for engineering purposes.

The present code requires approximately 300K bytes of storage. It will run a pattern cut of 360 points for a commerical aircraft model (Example 3, 6 plates included) with one antenna element in approximately 4 minutes on a VAX 11/780 Computer.

This user's manual is designed to give an overall view of the operation of the computer code, to instruct a user in how to use it to model structures, and to show the validity of the code by comparing various computed results against measured data whenever available. Section II describes an overall view of the organization of the program. The definition of the input is given in Section III. How to apply the capabilities of this input data to a practical structure is briefly discussed in Section IV. This includes a clarification of the subtle points of interpreting the input data. The representation of the output is discussed in Section V. Various sample problems are presented in Section VI to illustrate the operation, versatility, and validity of the code.

II. PRINCIPLES OF OPERATION

The analytical modeling of complex scattering shapes in order to predict the radiation patterns of antennas has been accomplished by the use of the Uniform Geometrical Theory of Diffraction (UTD)[1,2]. This is a high frequency technique that allows a complicated structure to be approximated by basic shapes representing canonical problems in the UTD. These shapes include flat or curved wedges and convex curved surfaces. The UTD is a ray optical technique and it therefore allows one to gain some physical insight into the various scattering and diffraction mechanisms involved. Consequently, one is able to quickly seek out the dominant or significant scattering and diffraction mechanism for a given geometrical configuration. This, in turn, leads to an accurate

engineering solution to practical antenna problems. This approach has been used successfully in the past to model aircraft shapes [5,6,7,8,9] and ship-like structures [10,11,12].

This section briefly describes the basic operation of this code for the analysis of antennas in an aircraft environment. The present version of the code allows analysis of a structure that can be modeled by flat plates and a composite prolate spheroid, all of which are built up from the basic canonical problems. These shapes allow one to model a wide variety of structures in the UHF range and above where the scattering structures are large in terms of a wavelength. The general rule is that the lower frequency limit of this solution is dictated by the spacings between the various scattering centers and their overall size. In practice this means that the smallest dimensions should be on the order of a wavelength.

The positive time convention $e^{j\omega t}$ has been used in this code, and, all the structures are assumed to be perfectly conducting and surrounded by free space.

As mentioned above, the UTD approach is ideal for a general high frequency study of aircraft antennas in that only the most basic structural features of an otherwise very complicated structure need to be modeled. This is because ray optical techniques are used to determine components of the field incident on and diffracted by various structures. Components of the diffracted fields are found using the UTD solutions in terms of the individual rays which are summed with the geometrical optics terms at the field point. The rays from a given

scatterer tend to interact with other structures causing various higher-order terms. In this way one can trace out the various possible combinations of rays that interact between scatterers and determine and include only the dominant terms. Thus, one need only be concerned with the important scattering components and neglect all other higher-order terms. This method leads to accurate and efficient computer codes that can be systematically written and tested.

Complex problems are built up from similar components in terms of a modular computer code. This modular approach is illustrated in the block diagram of the main program shown in Table I. The code is broken up into many subroutines that represent different scattered field components, ray tracing sections, (by composite prolate spheroid surface) geodesic path finding algorithms [13,14], plate attachment calculation [15], and shadowing routines. As can be seen from the flow chart, the code is structured so that all of one type of scattered field is computed at one time for the complete pattern cut so that the amount of core swapping is minimized thereby reducing overlaying and increasing efficiency. This also is an important feature that allows the code to be used on small computers that are not large enough to accept the entire code at one time. The code can be broken into smaller overlay segments which will individually fit in the machine. The results are, then, superimposed in the main program as the various segments are executed.

The subroutines for each of the scattered field components are all structured in the same basic way. First, the ray path is determined

TABLE I

BLOCK DIAGRAM OF THE MAIN PROGRAM

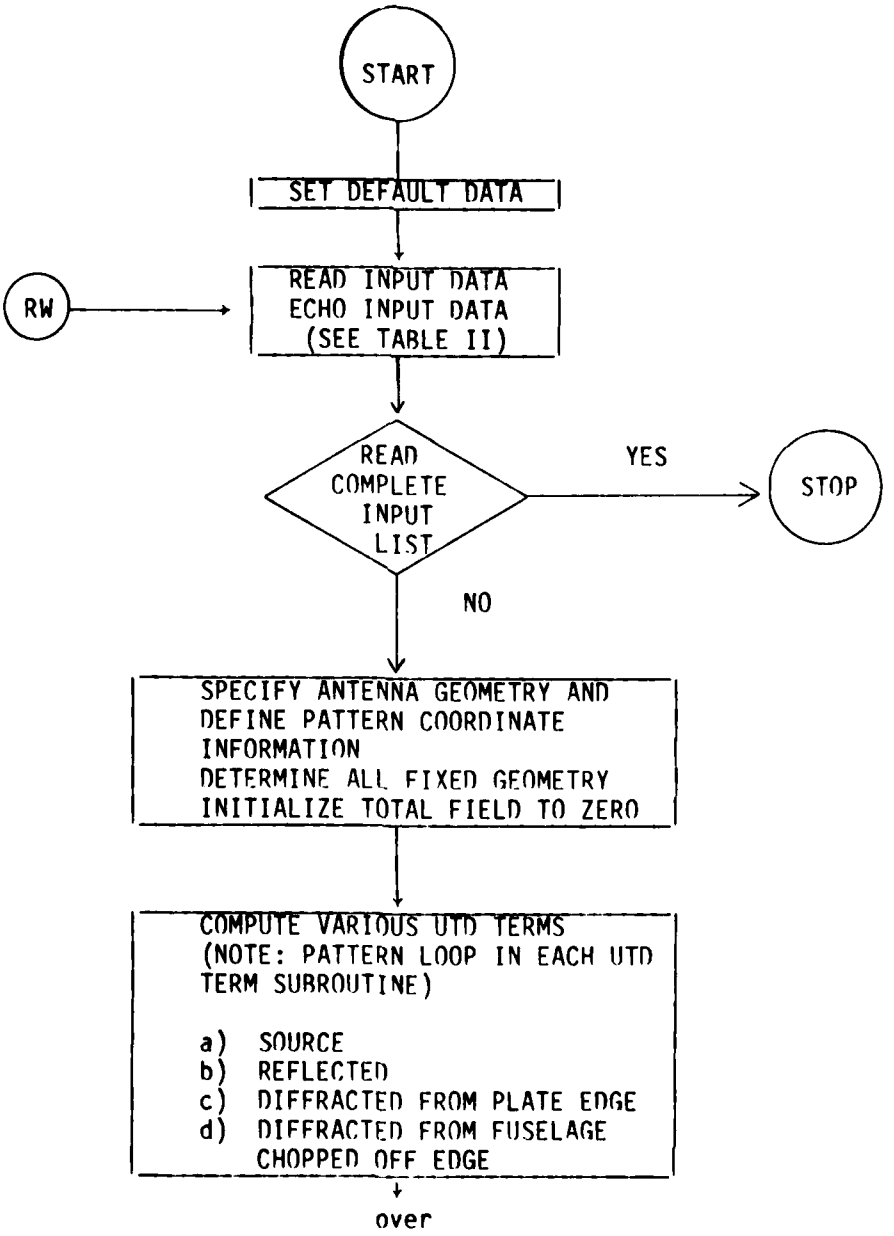

over

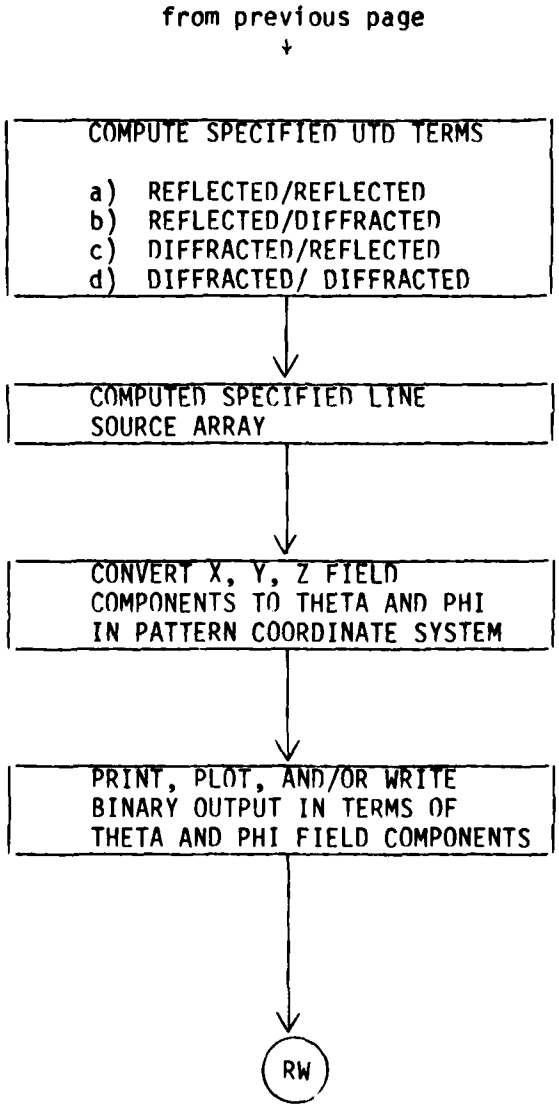
from previous page
COMPUTE SPECIFIED UTD TERMS
a) REFLECTED/REFLECTED
b) REFLECTED/DIFFRACTED
c) DIFFRACTED/REFLECTED
d) DIFFRACTED/ DIFFRACTED
COMPUTED SPECIFIED LINE SOURCE ARRAY
CONVERT X, Y, Z FIELD COMPONENTS TO THETA AND PHI IN PATTERN COORDINATE SYSTEM
PRINT, PLOT, AND/OR WRITE BINARY OUTPUT IN TERMS OF THETA AND PHI FIELD COMPONENTS
RW

from the source to a particular scatterer and subsequently to the observation point using either the laws of reflection or diffraction. Each ray path, assuming one is possible, is then checked to see if it is shadowed by any structure along the complete ray path. If it is shadowed the field is not computed and the code proceeds to the next scatterer or observation point. If the path is not interrupted the scattered field is computed using the appropriate GTD solutions. The fields are then superimposed in the main program. This shadowing process is often speeded up by making various decisions based on bounds associated with the geometry of the structure. This type of knowledge is used wherever possible.

The shadowing of rays is a very important part of the GTD scattering code. It is obvious that this approach should lead to various discontinuities in the resulting pattern. However, the UTD diffraction coefficients are designed to smooth out the discontinuities in the field such that a continuous field is obtained. When a scattered field is not included in the result, the lack of its presence is apparent. This can be used to advantage in analyzing complicated problems. Obviously, in a complex problem not all the possible scattered fields can be included. In the GTD code the importance of the neglected terms are determined by the size of the so-called glitches or jumps in the pattern trace.

If the glitches are small, no additional terms are needed for a good engineering solution. If the glitches are large, it may be necessary to include more terms in the solution. In any case the user has a gauge

with which he can examine the accuracy of the results and is not falsely led into believing a result is correct when in fact there could be an error associated with neglecting a higher order interaction term.

The brief discussion of the operation of the scattering code given above should help the user get a feel for the overall code so that he might better understand the code's capabilities and interpret its results. The code is designed, however, so that a general user can run the code without knowing all the details of its operation. Yet, he must become familiar with the input/output details which will be discussed in the next three sections.

III. DEFINITION OF INPUT DATA

The method used to input data into the computer code is presently based on a command word system. This is especially convenient when more than one problem is to be analyzed during a computer run. The code stores the previous input data such that one need only input that data which needs to be changed from the previous execution. Also, there is a default list of data so, for any given problem the amount of data that needs to be input has been shortened. The organization of the input data is illustrated in Table II.

In this system, all linear dimensions may be specified in either meters, inches, or feet; whereas all angular dimensions are in degrees. All the dimensions are eventually referred to a fixed cartesian coordinate system used as a common reference for the source and structures. There is, however, a geometry definition coordinate system

TABLE II

BLOCK DIAGRAM OF THE INPUT DATA
ORGANIZATION FOR THE COMPUTER CODE

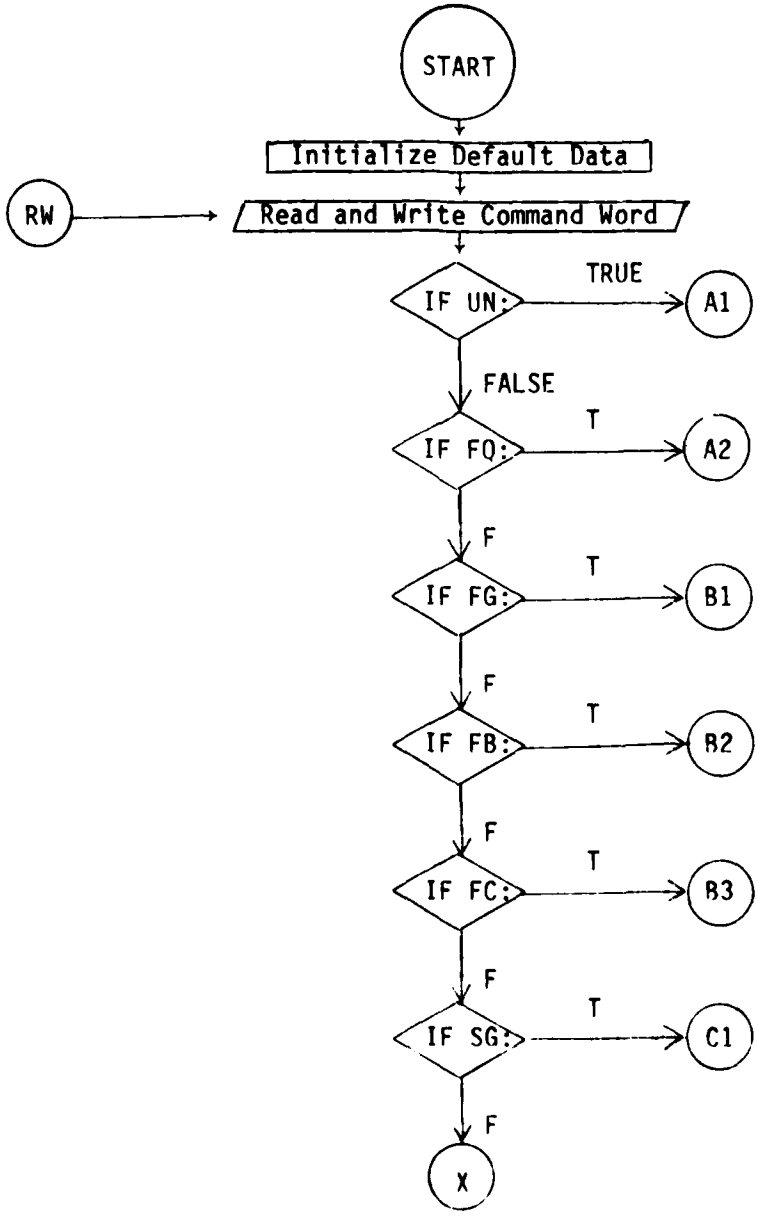

TABLE II. (continued)

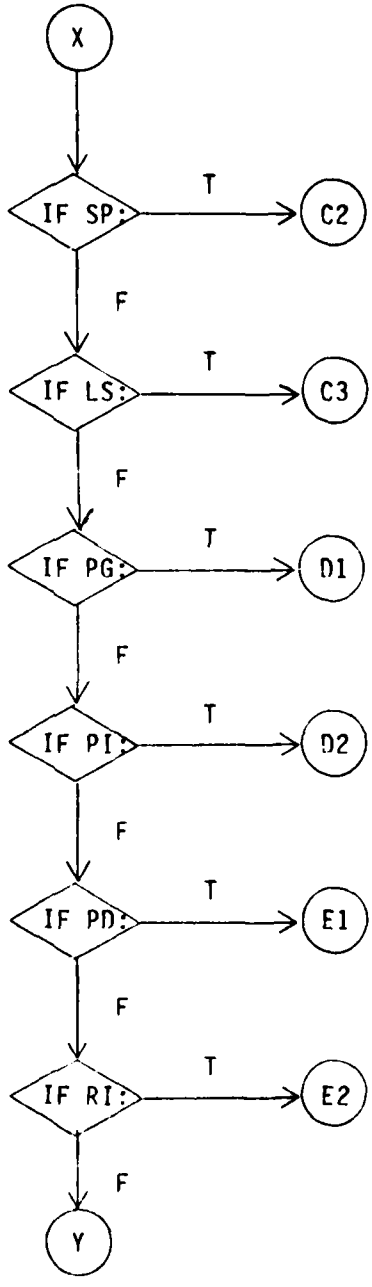

TABLE II. (continued)

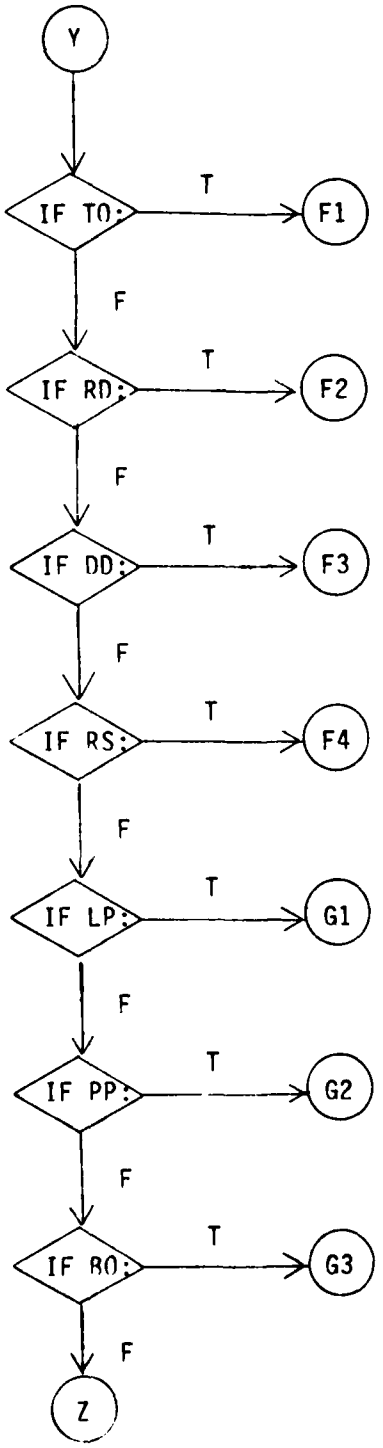

TABLE II. (continued)

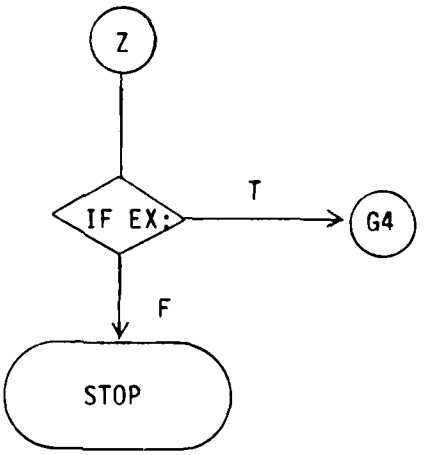

that may be defined using the "RT:" command. This command enables the user to rotate and translate the coordinate system to be used to input any select data set into the best coordinate system for that particular geometry. Once the "RT:" command is used all the input following the command will be in that rotated and translated coordinate system until the "RT:" command is called again. The only exception to this is that the composite prolate spheroid will always be in the reference coordinate system. See below for more details. There is also a separate coordinate system that can be used to define the pattern coordinates. This is discussed in more detail in Section III-C in terms of the "PD:" command.

It is felt that the maximum usefulness of the computer code can be achieved using it on an interactive computer system. As a consequence, all input data are defined in free format such that the operator need only put commas or spaces between the various input variables. This allows the user on an interactive terminal to avoid the problems associated with typing in the field length associated with a fixed format. This method also is useful on batch processing computers. Note that all read statements are made on unit #5, i.e., READ (5,*), where the "*" symbol refers to free format. Other machines, however, may have different symbols representing free format.

In all the following discussions associated with logical variables a "T" will imply true, and an "F" will imply false. The complete words true and false need not be input since most compilers just consider the first character in determining the state of the logical variable.

The following list defines in detail each command word and the variables associated with them. Section VI will give specific examples using this input method. Note that the program halts execution by sensing the end-of-file mark associated with the input data stream.

COMMAND PART:

A. Unit and Frequency Commands:

A1. COMMAND UN: Set Linear Units Used for Input

A2. COMMAND FQ: Frequency Input

B. Fuselage Geometry Related Commands:

B1. COMMAND FG: Fuselage Geometry Input

B2. COMMAND FB: Fuselage Blockage Modeled by Plates

B3. COMMAND FC: Fuselage Chopped Off

C. Source Geometry Related Commands:

C1. COMMAND SG: Source Geometry Input

C2. COMMAND SP: Superposition Fields from Several Sources

C3. COMMAND LS: Line Source Distribution Along Z-axis Used in Array Pattern

D. Plate Geometry Related Commands:

D1. COMMAND PG: Plate Geometry Input

D2. COMMAND PI: Initialize Number of Plates to be Retained

E. Pattern Cut Related Commands:

E1. COMMAND PD: Conical Pattern Data Desired

E2. COMMAND RT: Translate and/or Rotate Coordinates

F. Specific Calculation Related Commands:

F1. COMMAND TO: Test Data Generation Option

F2. COMMAND RD: Reflection/Diffraction Included in Computation

F3. COMMAND DD: Double Diffraction Included in Computation

F4. COMMAND RS: Reset Input Data to Default Case

G. Execute and Output Related Commands:

G1. COMMAND LP: Line Printer Listing of Results

G2. COMMAND PP: Pen Plot of Results

G3. COMMAND BO: Binary Outputs of E-THETA and E-PHI Pattern Results

G4. COMMAND EX: Execute Program

A. Unit and Frequency Commands:

A1. COMMAND UN:

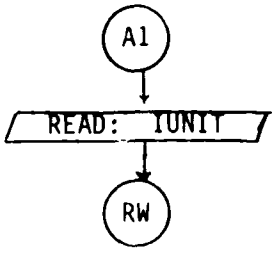

This command enables the user to specify the units used for all following linear dimensions in the input data list.

1. READ: IUNIT

a) IUNIT: This is an integer variable that defines the units.

If

$$IUNIT = \begin{cases} 1 \rightarrow \text{meters} \\ 2 \rightarrow \text{feet} \\ 3 \rightarrow \text{inches} \end{cases}$$

A2. COMMAND FQ:

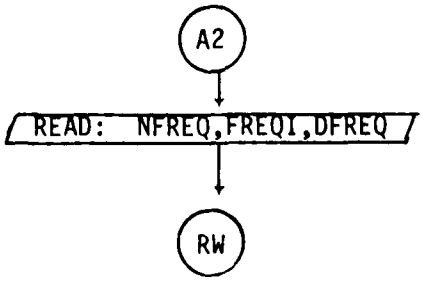

NFREQ: This is an integer variable that specifies the number of different frequencies.

FREQI, DFREQ: They are real variables that specify the start and increment of the frequency loop, respectively, in Gigahertz.

B. Fuselage Geometry Related Commands:

B1. COMMAND FG:

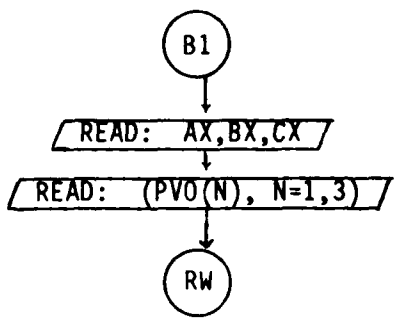

This command enables the user to model the fuselage by a composite spheroid.

1. READ: AX,BX,CX

a) AX,BX,CX: These are real variables that specify the semi-major and semi-minor axes of the composite prolate spheroid used to model the fuselage as shown in Figure 1. Note that the prolate spheroid is a surface of revolution about the Z-axis.

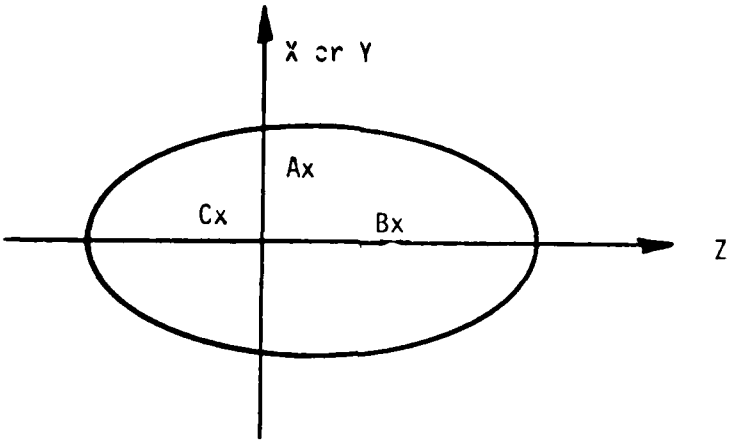

Figure 1. Definition of fuselage geometry.

2. READ: (PVO(N), N=1,3)

   a) PVO(N): This is a real dimensioned array that defines the location of the origin about which the pattern is taken, i.e., PVO(N) = (x,y,z).

B2. COMMAND FB:

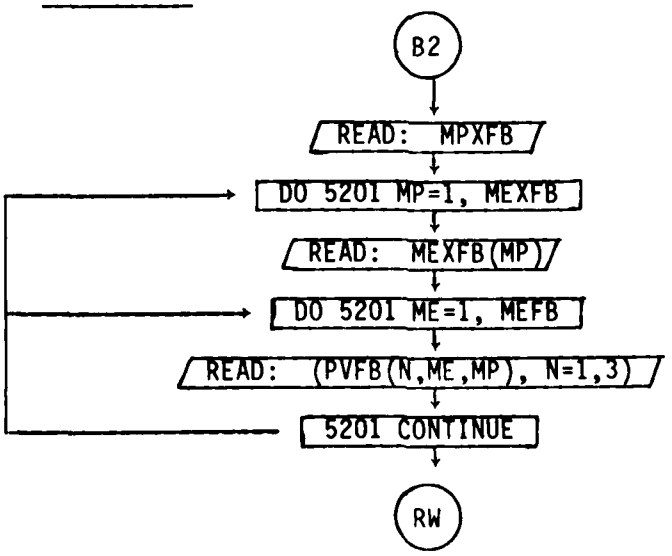

This command enables the user to model the fuselage blockage by plates.

1. READ: MPXFB

   MPXFB: This is an integer variable which defines the maximum number of plates to be used in modeling the fuselage blockage. MPXFB can not exceed 2!

2. READ: MEXFB(MP)

   MEXFB(MP): This is a dimensional integer variable which defines the maximum number of corners of each fuselage blockage plate. MEXFB(MP) can not exceed 6!

3. READ: (PVFB(N,ME,MP), N=1,3

   PVFB(N,ME,MP): This is a triply dimensioned real variable. It is used to specify the location of the MEth corner of the MPth plate. It is input on a single line with the real numbers being the X,Y,Z coordinates of the corner which corresponds to N=1,2,3, respectively, in the arrray. For example, the first plate and 2nd corner located at x=2., y=0., z=20. is represented by.

   PVFB(1,2,1)=2.

   PVFB(2,2,1)=0.

   PVFB(3,2,1)=20.

This data is input as: 2., 0., 20.

B3. COMMAND FC:

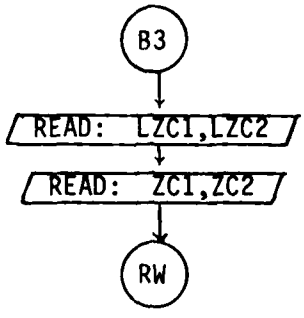

This command enables the user to chop off the fuselage. This command is useful in modeling the radome bulk/head portion of an aircraft fuselage. Using this command the fuselage spheroid is cut at right angles to the z-axis which forms an abrupt termination of the fuselage.

1. READ: LZC1,LZC2

   LZC1/LZC2: These are logical variables defined by T or F. They are used to indicate if the fuselage will be chopped off in the ZC1/ZC2 location.

2. READ: ZC1, ZC2

   ZC1/ZC2: This is a real variable which defines positive/ negative Z location at which the fuselage is chopped, respectively. Note ZC1(ZC2) can be any number when LZC1(LZC2) is .FALSE.

C. Source Geometry Related Commands:

C1. COMMAND SG:

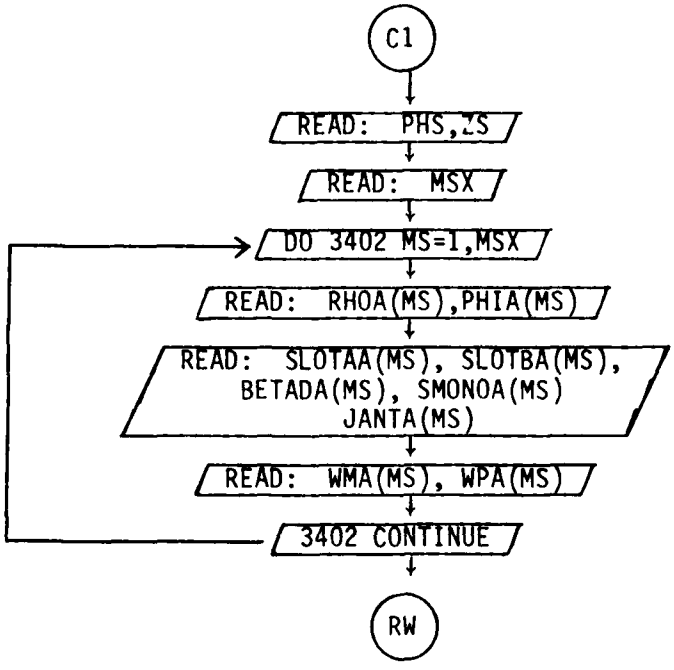

This command enables the user to specify the location and type of antenna to be used. The geometry is illustrated in Figure 2.

1. READ: PHS,ZS

   PHS,ZS: These are real variables used to specify the phi-angle (in degrees) and Z location of the antenna phase center. (Refer to Figure 2) Note: $-90° < PHS < 90°$

2. READ: MSX

   a) MSX: This is an integer variable which defines the maximum number of elemental radiators to be considered during execution of the program. Presently, $1 < MSX < 10$.

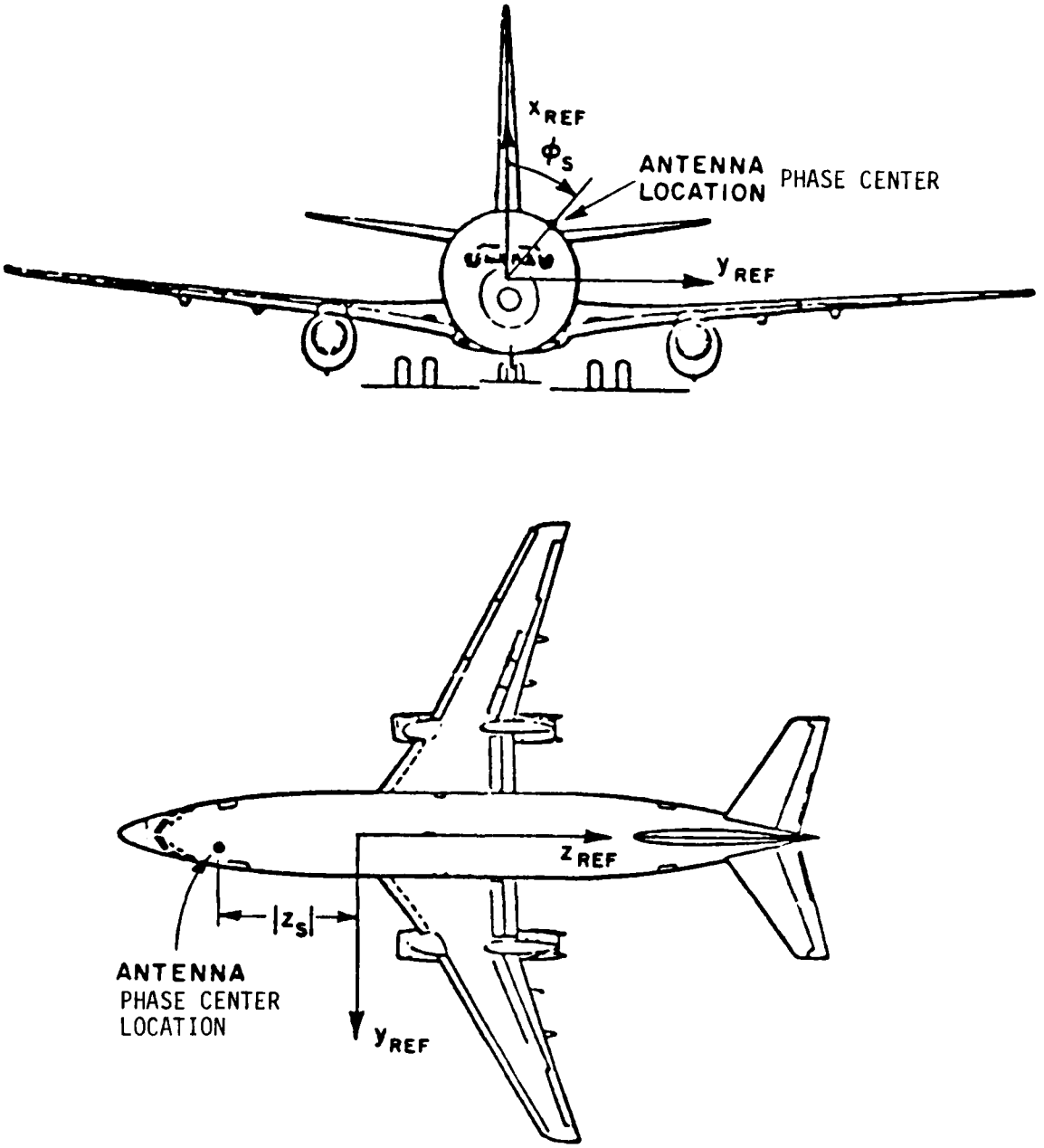

Figure 2. Definition of the antenna phase center location for computer code. Note that PHS = ϕ_S and ZS = - $|Z_S|$ in the above drawings.

3. READ: PHOA(MS), PHIA(MS)

   a) RHOA(MS): This is a dimensioned real variable which defines the distance that a single antenna element is positioned away from the antenna phase center. It is shown in Figure 3 in terms of ρ_A.

   b) PHIA(MS): This is a dimensioned real variable used to specify the angle (in degrees) relative to antenna phase center. It is shown in Figure 3 in terms of ϕ_A.

4. READ: SLOTAA(MS), SLOTBA(MS), BETADA(MS), SMONOA(MS), JANTA(MS)

   a) SLOTAA(MS), SLOTBA(MS): These are real variables used to specify the narrow (parallel with E field) and broad (perpendicular to E field) dimensions of the slot in specified units.

   b) BETADA(MS): This is a real variable used to specify the angle (in degrees) of the slot relative to the fuselage axis. If BETADA=0., then it is an axial slot. If BETADA=90., then it is a circumferential slot.

   c) SMONOA(MS): This is a real variable used to specify the length of monopole in specified unit. Note that SMONOA should not exceed a quarter wavelength.

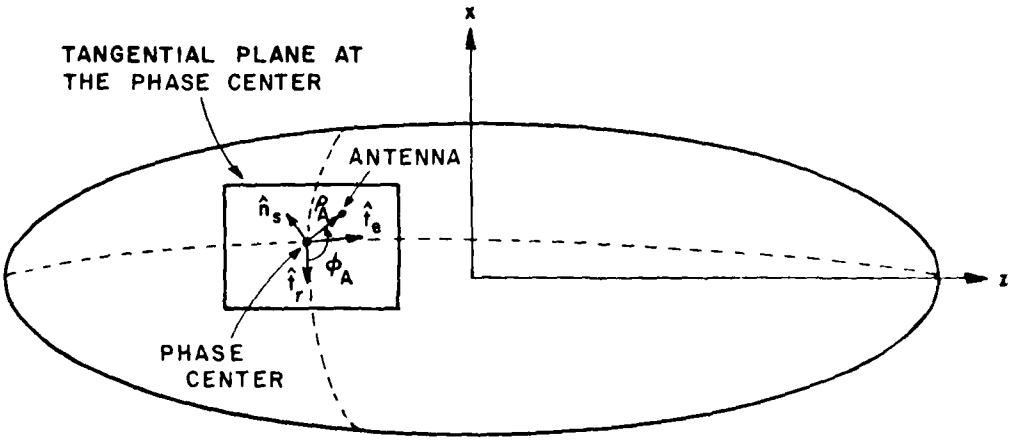

Figure 3. Source geometry.

(Note that RHOA(MS)=ρ_A and PHIA(MS)=ϕ_A)

d) JANTA(MS): This is an integer variable used to specify the type of antenna considered in computation:

$$JANTA = \begin{cases} 1 \rightarrow \text{arbitrary oriented slot} \\ 3 \rightarrow \text{radial monopole.} \end{cases}$$

5. READ: WMA(MS), WPA(MS)

a) WMA(MS), WPA(MS): These are real variables used to specify the magnitude and phase (in degrees) of excitation of the MSth antenna. If an array is used, then the excitation including the coupling effect on the radiators may be obtained using a thin-wire code as shown in the results section.

C2. COMMAND SP:

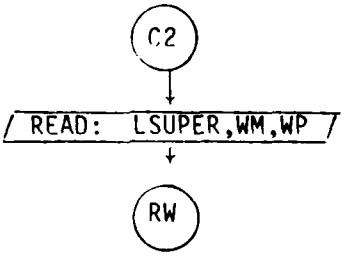

This command enables the user to superimpose the field calculated for several sources. But, one should note that this command can be used only when sources are operating at the same frequency.

1. READ: LSUPER,WM,WP

a) LSUPER: This is a logical variable defined by T or F. It is used to indicate if one wishes to superimpose fields or not.

WM,WP: These are real variables used to specify the magnitude and phase (in degrees) of the source relative to the first source in the superposition string.

- COMMAND LS:

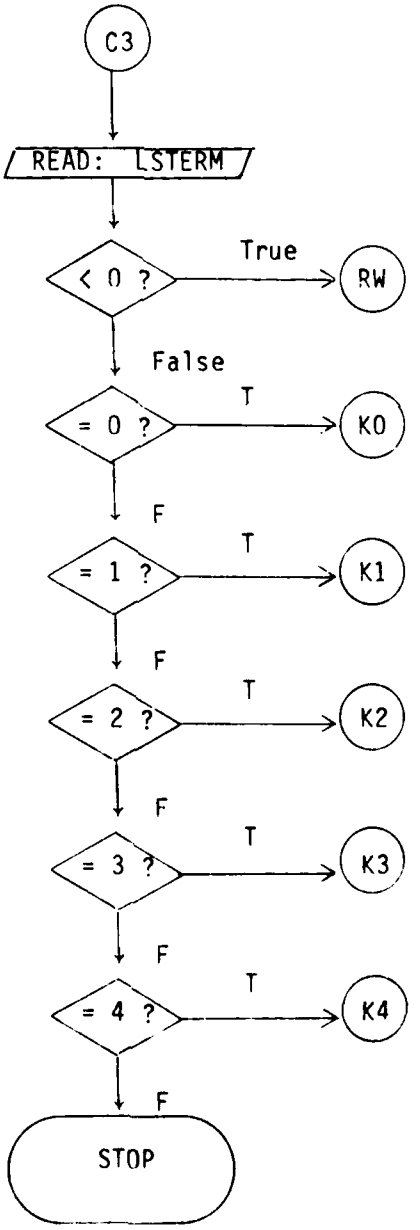

COMMAND LS (continued)

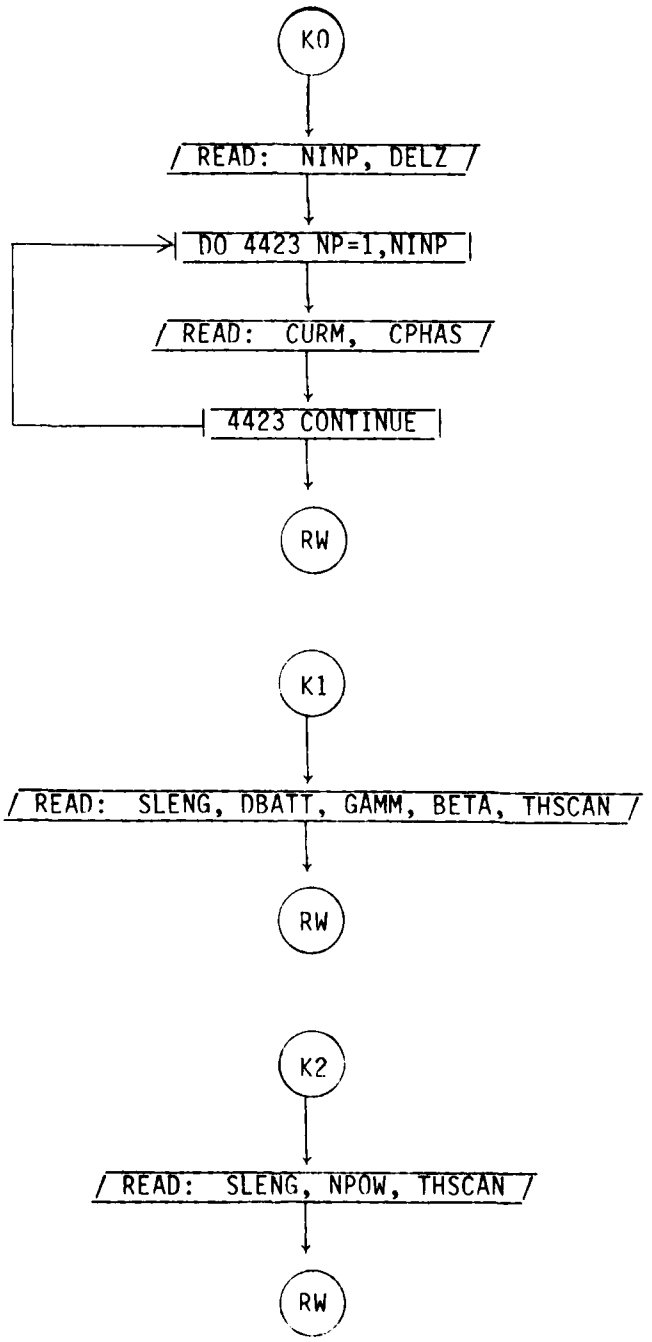

COMMAND LS (continued)

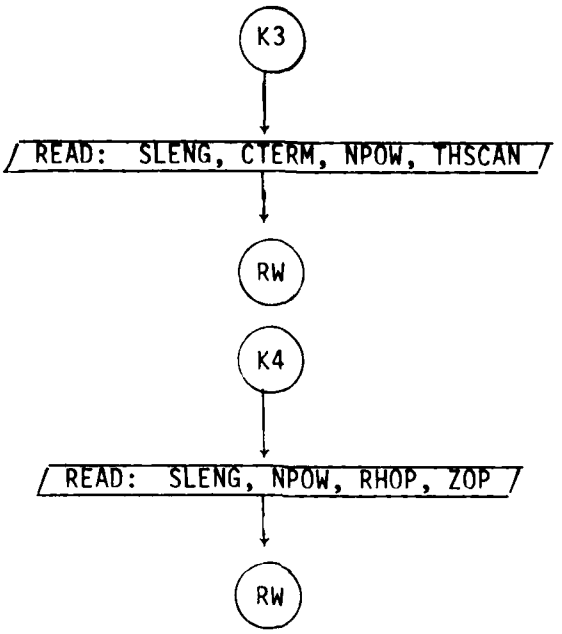

This command enables the user to specify a line source distribution along the z-axis. It is used in an array pattern multiplication analysis. This command applies only when one has a uniform geometry along the axis of the fuselage.

1. READ: LSTERM

   a) LSTERM: This is an integer variable that indicates the type of line source distribution treated. The current distribution and, therefore, the following inputs vary according to the following table.

LSTERM=0: $I(z) = \sum_{N=1}^{NINP} |I_N| \, e^{j\phi_N} \, \delta(z-(N-1/2)\Delta z)$

2. READ: NINP,DELZ

3. READ: CURM,CPHAS

LSTERM=1: $I(z) = \left[e^{-\alpha z} + \Gamma e^{-j\beta} e^{-\alpha(2L-z)} \right] e^{-jkz\cos\theta_s}$

2. READ: SLENG,DBATT,GAMM,BETA,THSCAN

LSTERM=2: $I(z) = \left\{ 1 - \left[\frac{2(z-L/2)}{L} \right]^2 \right\}^N e^{-jkz\cos\theta_s}$

2. READ: SLENG,NPOW,THSCAN

LSTERM=3: $I(z) = \left[\left(\cos \frac{\pi z}{L} \right)^N + C \right] e^{-jkz\cos\theta_s}$

2. READ: SLENG,CTERM,NPOW,THSCAN

LSTERM=4: $I(z) = \left(\cos \frac{\pi z}{L} \right)^N e^{-jk(\rho-\rho_0)}$

where $\rho = \sqrt{\rho_0^2 + (z-z_0)^2}$

2. READ: SLENG,NPOW,RHOP,ZOP

The input data is interpreted as follows.

a) NINP: This is an integer variable that defines the number of current samples.

b) DELZ: This is a real variable (Δz) that defines the current sample spacing in wavelengths.

c) CURM,CPHAS: These are real variables that define the magnitude ($|I_N|$) and phase (ϕ_N) of the current elements.

d) SLENG: This is a real variable (L) that defines the length of the linear array, in wavelengths.

e) DBATT: This is a real variable that defines the attenuation (in dB) along the total length (SLENG) of the array. Note that α is related to DBATT.

f) GAMM,BETA: These are real variables (Γ and β) that define the magnitude and phase (in degrees) of the reflection coefficient at the end of the traveling wave antenna (LSTERM=1).

g) THSCAN: This is a real variable that defines the scan angle (in degrees) of the array.

h) NPOW: This is an integer variable (N) that defines the exponent in the previous equations.

i) CTERM: This is a real variable that defines the constant (C) in the previous equations.

j) RHOP,ZOP: These are real variables that define the phase distribution across an aperture. Note that RHOP and ZOP are specified in wavelengths. In terms of the previous definition for the case (LSTERM=4) RHOP=ρ_o and ZOP=Z_o.

D. Plate Geometry Related Commands:

D1. COMMAND PG:

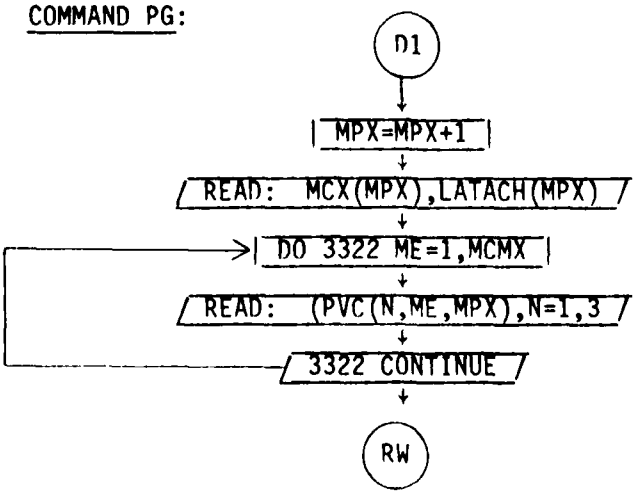

This command enables the user to define the geometry of the flat plate structures to be considered. The geometry is illustrated in Figure 4. It can be called repeatedly up to 25 times.

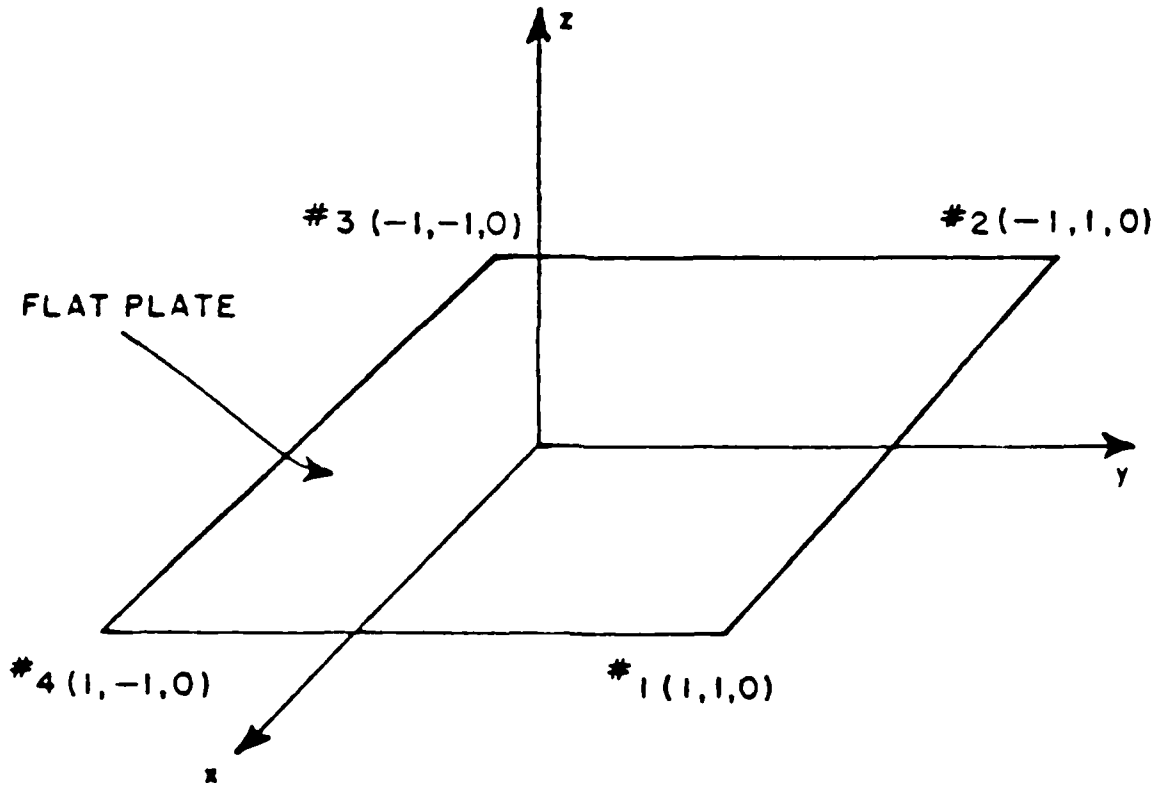

Figure 4. Definition of flat plate geometry.

1. READ: MCX(MPX),LATACH(MPX)

   a) MCX(MPX): This is a dimensioned integer variable. It is used to define the number of corners (or edges) on the MPXth plate. Presently, $1 \leq MCX(MPX) \leq 6$ with $1 \leq MPX \leq 25$.

   b) LATACH(MPX): This is a logical variable defined by T or F. It is used to indicate if the MPXth plate is attached to the fuselage (T) or not (F). Note that all attached plates should be defined within the first six plates. The first and last corners of attached plates should be specified on or near the fuselage. If they are not attached, the program will automatically attach the first and last corners if LATACH=.TRUE. .

2. READ: (PVC(N,ME,MPX),N=1,3)

As stated earlier the locations of the corners of the flat plates are input in terms of the x, y, z coordinates in the specified cartesian coordinate system.

   a) PVC(N,ME,MPX): This is a triply dimensioned real variable. It is used to specify the location of the MEth corner of the MPXth plate. It is input on a single line with the real numbers being the x,y, z coordinates of the corner which correspond to N=1,2,3, respectively, in the array. For example, the array will contain the following

for plate #1 and corner #2 located at x=2.,

y=4., z=6.:

PVC(1,2,1) = 2.

PVC(2,2,1) = 4.

PVC(3,2,1) = 6.

This data is input as: 2., 4.,6.

Considering the flat plate structure given in Figure 4, the input data is given by

```
 1., 1., 0.        : corner #1
-1., 1., 0.        : corner #2
-1.,-1., 0.        : corner #3        plate #1
 1.,-1., 0.        : corner #4
```

Presently, $1 \leq MPX \leq 25$

$1 \leq ME \leq 6$

$1 \leq N \leq 3$

(See Section IV for further details in defining the corner points.)

D2. COMMAND PI:

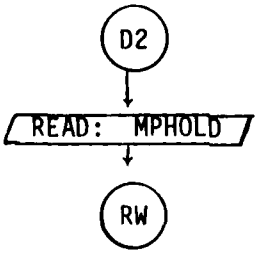

This command enables the user to specify those consecutive plates which will remain for the next calculation. Its useful when one simulates a complicated model by many plates and wants to know the effect of eliminating some plates from a configuration. The useage is illustrated in the example 2.

1. READ: MPHOLD

MPHOLD: This is a real variable used to specify the number of plates to be retained for the next calculation. One should note that the first MPHOLD plates are retained. For example, if MPHOLD=2, then plates #1 and #2 remain in the input data list for the next computation.

E. Pattern Cut Related Commands:

E1. COMMAND PD:

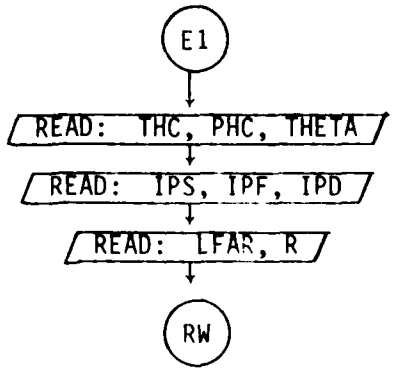

This command enables the user to define the pattern axis of rotation, the angular range, and the range from origin to receiver for the desired conical pattern.

This set of data is associated with the conical pattern desired during execution of the program. The pattern axis is defined by the spherical angles (THC,PHC) as illustrated in Figure 5. These angles define a radial vector direction which points in the direction of the pattern axis of rotation. These angles actually set-up a new coordinate system in relation to the original fixed coordinates. The new cartesian coordinates defined by the subscript "p" are found by first rotating about the z-axis the angle PHC and, then, about the y_p-axis the angle

THC. The pattern is, then, taken in the "p" coordinate system in terms of spherical angles. The theta angle of the pattern taken about the z_p-axis is defined by THETA. The phi angle is defined by the next read statement. In the present form the program will, then, compute any conical pattern in that THETA is used as the conical pattern angle about the z_p-axis for the complete pattern calculation.

As an aid in setting up the "p" coordinate system the following set of equations give the relationships between (THC, PHC) and the x_p, y_p, and z_p-axes. Note that the "p" axes are defined as radial vector directions in a spherical coordinate system:

$$\hat{x}_p = \cos(PHC)\sin(THC+90°)\hat{x}+\sin(PHC)\sin(THC+90°)\hat{y}+\cos(THC+90°)\hat{z}$$

$$\hat{y}_p = \cos(PHC+90°)\hat{x}+\sin(PHC+90°)\hat{y}$$

$$\hat{z}_p = \cos(PHC)\sin(THC)\hat{x}+\sin(PHC)\sin(THC)\hat{y}+\cos(THC)\hat{z}$$

where $0 \leq THC \leq 180°$ and $0 \leq PHC \leq 360°$. In its present form it should be noted that the user may not be able to define the x_p-axis at the starting location that he desired. In addition, the rotation of the pattern may be in the opposite sense using this approach. However, these problems can be easily overcome with properly written plot routines.

1. READ: THC,PHC,THETA

   a) THC,PHC: These are real variables. They are input in degrees and define the axis of rotation about which a conical pattern will be computed (see Figure 5).

b) THETA: This is a real variable. It is input in degrees and used to define the conical angle about the axis of rotation for the desired pattern.

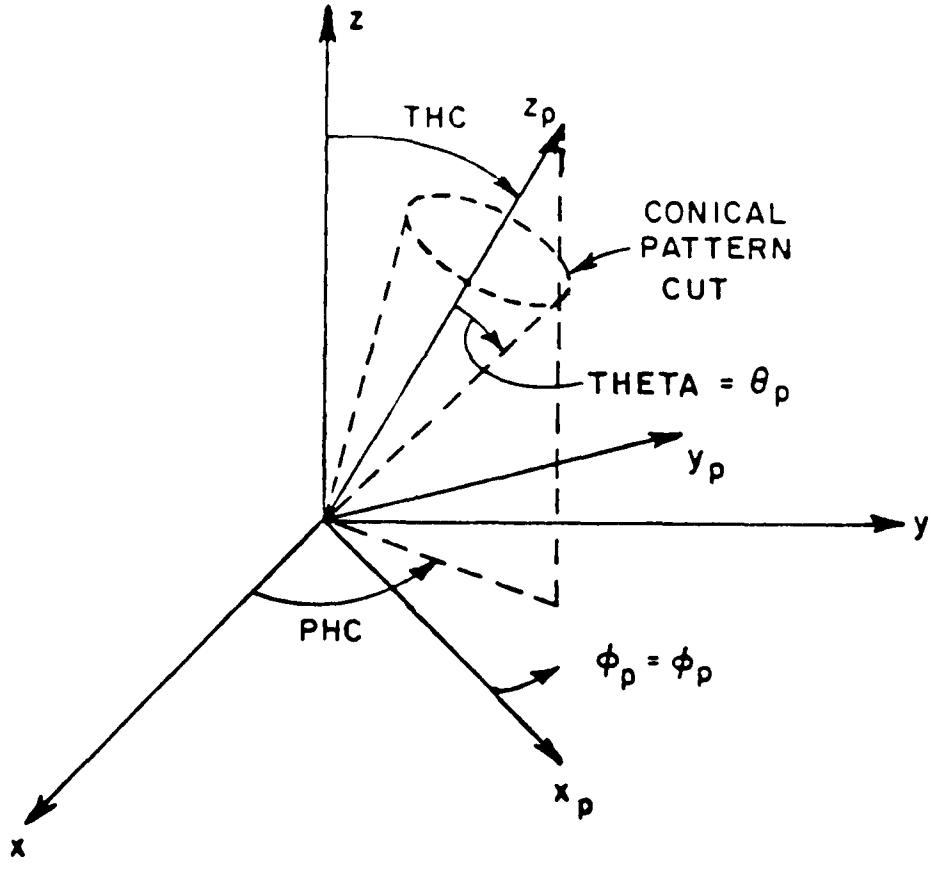

Figure 5. Definition of pattern axis.

2. READ: IPS,IPF,IPD

a) IPS,IPF,IPD: These are integer variables used to define angles in degrees. They are, respectively, the beginning, ending, and incremental values of the phi pattern angle.

As a result of the input given by the two previous read statements, the operator has completely defined the desired conical pattern to be computed during execution of the program.

3. READ: LFAR,R

a) LFAR: This is a logical variable defined by T or F. It is used to specify if the far field pattern is desired or not.

b) R: This is a real variable which is used to define the range in linear units from the origin to the receiver. Note R can be any number when LFAR is .TRUE. in that it is not used in the calculation.

E2. COMMAND RT:

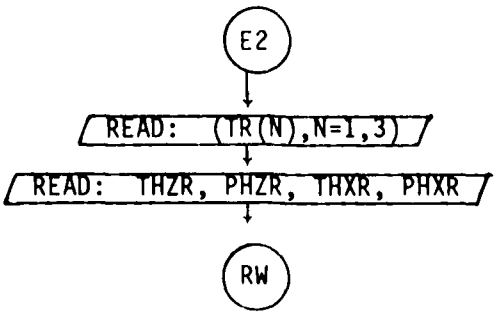

This command enables the user to translate and/or rotate the coordinate system used to define the input data in order to simplify the specification of the plate geometry. The geometry is illustrated in Figure 6.

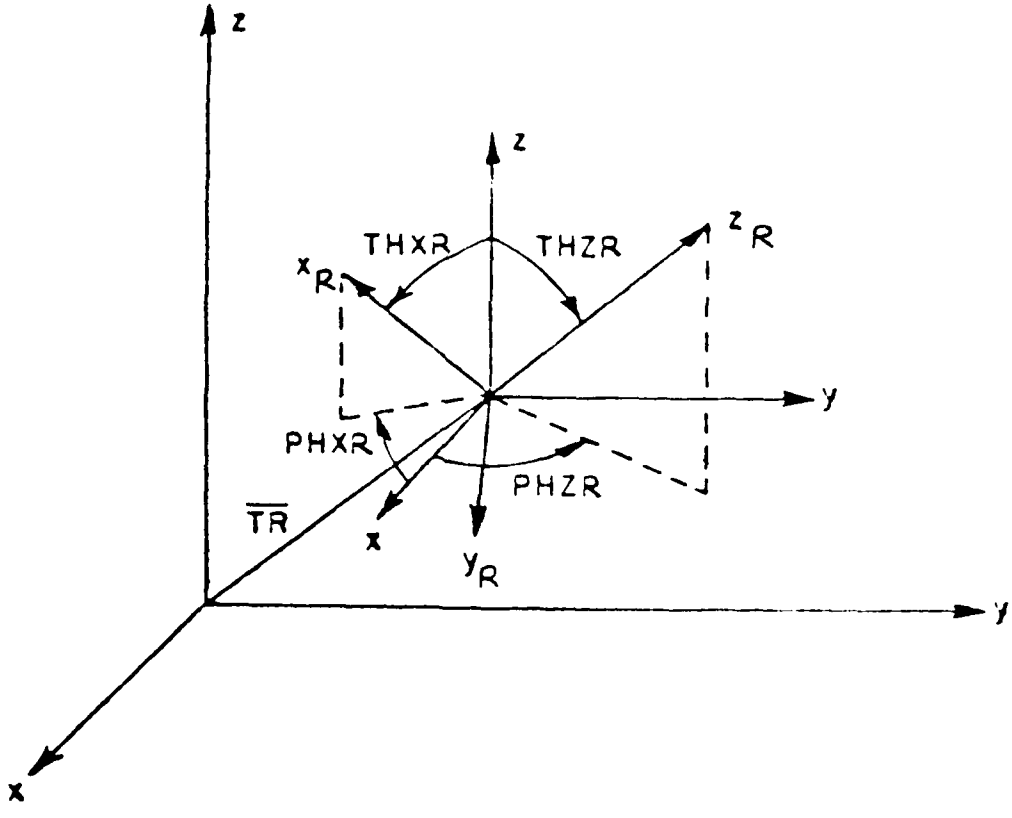

Figure 6. Definition of rotate-translate coordinate system geometry.

1. READ: (TR(N), N=1,3)

   a) TR(N): This is a dimensioned real variable. It is used to specify the origin of the new coordinate system to be used to input the data for the plate structures. It is input on a single line with the real numbers being the x,y,z coordinates of the new origin which corresponds to N=1,2,3, respectively.

2. READ: THZR, PHZR, THXR, PHXR

   a) THZR,PHZR: These are real variables. They are input in degrees as spherical angles that define the z_R-axis of the new coordinate system as if it was a radial vector in the reference coordinate system.

   b) THXR,PHXR: These are real variables. They are input in degrees as spherical angles that define the x_R-axis of the new coordinate system as if it was a radial vector in the reference coordinate system.

The new x_R-axis and z_R-axis must be defined orthogonal to each other. The new y_R-axis is found from the cross product of the x_R and z_R axes. All the subsequent inputs will be made relative to this new coordinate system, which is shown as (x_R, y_R, z_R) unless command "RT:" is called again and redefined.

F. Specific Terms Related Commands:

F1. COMMAND TO:

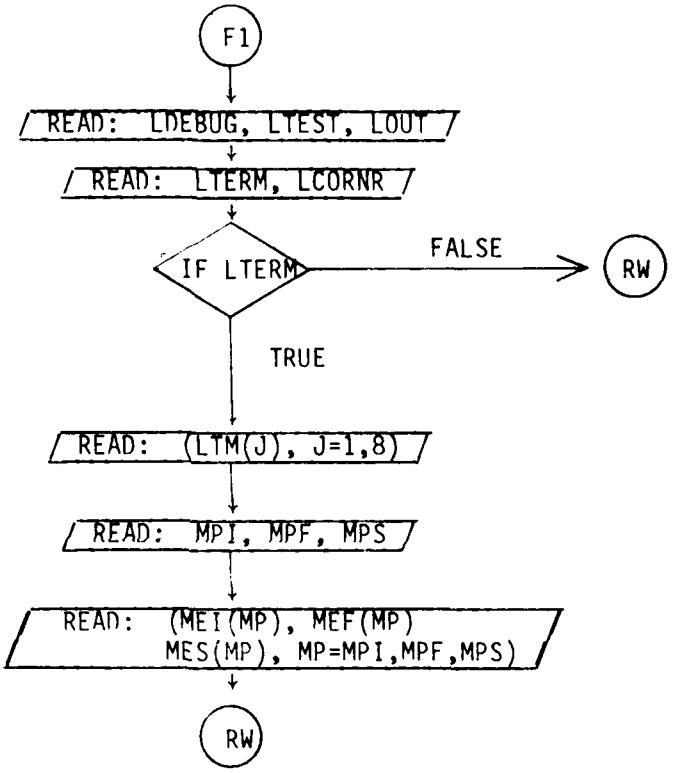

This command enables the user to obtain an extended output of various intermediate quantities in the computer code. This is useful in testing the program or in analyzing the contributions from various scattering mechanisms in terms of the total solution.

1. READ: LDEBUG, LTEST, LOUT

   a) LDEBUG: This is a logical variable defined by T or F. It is used to debug the program if errors are suspected within the program. If set true, the program prints out data on unit #6 associated with each

of its internal operations. These data can, then, be compared with previous data which are known to be correct. It is, also, used to insure initial operation of the code. Only one pattern angle is considered. (normally set false)

b) LTEST: This a logical variable defined by T or F. It is used to test the input/output associated with each subroutine. The data written out on unit #6 are associated with the data in the window of the subroutine. They are written out each time the subroutine is called. It is, also, used to insure initial operation of the code. Only one pattern angle is considered. (normally set false)

c) LOUT: This is a logical variable defined by T or F. It is used to output data on unit #6 associated with the main program. It also is used to initially insure proper operation. It can be used to examine the various components of the pattern. (normally set false)

2. READ: LTERM, LCORNR

a) LTERM: This is a logical variable defined by T or F. It is used to tell the code whether or not individual terms are desired during the computation. (normally set false)

b) LCORNR: This is a logical variable defined by T or F. It

is used to tell the code whether or not corner diffraction is desired during the computation. (normally set true)

3. READ: (LTRM(J), J=1,8)

   a) LTRM(J): These are logical variables defined by T or F to specify a set of individual scattering components that are to be included in the scattered field computation. The components are defined by the following number designations.

   J=1: source field

   J=2: single reflected field

   J=3: single diffracted field

   J=4: diffracted field from chopped fuselage

   J=5: double reflected field

   J=6: reflected-diffracted field

   J=7: diffracted reflected field

   J=8: double diffracted field

(Note: To get the reflected-diffracted and/or double diffracted field one must accompany this command with COMMAND "RD:" and/or "DD:", respectively.)

4. READ: MPI,MPF,MPS

   a) MPI,MPF,MPS: These are integer variables to define plates used in computation, where

   MPI = initial plate,

MPF = final plate, and

MPS = increment in plates going from initial to final plate.

(Note: MPI=1, MPF=3, and MPS=2 implied plates 1 and 3 are included in the computation.)

5. READ: (MEI(MP), MEF(MP), MES(MP), MP=MPI,MPF,MPS)

a) MEI(MP),MEF(MP),MES(MP): These are dimensioned integer variables to define the edges on the MPth plate used in the computation, where

MEI(MP) = initial edge on plate MP,

MEF(MP) = final edge on plate MP, and

MES(MP) = increment in edges going from MEI(MP) to MEF(MP).

F2. COMMAND RD:

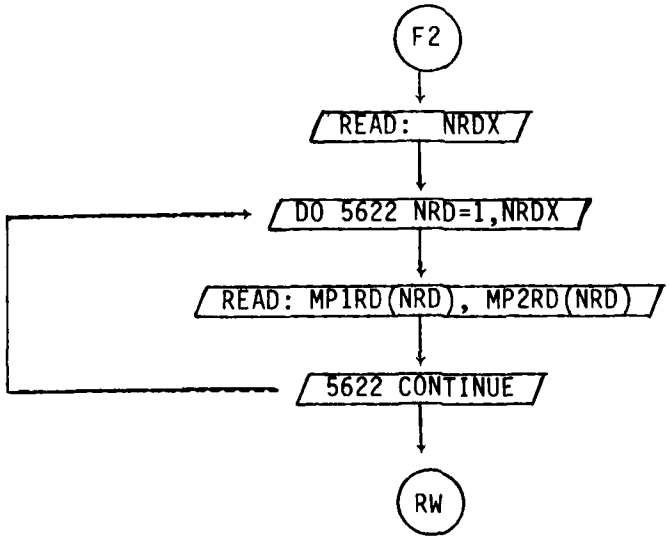

1. READ: NRDX

   NRDX: This is a real variable used to specify the number of reflection-diffraction terms desired. Presently, $0 \leq NRDX \leq 40$.

2. READ: MP1RD(NRD), MP2RD(NRD)

   MP1RD(NRD): This is an integer dimensioned array used to specify the plate number from which the first reflection occurs.

   MP2RD(NRD): This is an integer dimensioned array used to specify the plate number from which the diffraction occurs.

(Note: The useage of this command is illustrated in example 2.)

F3. COMMAND DD:

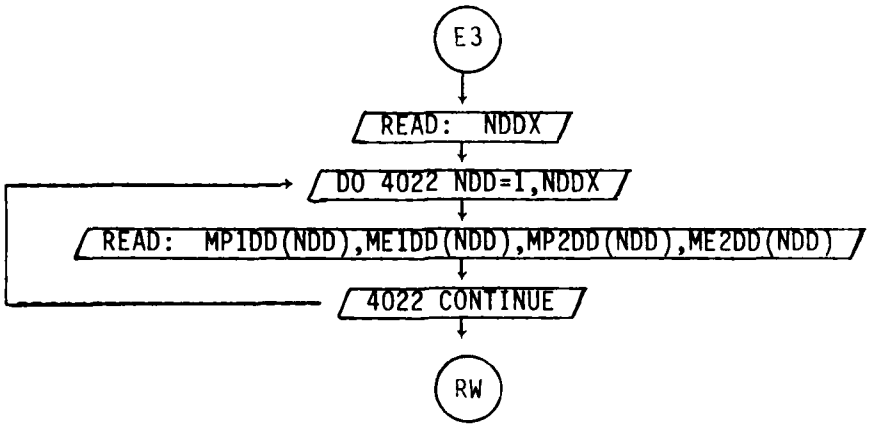

1. READ: NDDX

   a) NDDX: This is an integer variable that specifies the total number of double diffraction terms desired. Presently, $0 \leq NDDX \leq 10$.

2. READ: MP1DD(NDD), ME1DD(NDD), MP2DD(NDD), ME2DD(NDD)

a) MP1DD(NDD), ME1DD(NDD): These are integer dimensioned arrays used to specify the plate and edge number, respectively, from which the first diffraction occurs.

b) MP2DD(NDD), ME2DD(NDD): These are integer dimensioned array used to specify the plate and edge number, respectively, from which a second diffraction occurs.

(Note: The useage of this command is illustrated in example 2.)

F4. COMMAND RS:

This command enables the user to reset the input data to the default case. There is no input data associated with this command.

G. Execute and Output Related Commands:

G1. COMMAND LP:

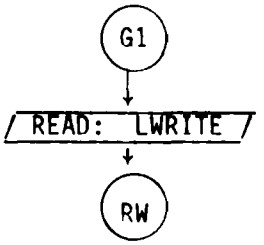

This command enables the user to obtain a line printer listing of the total fields ($E_{\theta p}$, $R_{\phi p}$).

1. READ: LWRITE

LWRITE: This is a logical variable defined by T or F. It is used to indicate if a line printer output is desired or not.

G2. COMMAND PP:

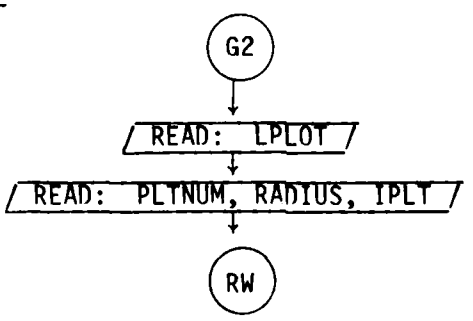

This command enables the user to obtain a pen plot of the total fields ($E_{\theta p}$, $E_{\phi p}$).

1. READ: LPLOT

   LPLOT: This is a logical variable defined by T or F. It is used to indicate if a pen plot is desired or not.

2. READ: PLTNUM, RADIUS, IPLT

   PLTNUM: This is a real variable used to indicate the type of polar plot desired, such that

$$\text{PLINUM} = \begin{cases} 1 \rightarrow \text{E-THETA and E-PHI are plotted separately.} \\ 2 \rightarrow \text{E-THETA and E-PHI are plotted in the same plot.} \\ 3 \rightarrow \text{Both 1 and 2.} \end{cases}$$

   RADIUS: This is a real variable that is used to specify the radius of the polar plot.

   IPLT: This is an integer variable that indicates the type of polar plot desired, such that

$$\text{IPLT} = \begin{cases} 1 \rightarrow \text{field plot} \\ 2 \rightarrow \text{power plot} \\ 3 \rightarrow \text{dB plot} \end{cases}$$

G3. COMMAND BO:

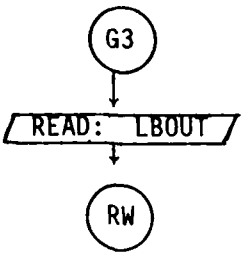

This command enables the user to obtain a binary output of the complex E-THETA and E-PHI patterns values.

1. READ: LBOUT

   (a) LBOUT: This is a logical variable defined by T or F. It is used to indicate if the binary output is desired *or not*.

G4. COMMAND EX:

This command is used to execute the code so that the total fields may be computed. After execution the code returns for another possible command word.

This concludes the definition of all the input parameters to the program. The program would, then, run the desired data and output the results on unit #6. However as with any sophisticated program, the definition of the input data is not sufficient for one to fully understand the operation of the code. In order to overcome this difficulty the next section discusses how the input data are interpreted and used in the program.

IV. INTERPRETATION OF INPUT DATA

This computer code is written to require a minimum amount of user information such that the burden associated with a complex geometry will be organized internal to the computer code. For example, the operator need not instruct the code that two plates are attached to form a convex or concave structure. The code flags this situation by recognizing that two plates have a common set of corners (i.e., a common edge). So if the operator wishes to attach two plates together he needs only define the two plates as though they were isolated. However, the two plates will have two identical corners. All the geometry information associated with plates having common edges is then generated by the code. The present code also will allow a plate to intersect another plate as shown in Figure 7. It is necessary that the corners defining the attachment be positioned a small amount through the plate surface to which it is being connected.

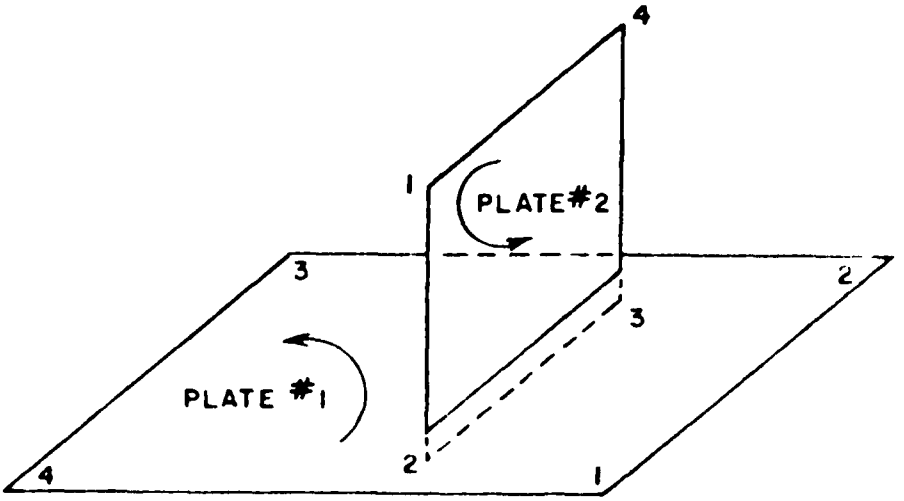

Figure 7. Data format used to define a flat plate intersecting another flat plate.

In defining the plate corners it is necessary to be aware of a subtlety associated with simulating convex or concave structures in which two or more plates are used in the computation. This problem results because each plate has two sides. If the plates are used to simulate a closed or semi-closed structure, then possibly only one side of the plate will be illuminated by the antenna. Consequently, the operator must define the data in such a way that the code can infer which side of the plate is illuminated by the antenna. This is accomplished by defining the plate according to the right-hand rule. As one's fingers of the right hand follow the edges of the plate around in the order of their definition, his thumb should point toward the illuminated region above the plate. To illustrate the constraint associated with the data format, let us consider the definition of a rectangular box. In this case, all the plates of the box must be specified such that they satisfy the right-hand rule with the thumb pointing outward as illustrated in Figure 8. If this rule were not satisfied for a given plate, then the code would assume that the antenna is within the box as far as the scattering from that plate is concerned.

In the "PG:" command, if LATACH(MPX)=T (i.e., the plate is attached to the fuselage), the program assumes that the first and last plate corners (PVC(N,1,MPX) and PVC(N,MCMX,MPX)) are positioned on the fuselage. The user must define the geometry accordingly. However, he need not exactly attach the first and last corners to the fuselage since the code will extend the edges and reset the first and final corner points on the fuselage as shown in Figure 9.

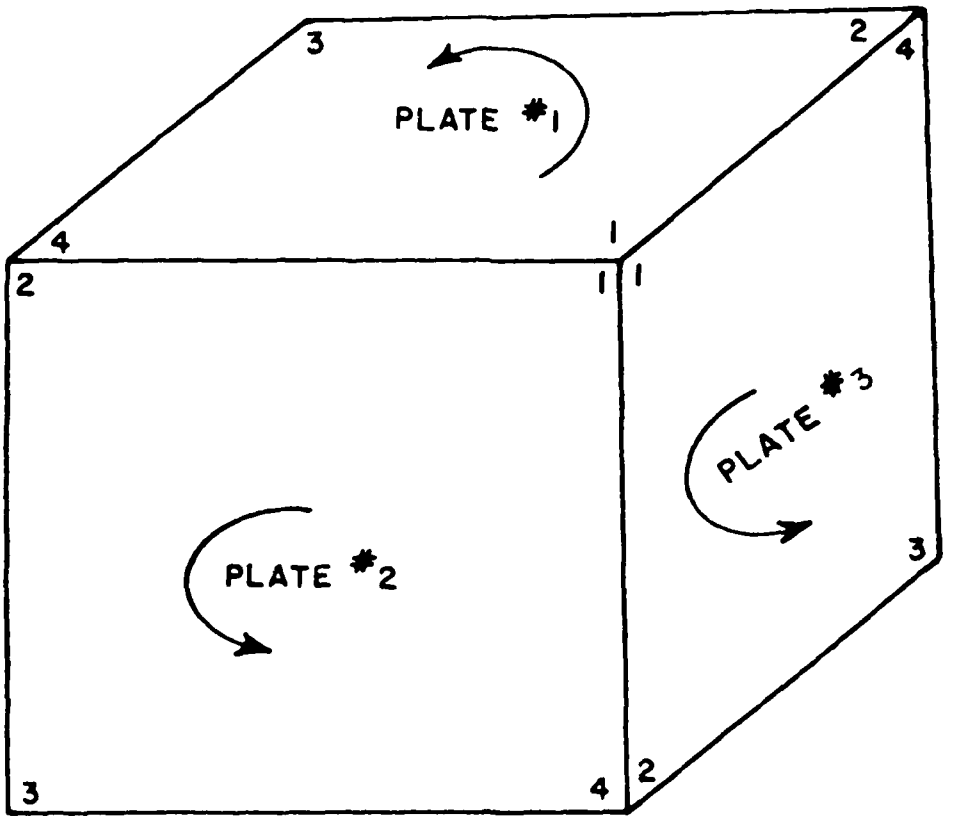

Figure 8. Data format used to define a box structure.

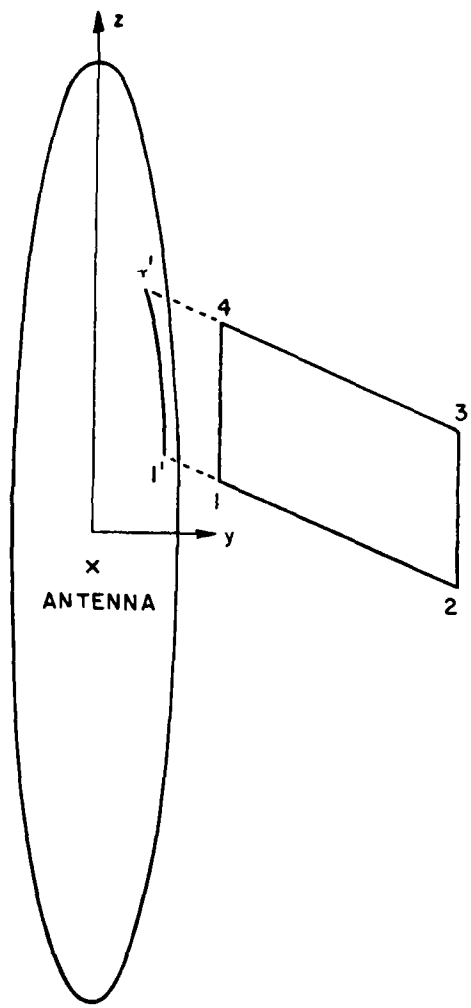

Figure 9. Data format used to define a flat plate attaching to a fuselage.

Using the "SG:" command, it is necesary that $-90° \leq PHSA(MS) \leq 90°$. In case the antenna is placed on the bottom part of the fuselage, the user must redefine the geometry such that $\phi_S(PHSA(MS))$ falls within the required angular range. This requires turning the aircraft upside-down. The code simulates fuselage blockage by using "FB:" COMMAND. If this command is activated the code will determine if a ray strikes a fuselage blockage plate. If so, it will set that field component to zero. Thus, the shadowing effect of the fuselage can be simulated in this way. It is assumed that the higher-order diffraction and reflection fields from the fuselage are small in which case they can be neglected. Thus, even though higher-order interactions between structures and the fuselage are not added in computation, their absence will be apparent in the results.

Finally, it must be kept in mind that the antenna should be kept at least a wavelength away from any diffracting edge. In fact all dimensions should be at least a wavelength.

V. PROGRAM OUTPUT

The basic output option from the computer code is a line printer listing of the results. If LWRITE=T in the input data list the program will automatically generate a line printer output of the complex field values. Recall that the results of the program are the $E_{\theta p}$ and $E_{\phi p}$ radiation pattern values. In order to again describe these pattern components, let us consider the various principal plane patterns treated in the previous section. The computer code allows for a rotation of coordinates such that one can take a pattern about an angles (THC, PHC).

The geometry that applies for each of the roll, elevation, and azimuth patterns used in the next section is illustrated in Figure 10. Note that the θp and ϕp angles are defined relative to the rotated pattern coordinates and that they change as THC and PHC are changed. Thus, $E_{\theta p}$ is the theta component of the field (i.e., $E_{\theta p}=\vec{E}\cdot\hat{\theta p}$) in the pattern coordinate system. Likewise, $E_{\phi p} = \vec{E}\cdot\hat{\phi p}$. The total radiated electric field is denoted by $\vec{E}$.

In addition to the printed results, one has the option of obtaining a set of polar patterns. If LPLOT=T in the input data list, using the "PP:" command, the program will automatically plot the $E_{\theta p}$ and $E_{\phi p}$ polar patterns. These patterns are plotted such that the outer ring corresponds to the pattern maximum in each case. This polar plot routine was used to plot the data presented in the next section.

One more output option is to get the binary output of the $E_{\theta p}$ and $E_{\phi p}$ patterns. If LBOUT=T in the input data list, using the "BO:" command, the program will automatically write the $E_{\theta p}$ and $E_{\phi p}$ results on unit number #1, i.e., WRITE (1). This is a very useful output when one wishes to interface this program with another one.

VI. APPLICATION OF CODE TO SEVERAL SIMPLE EXAMPLES

The following two examples are used to illustrate some features and demonstrate the usage of the basic COMMANDS of the computer code. The effect of higher order terms on the solution is shown in example 2. Note that the patterns are plotted in decibels with each division being 10 dB, and the labeling is not included.

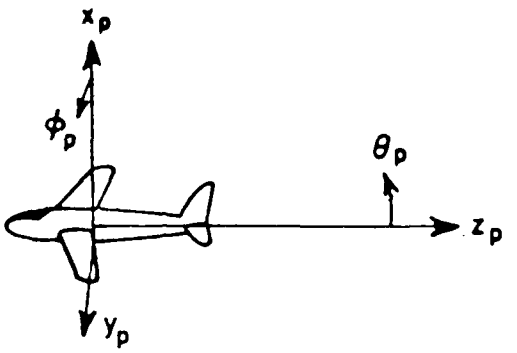

(a) ROLL PLANE COORDINATES (THC=0°, PHC=0°)

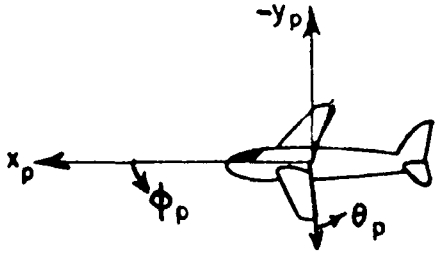

(b) ELEVATION PLANE COORDINATES (THC=90°, PHC = ± 90°)

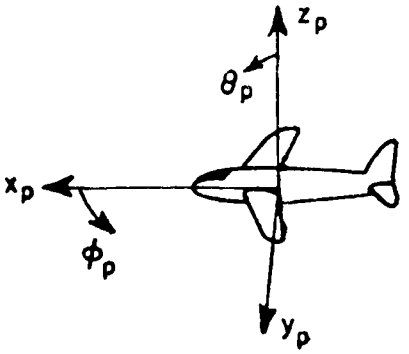

(c) AZIMUTH PLANE COORDINATES (THC=90°, PHC=0°)

Figure 10. Illustration of pattern coordinates for the principal plane pattern calculations.

Example 1. Consider the radiation pattern of an antenna mounted on a composite prolate spheroid (5^{λ} x 60^{λ} x 20^{λ}) for different pattern cuts. This example illustrates the useage of the COMMAND "FC:" and its effect on the pattern. The geometry is shown in Figure 11.

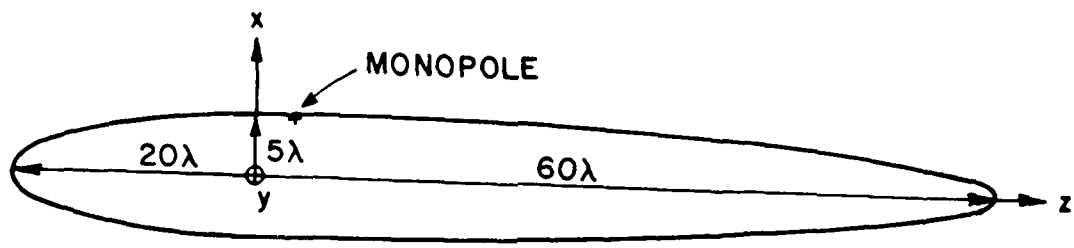

(a) SIDE VIEW

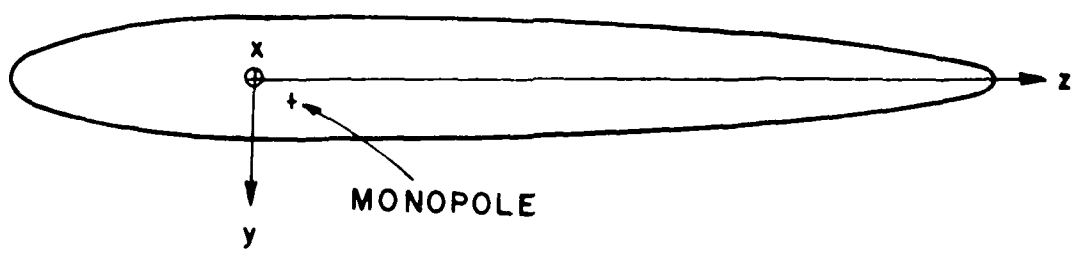

(b) TOP VIEW

Figure 11. A monopole mounted on a composite prolate spheroid.

The input data is given by

```
FG:
5.,60.,20.
0.,0.,0.
SG:MONOPOLE
25.,3.
1
0.,0.
.4,.8,0.,.25,3
1.,0.
PD:ROLL PLANE (FAR FIELD)
0.,90.,90.
0,360,1
T,1000.
PP:
T
2,1.,3
EX:
PD:AZIMUTH PLANE (FAR FIELD)
90.,0.,90.
0,360,1
T,1000.
EX:
PD:ELEVATION PLANE (FAR FIELD)
90.,90.,90.
0,360,1
T,1000.
EX:
SG:MONOPOLE
25.,-12.
1
0.,0.
.4,.8,0.,.25,3
1.,0.
EX:
FC:FUSELAGE CHOPPED OFF
F,T
40.,-14.
EX:
```

The computation results are shown in Figure 12.

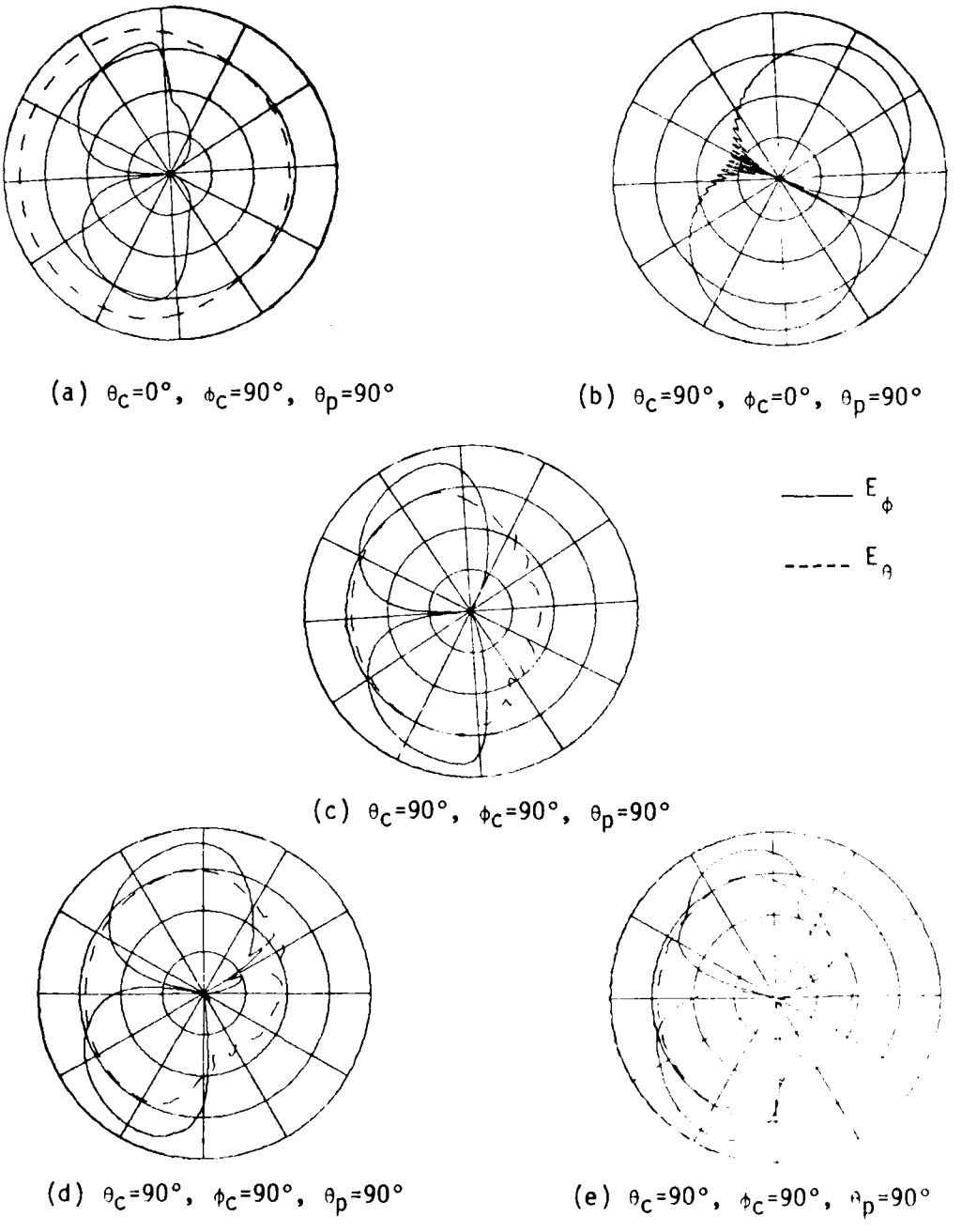

Figure 12. Radiation pattern of monopole mounted on spheroid at frequency .3GHz. (a)(b)(c) source located at PHS=25°, ZS=3$^\lambda$ (d)(e) source locate at PHS=25°, ZS=-12$^\lambda$ and fuselage chopped off at ZC2=-14$^\lambda$ for (e).

Example 2: Consider the roll plane radiation pattern for a bent plate attached to a composite spheroid (5^{λ} x 200^{λ} x 200^{λ}). The geometry is shown in Figure 13. The useage of "TO:" and "PI:" commands and their effect on the radiation pattern will be shown in this example. Various GTD terms involved in the computation are shown in Figure 14.

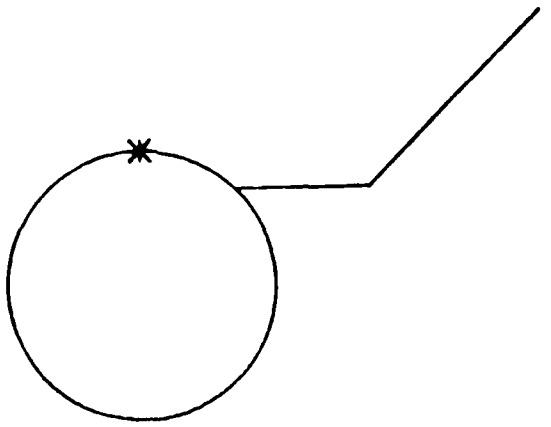

Figure 13. A bent plate attached to a composite spheroid.

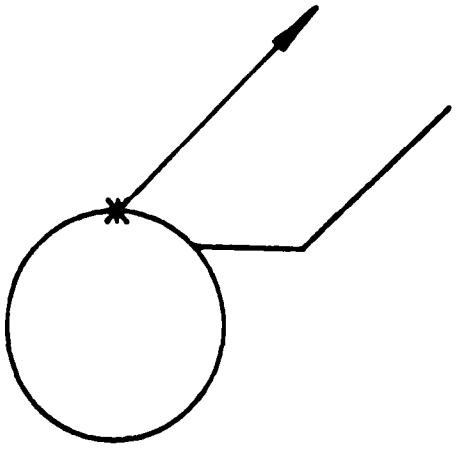

source field

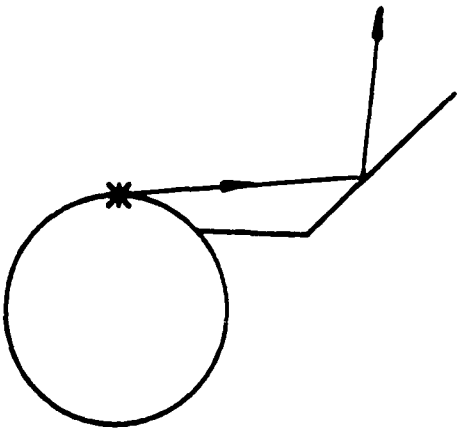

reflected field

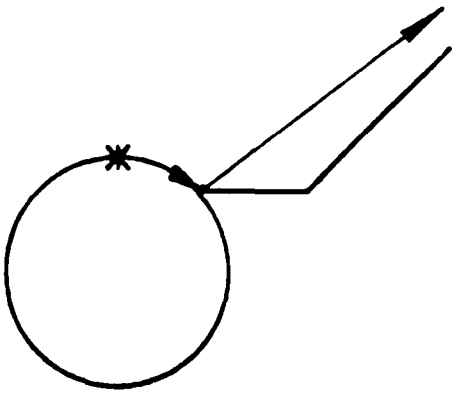

diffracted field

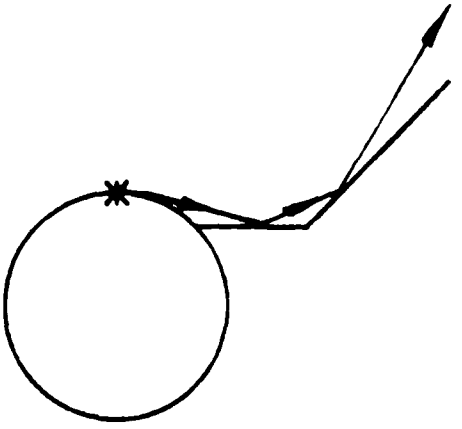

reflected-reflected field

Figure 14. Various GTD terms.

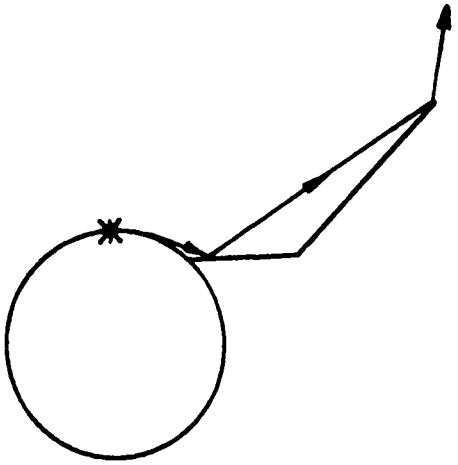

reflected-diffracted field

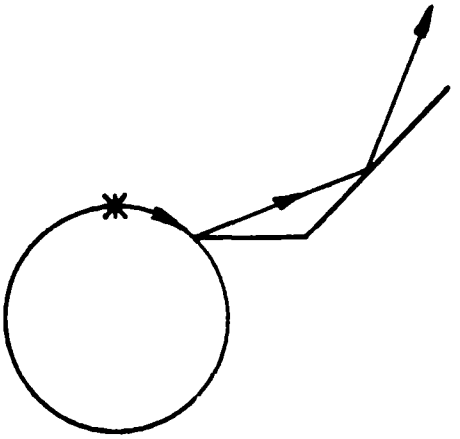

diffracted-reflected field

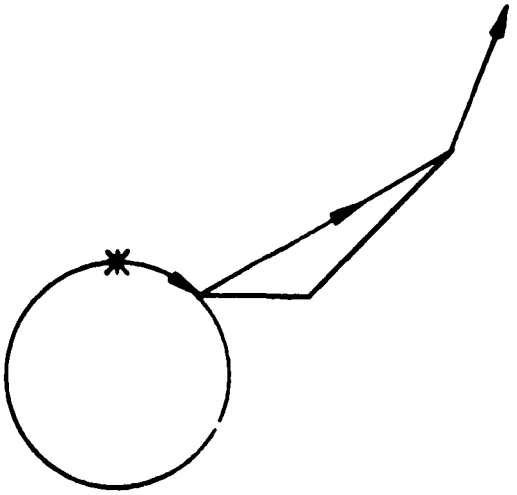

diffracted-diffracted field

Figure 14. (continued) Various GTD terms.

```
FG:
5.,200.,200.
0.,0.,0.
FB:
2
4
4.5,0.,40.
4.5,0.,-40.
-4.5,0.,-40.
-4.5,0.,40.
4
0.,-4.5,40.
0.,4.5,40.
0.,4.5,-40.
0.,-4.5,-40.
SG:MONOPOLE
0.,0.
1
0.,0.
.4,.8,0.,.25,3
1.,0.
PP:PEN PLOT
T
1,1.35,3
PD:ROLL PLANE (NEAR FIELD)
0.,90.,90.
0,360,1
F,1000.
PG:
4,T
3.,5.,-40.
3.,9.,-40.
3.,9.,40.
3.,5.,40.
PG:
4,F
3.,9.,-40.
10.,18.,-40.
10.,18.,40.
3.,9.,40.
RD:
1
1,2
```

```
DD:
4
2,4,2,2
1,4,2,2
2,2,1,4
2,2,2,4
TO:TOTAL FIELD (INCLUDE DOUBLE TERMS)
F,F,F
T,T
T,T,T,F,T,T,T,T
1,2,1
1,4,1
1,4,1
EX:
TO:SOURCE FIELD ONLY
F,F,F
T,T
T,F,F,F,F,F,F,F
1,2,1
1,4,1
1,4,1
EX:
TO:REFLECTED FIELD ONLY
F,F,F
T,T
F,T,F,F,F,F,F,F
1,2,1
1,4,1
1,4,1
EX:
TO:DIFFRACTED FIELD ONLY
F,F,F
T,T
F,F,T,F,F,F,F,F
1,2,1
1,4,1
1,4,1
EX:
TO:S+R
F,F,F
T,T
T,T,F,F,F,F,F,F
1,2,1
1,4,1
1,4,1
EX:
```

```
TO:S+R+D (ONLY FIRST ORDER TERM INCLUDE)
F,F,F
T,T
T,T,T,F,F,F,F,F
1,2,1
1,4,1
1,4,1
EX:
TO:DOUBLE REFLECTION (R/R)
F,F,F
T,T
F,F,F,F,T,F,F,F
1,2,1
1,4,1
1,4,1
EX:
TO:S+R+R/R
F,F,F
T,T
T,T,F,F,T,F,F,F
1,2,1
1,4,1
1,4,1
EX:
TO:REFLECTION/DIFFRACTION TERM (R/D)
F,F,F
T,T
F,F,F,F,F,T,F,F
1,2,1
1,4,1
1,4,1
EX:
TO:R/R+R/D
F,F,F
T,T
F,F,F,F,T,T,F,F
1,2,1
1,4,1
1,4,1
EX:
TO:S+R+D+R/R+R/D
F,F,F
T,T
T,T,T,F,T,T,F,F
1,2,1
1,4,1
1,4,1
EX:
```

```
TO:DIFFRACTION/REFLECTION TERM (D/R)
F,F,F
T,T
F,F,F,F,F,F,T,F
1,2,1
1,4,1
1,4,1
EX:
TO:S+R+D+R/R+R/D+D/R
F,F,F
T,T
T,T,T,F,T,T,T,F
1,2,1
1,4,1
1,4,1
EX:
TO:DOUBLE DIFFRACTION TERM (D/D)
F,F,F
T,T
F,F,F,F,F,F,F,T
1,2,1
1,4,1
1,4,1
EX:
TO:D/R+D/D
F,F,F
T,T
F,F,F,F,F,F,T,T
1,2,1
1,4,1
1,4,1
EX:
TO:ALL DOUBLE TERM
F,F,F
T,T
F,F,F,F,T,T,T,T
1,2,1
1,4,1
1,4,1
EX:
TO:
F,F,F
T,T
T,T,T,F,F,F,F,F
1,2,1
1,4,1
1,4,1
PI:TAKE OFF SECOND PLATE
1
PG:ADD ONE PLATE
4,T
3.,-5.,40.
3.,-9.,40.
3.,-9.,-40.
3.,-5.,-40.
PP:
T
1,2.,3
EX:
```

The computed results are shown in Figure 15 and 16. Note that each pattern in Figure 15 is normalized to the same level such that one can see the relative significance of each term. An interesting result is shown in Figure 15-(k) where the source and reflected fields are superimposed. These two terms form the classical "Geometrical Optics" (GO) solution. However, one should note that the GO solution is far from complete as can be observed from the discontinuities in the pattern. From Figure 15-(m), where the first order terms of GTD solution are superimposed. As can be seen that there is still some discontinuities in the pattern. Therefore, higher order terms (as shown in Figure 15 (d) ~ (j)) are being introduced such that the discontinuities in Figure 15-(m) are compensated by those higher order terms. The final result is shown in Figure 15-(p). From this example, it is clear that these higher order terms can be significant in certain regions of the pattern.

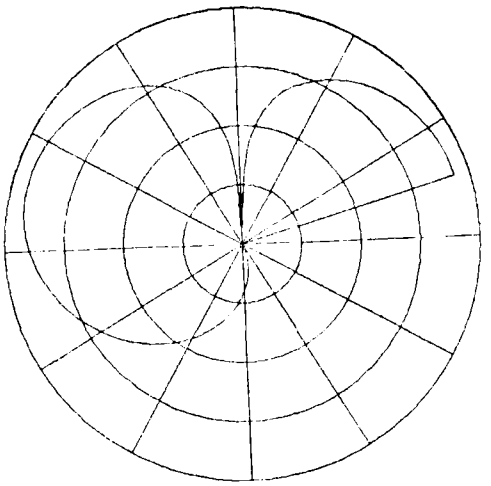

(a) source field (S)

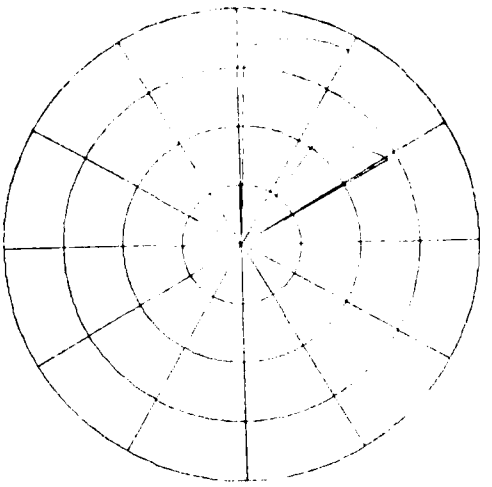

(b) reflected field (R)

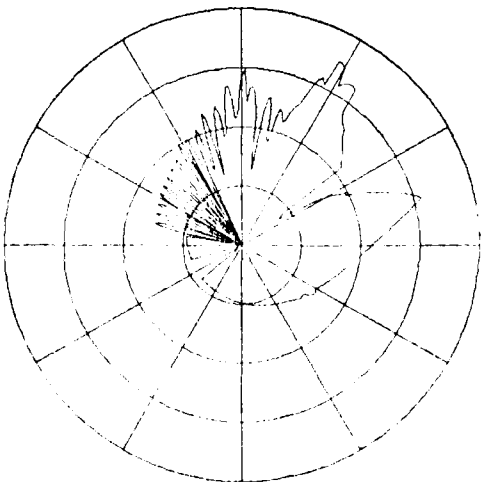

(c) diffracted field (D)

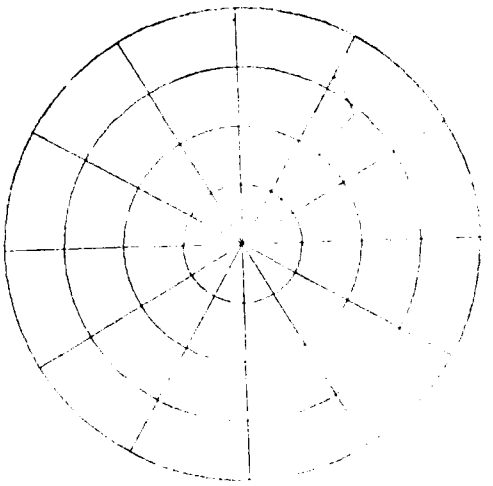

(d) reflected/reflected field (R/R)

Figure 15. Roll plane radiation pattern.

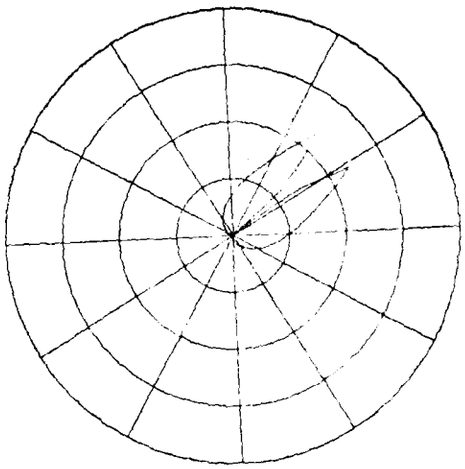

(e) reflected/diffracted field (R/D)

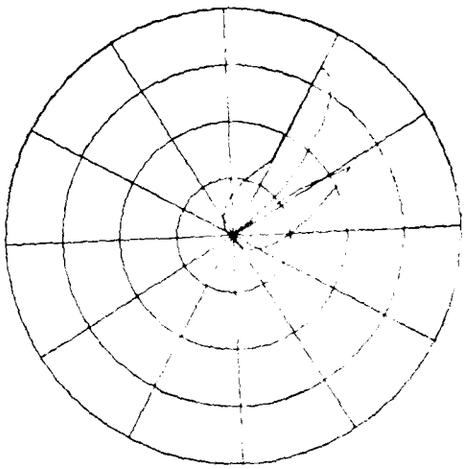

(f) R/R + R/D

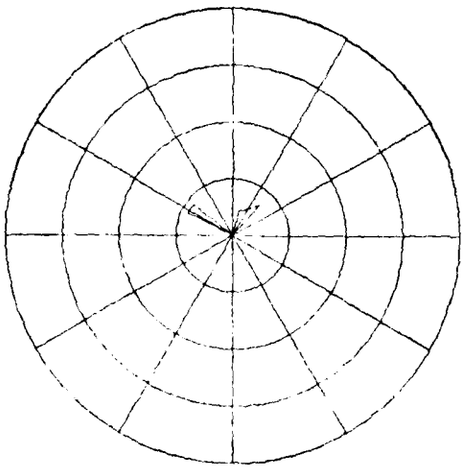

(g) diffracted/reflected field (D/R)

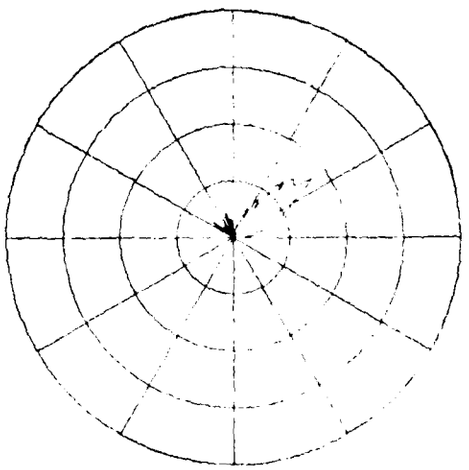

(h) diffracted/diffracted field (D/D)

Figure 15. (continued) Roll plane radiation pattern.

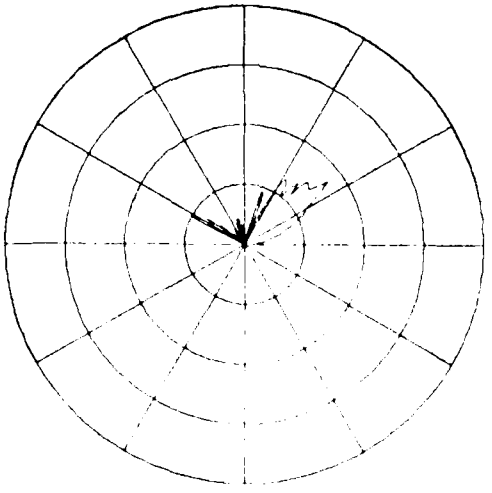

(i) D/R + D/D

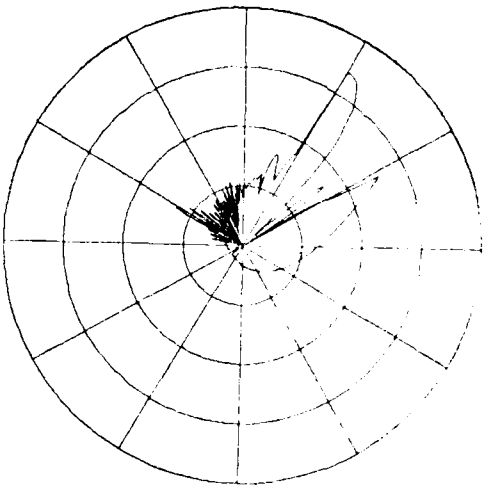

(j) second order interaction GTD terms (R/R + R/D + D/R + D/D)

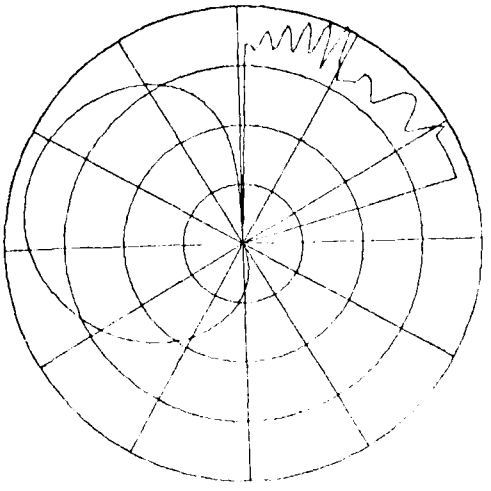

(k) S + R

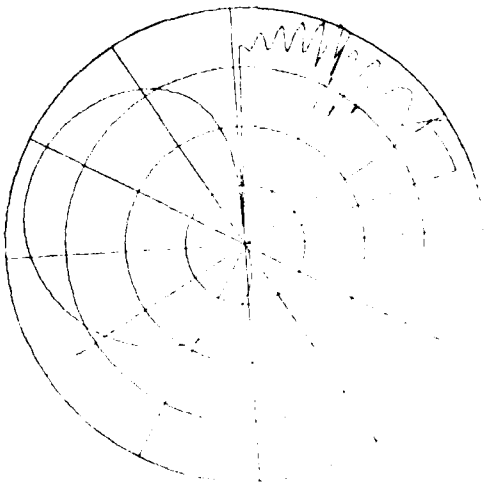

(l) S + R + R/R

Figure 15. (continued) Roll plane radiation pattern.

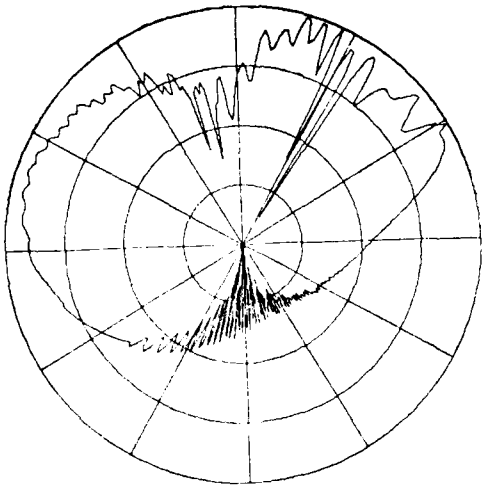

(m) S + R + D

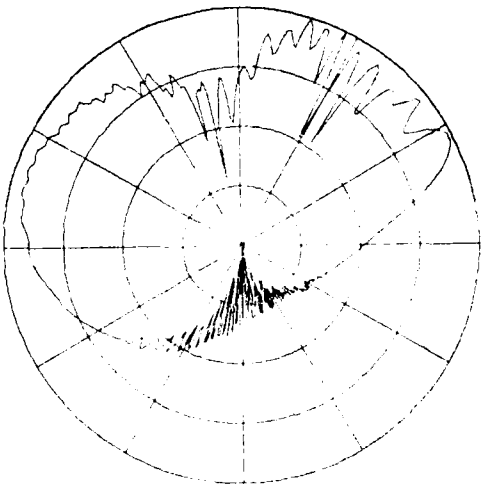

(n) S + R + D + R/R + R/D

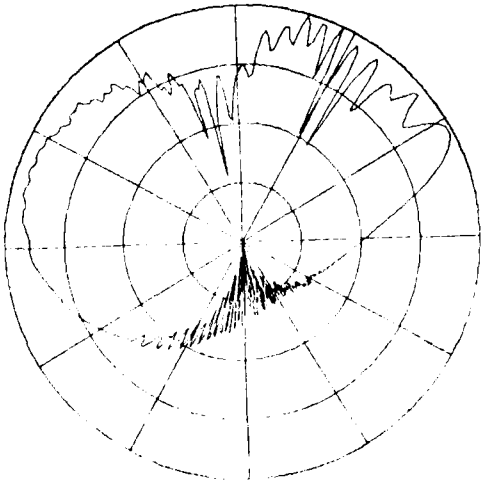

(o) S + R + R/R + R/D + D/R

(p) total solution
(S+R+D+R/R+R/D+D/R+D/D)

Figure 15. (continued) Roll plane radiation pattern.

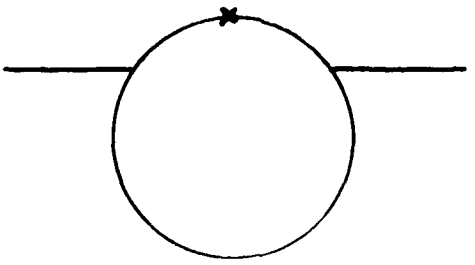

(a)

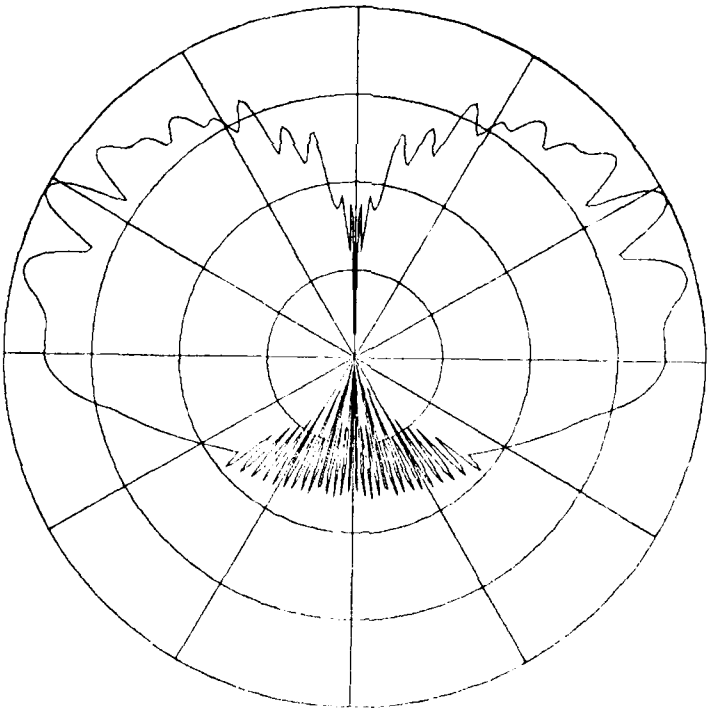

(b)

Figure 16. *Total solution (S+R+D) after using "PI:" and "PG:"* commands.

VII. APPLICATION OF CODE TO AIRCRAFT SIMULATIONS

To begin any simulation of an aircraft, one needs to start with a set of scale model drawings. A typical aircraft model consists of a composite prolate spheroid fuselage plus flat plates simulating the other structures such as wings, stabilizers, etc. One can also use the "COMMAND FC:" to model the radome part of the aircraft. The radome is constructed of low dielectric constant material such that it can be assumed to be free space for these calculations.

Several aircraft models such as BOEING 737, KC-135, and F-16 fighter will be given in the following examples.

To begin the simulation procedure, one first finds the composite prolate spheroid parameters for the aircraft fuselage. The spheroid surface should simulate the fuselage surface as accurately as possible near the antenna location. Once the composite prolate spheroid dimensions are specified the plates are added to the model.

This code allows for two different methods for defining one plate to be attached to another: 1) edge to edge attachment and 2) edge to surface attachment. Edge to edge attachment, as illustrated in Figure 17, often

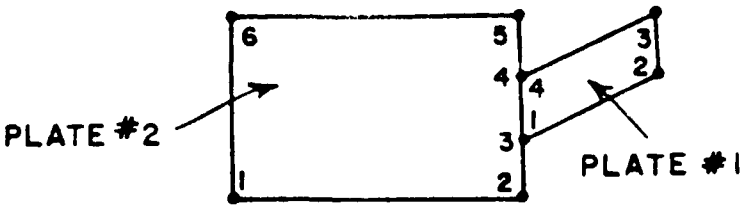

Figure 17. Edge to edge plate attachment.

requires that a plate edge be defined as two or three colinear edges as the program identifies this mode of attachment only by finding two identical pairs of corners. Note that the corners must be consecutive on both plates which means there actually exists an edge between them. In the case of edge to surface attachment, one plate is defined as penetrating a short distance through the surface of the second plate as illustrated in Figure 18. The program then defines the new junction edge and eliminates the smaller portion of plate #1 behind plate #2. Here care must be taken to assure that the new junction edge is completely contained within the bounds of plate #2, and is nowhere nearer than a half wavelength or so to an edge of plate #2.

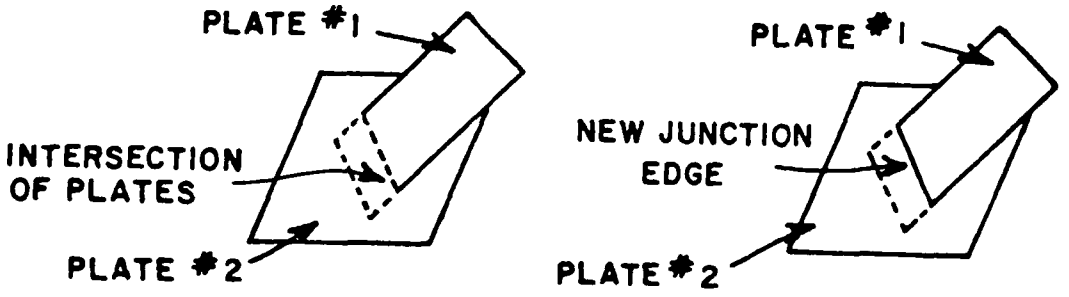

Figure 18. Edge to surface plate attachment.

One thing which should be noted is that the attachment of wings, stabilizers or plates to the fuselage is automatically done by the computer as illustrated in Figure 9 so the user need not worry about the input data attaching perfectly to the fuselage (composite prolate spheroid).

Example 3: Simulation of BOEING 737

Consider a λ/4 monopole located at PHS=0° and ZS=-278" mounted on the fuselage of Boeing 737. The line drawing model is shown in Figure 19, and the computer model based on the input data is shown in Figure 20. The input data is as follows:

```
UN:INCHES
3
FQ:3.18 GHZ
1,3.18,1.
FG:BOEING 737 (STATION 220)
65.86,1307.04,308.56
0.,0.,0.
SG:MONOPOLE
0.,-273.
1
0.,0.
.1,.2,0.,.928525,3
1.,0.
PG:RIGHT WING
4,T
0.,65.,67.952
0.,536.93,316.14
0.,536.93,379.86
0.,65.,240.26
PG:LEFT WING
4,T
0.,-65.,240.26
0.,-536.93,379.86
0.,-536.93,316.14
0.,-65.,67.952
PG:TAIL
4,T
60.,8.25,618.55
284.147,8.25,819.056
284.147,0.,683.696
60.,0.,483.19
PG:TAIL
4,T
60.,0.,483.19
284.147,0.,683.696
284.147,-8.25,819.056
60.,-8.25,618.55
PG:NOSE
4,T
0.,-27.07,-308.56
-5.6,-27.07,-321.6
-5.6,0.,-321.6
0.,0.,-308.56
PG:NOSE
4,T
0.,0.,-308.56
-5.6,0.,-321.6
-5.6,27.07,-321.6
0.,27.07,-308.56
FB:
2
6
0.,65.,0.
57.,32.,0.
57.,-32.,0.
0.,-65.,0.
-65.,-65.,0.
-65.,65.,0.
6
0.,-65.,470.
0.,-65.,0.
0.,-35.,-250.
0.,35.,-250.
```

```
0.,65.,0.
0.,65.,470.
PD:ELEVATION PLANE
90.,90.,89.
0,360,1
T,6000.
PP:
T
1,1.5,3
EX:
PD:ROLL PLANE
0.,90.,90.
0,360,1
T,6000.
EX:
PD:AZIMUTH PLANE
90.,0.,90.
0,360,1
T,6000.
EX:
```

```
PP:
T
1,1.625,3
PD:AZIMUTH PLANE
90.,0.,90.
0,360,1
T,6000.
FC:
T,F
820,0
EX:
PP:
T
1,1.62,3
PD:AZIMUTH PLANE
90.,0.,50.
0,360,1
T,6000.
EX:
PD:AZIMUTH PLANE
90.,0.,60.
0,360,1
T,6000.
EX:
```

```
PD:AZIMUTH PLANE
90.,0.,70.
0,360,1
T,6000.
EX:
PD:AZIMUTH PLANE
90.,0.,80.
0,360,1
T,6000.
EX:
PD:AZIMUTH PLANE
90.,0.,100.
0,360,1
T,6000.
EX:
PD:AZIMUTH PLANE
90.,0.,110.
0,360,1
T,6000.
EX:
PD:AZIMUTH PLANE
90.,0.,120.
0,360,1
T,6000.
EX:
```

The computed results are shown in Figure 21 to Figure 30 and found to be in very good agreement with measurements. (There is no measurement data available for E_ϕ in the azimuth plane.) The experimental work was performed by the technical staff at NASA (Hampton, Virginia) using a 1/11th scale model of a Boeing 737 aircraft. But it is noted that the measured results have some asymmetry in the patterns. This could be attributed to misalignment of the monopole with respect to the surface normal or the movement of the model due to shifting weight during the measurement. Also, it is found in Figure 30(a) that there is some deviation between computation and measurement in the region of the nose section (neighborhood of ϕ=0°). This could be attributed to the fact that the computer simulated model is not very good in simulating the nose section.

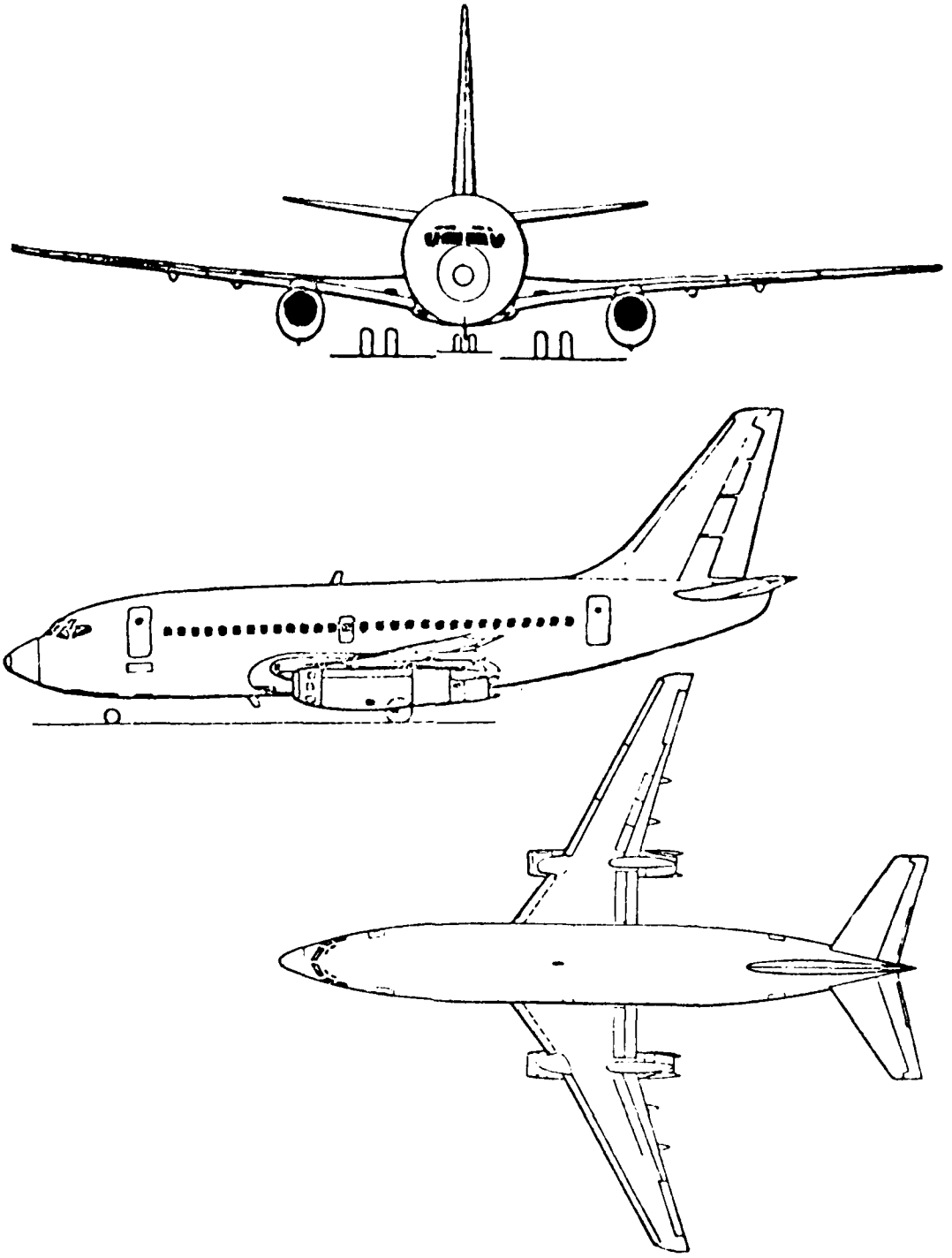

Figure 19. Line drawing model of Boeing 737.

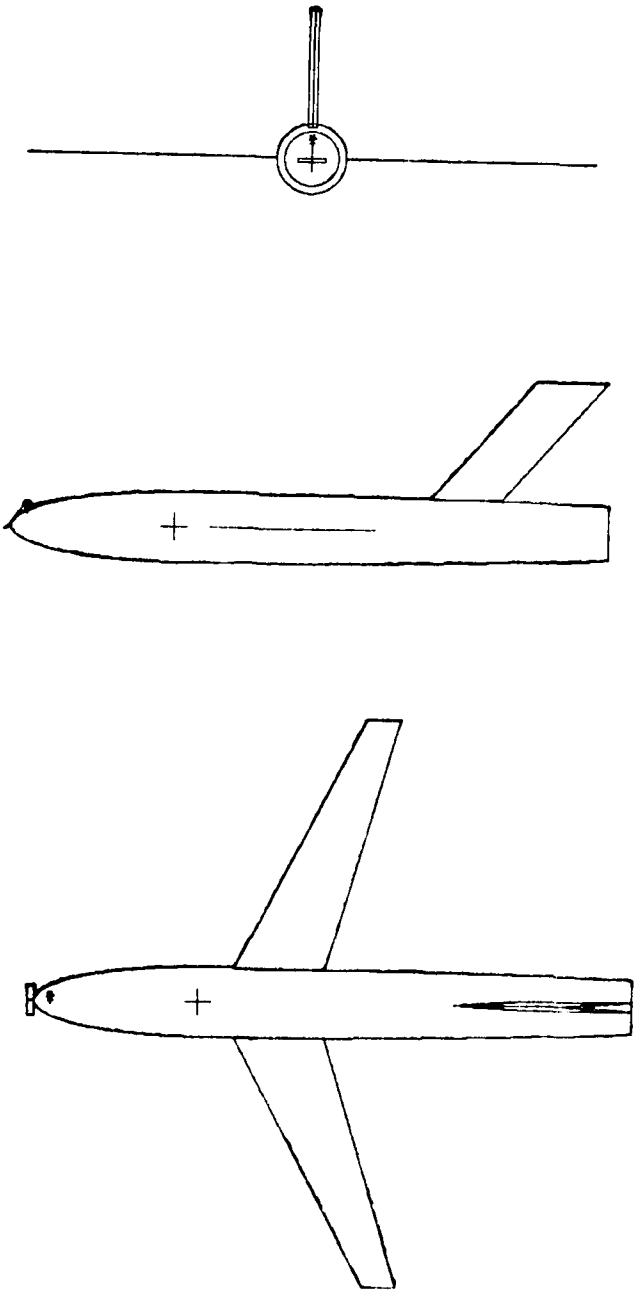

Figure 20. Computer model of Boeing 737.

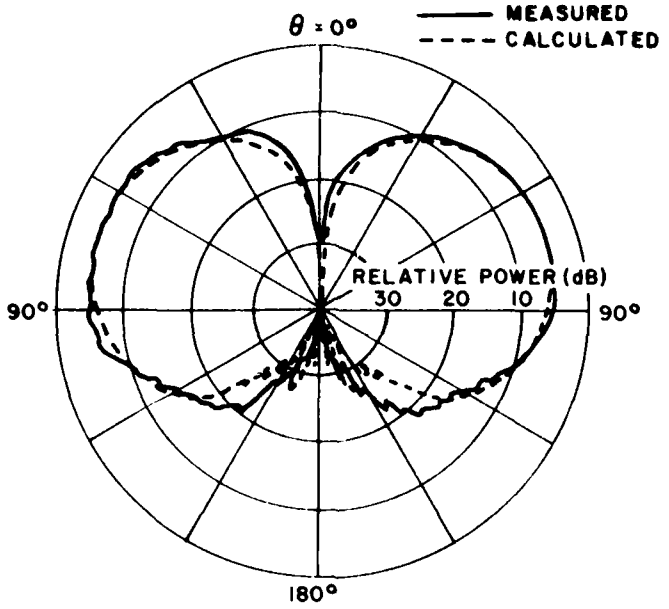

(a)

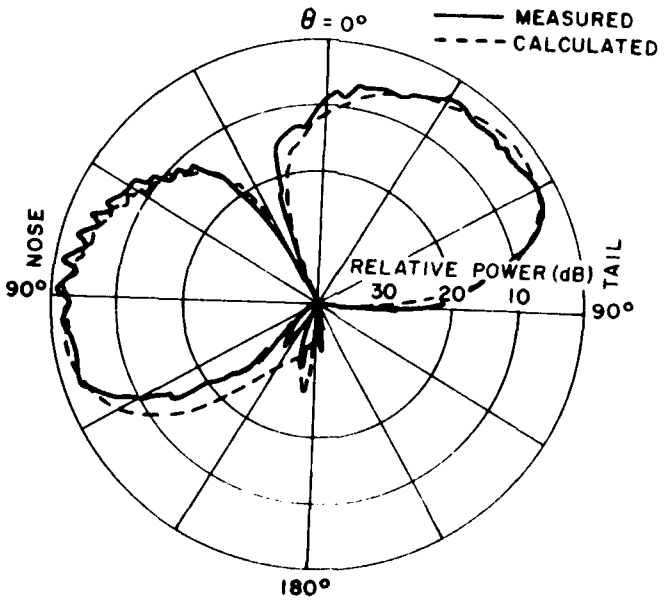

(b)

Figure 21. (a) Roll plane radiation pattern (E_ϕ)

(b) Elevation plane radiation pattern (E_ϕ)

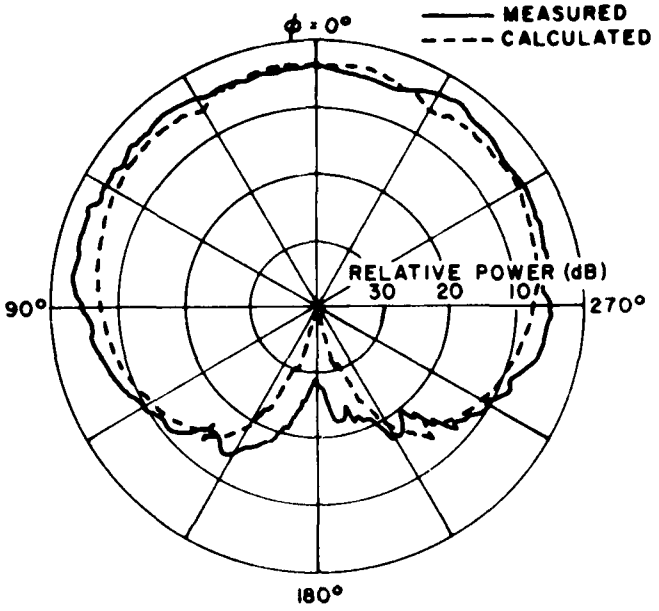

(a)

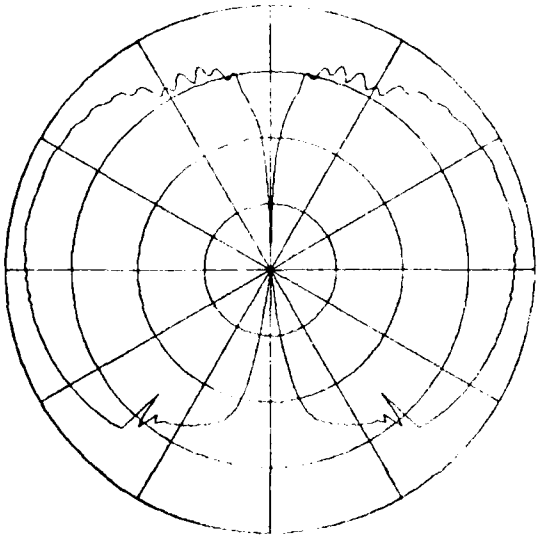

(b)

Figure 22. Azimuth plane radiation pattern (θ_p=92°)
(a) E_θ (b) E_ϕ (calculated pattern only).

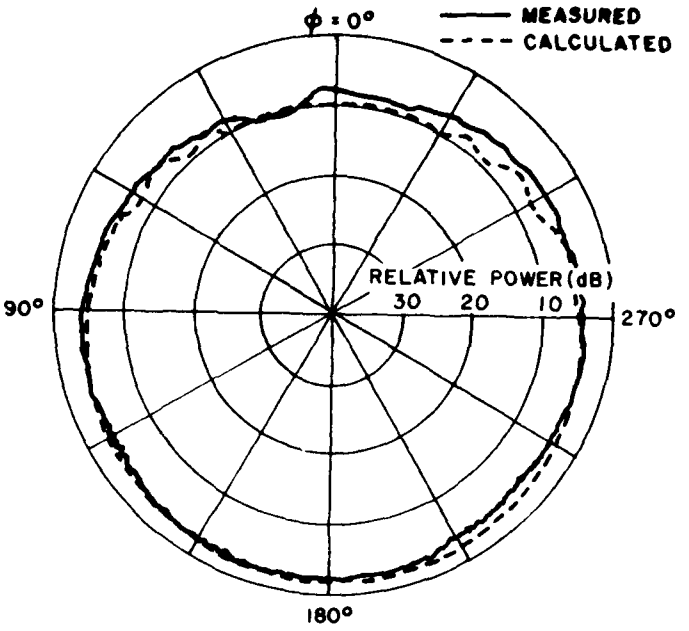

(a)

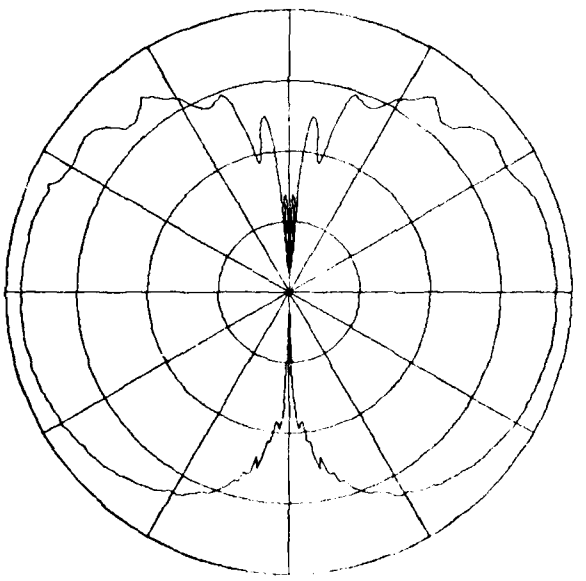

(b)

Figure 23. Azimuth plane radiation pattern (θ_p=50°)
(a) E_θ (b) E_ϕ (calculated pattern only)

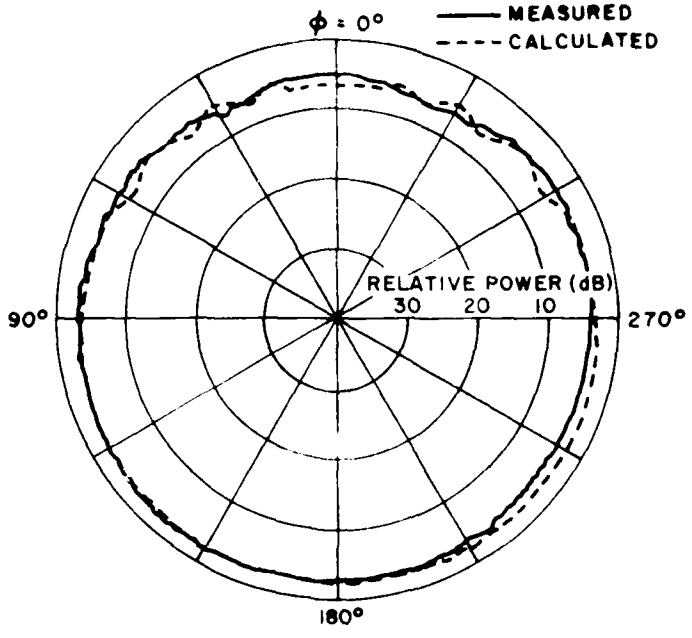

(a)

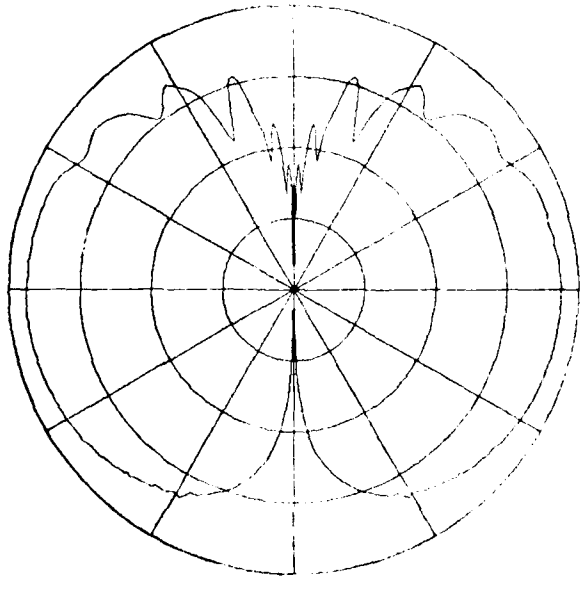

(b)

Figure 24. Azimuth plane radiation pattern (θ_p=60°)
(a) E_θ (b) E_ϕ (calculated pattern only)

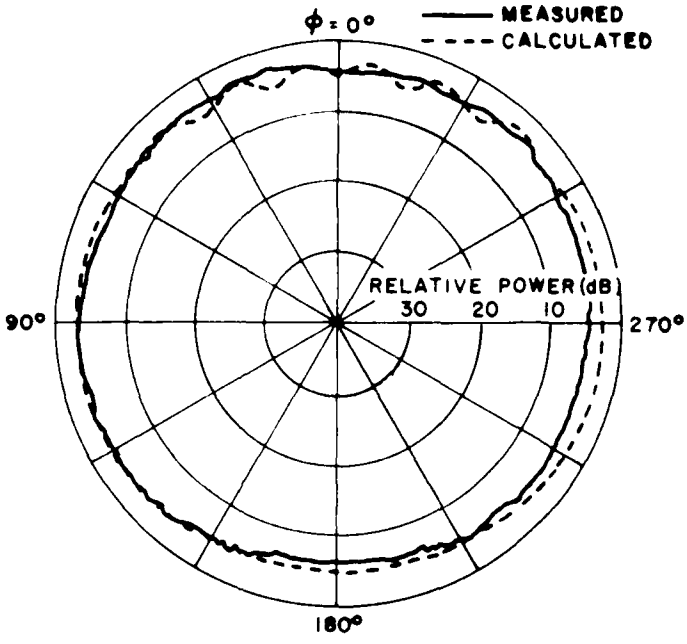

(a)

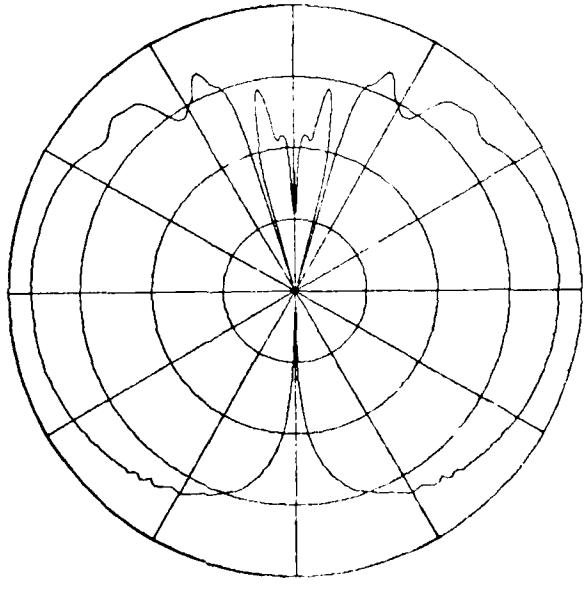

(b)

Figure 25. Azimuth plane radiation pattern (θ_p=70°)
(a) E_θ (b) E_ϕ (calculated pattern only)

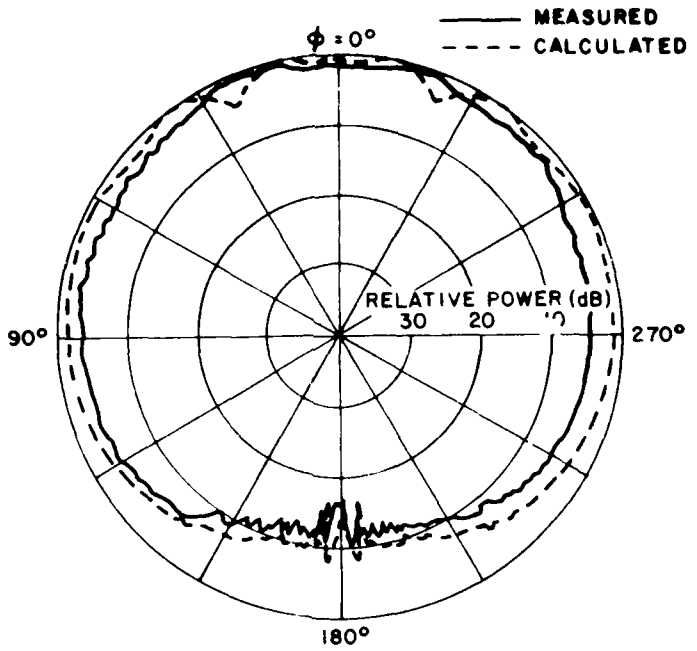

(a)

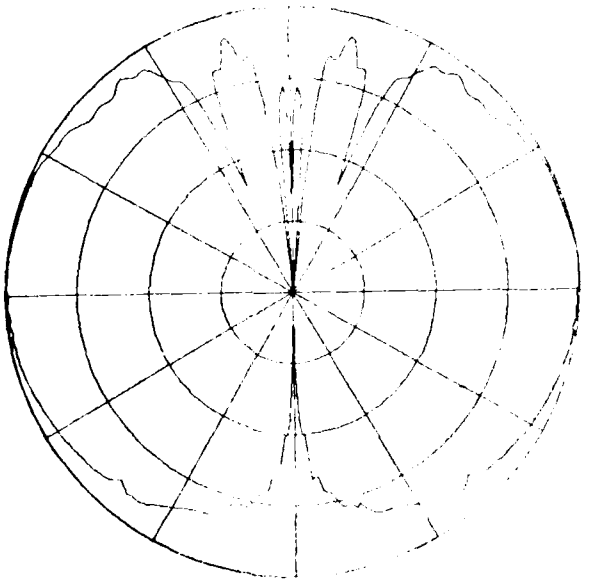

(b)

Figure 26. Azimuth plane radiation pattern (θ_p=80°)

(a) E_θ (b) E_ϕ (calculated pattern only)

AD-A130 359 GENERAL 3D AIRBORNE ANTENNA RADIATION PATTERN CODE USERS MANUAL(U) OHIO STATE UNIV COLUMBUS ELECTROSCIENCE LAB H H CHUNG ET AL. FEB 83 RADC-TR-83-39 1/2

UNCLASSIFIED F30602-79-C-0068 F/G 9/2 NL

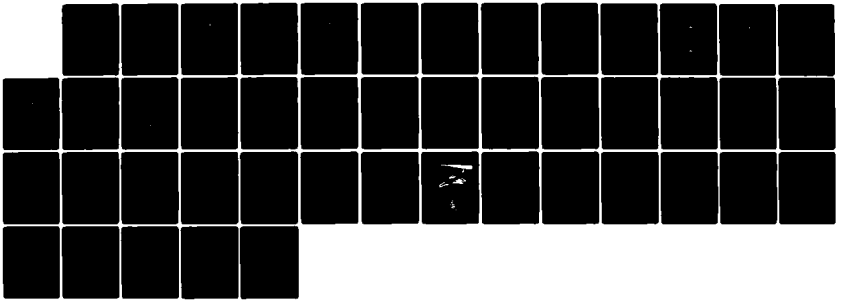

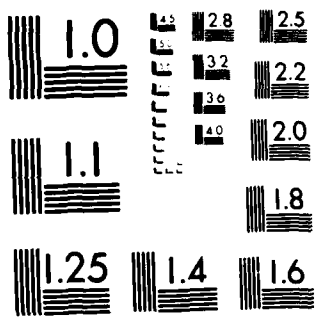

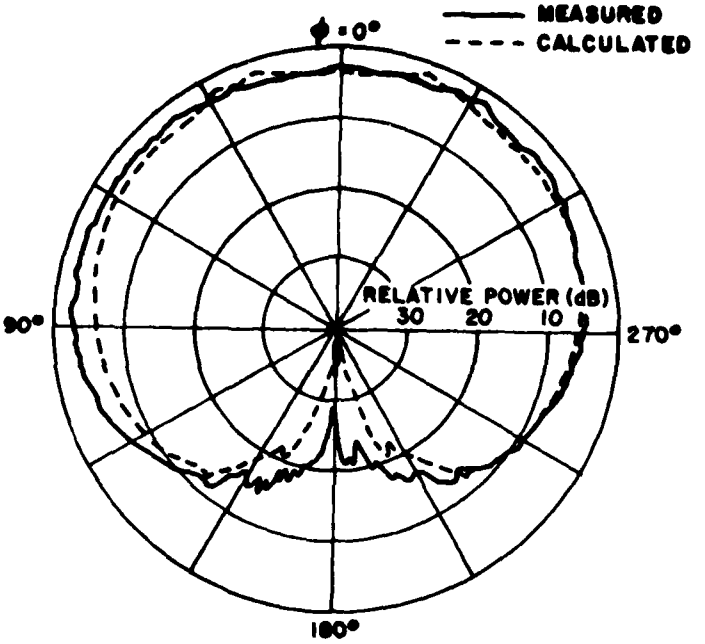

(a)

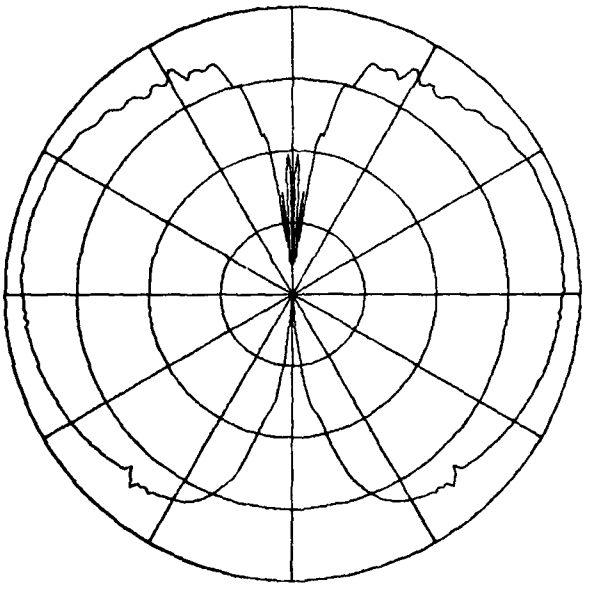

(b)

Figure 27. Azimuth plane radiation pattern (θ_p=90°)
(a) E_θ (b) E_ϕ (calculated pattern only)

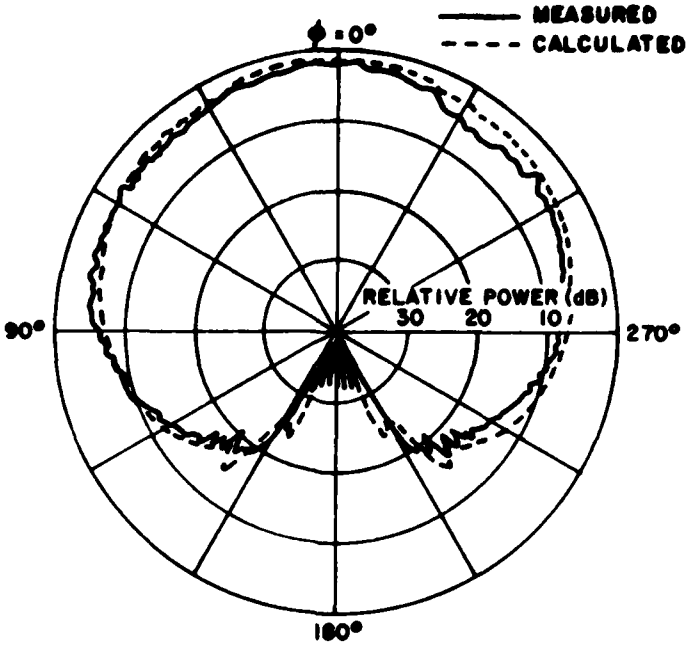

(a)

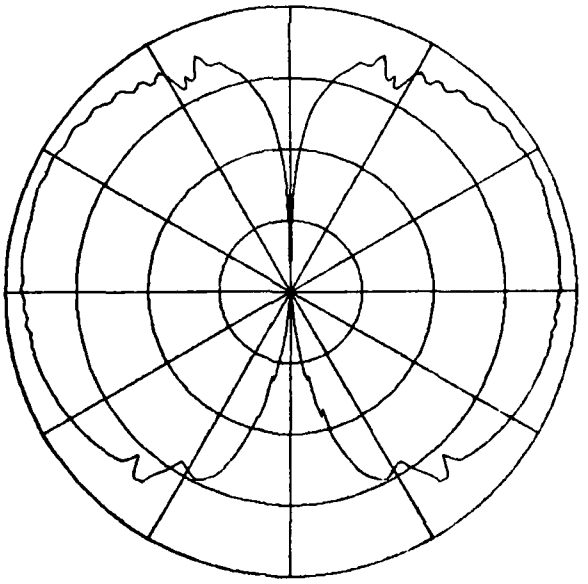

(b)

Figure 28. Azimuth plane radiation pattern (θ_p=100°)
(a) E_θ (b) E_ϕ (calculated pattern only)

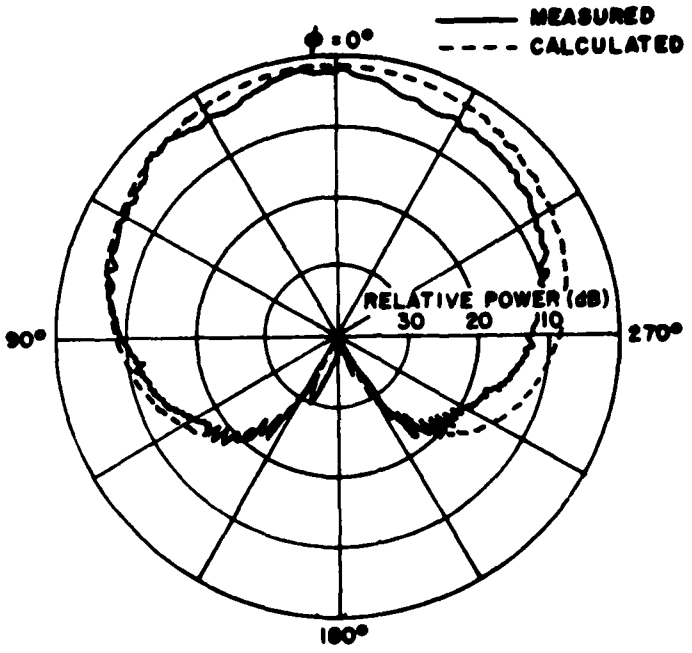

(a)

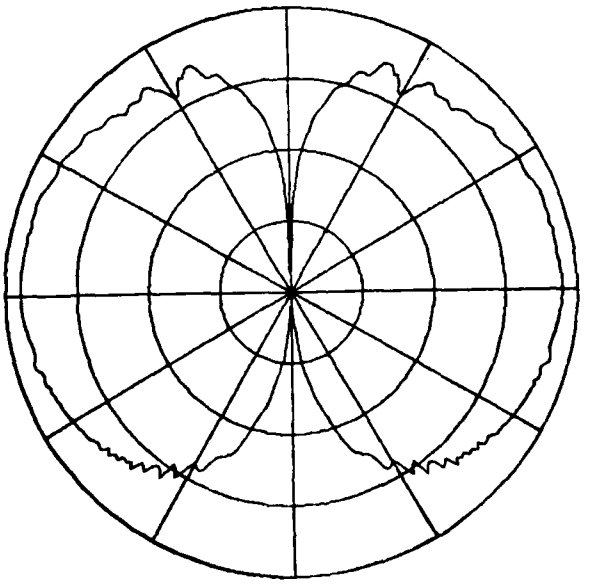

(b)

Figure 29. Azimuth plane radiation pattern (θ_p=110°)

(a) E_θ (b) E_ϕ (calculated pattern only)

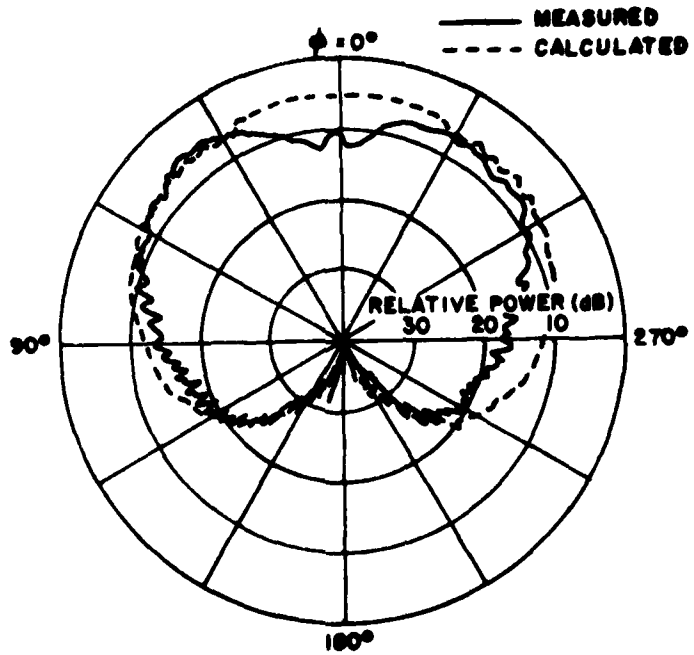

(a)

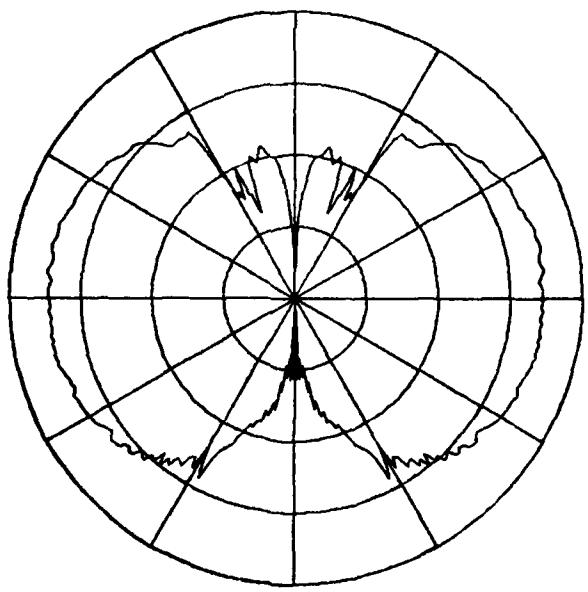

(b)

Figure 30. Azimuth plane radiation pattern (θ_p=120°)

(a) E_θ (b) E_ϕ (calculated pattern only)

Example 4: Simulation of KC-135

Consider an antenna mounted on the fuselage of KC-135. There are three different sources under study: $\lambda/4$ monopole, $.414^{\lambda} \times .828^{\lambda}$ axial slot and circumferential slot. The line drawing model of KC-135 is shown in Figure 31. The computer simulated model for antenna mounted forward of wings and over wings are shown in Figure 32 and Figure 33, respectively. The input data is as follows:

```
UN: CONVERT TO INCHES
3
FQ: 34.92GHZ
1,34.92,1.
FG: KC135 AIRCRAFT
3.,80.,8.
0.,0.,0.
PG: RIGHT WING
4,T
-1.,3.,12.31
-1.,28.5,36.41
-1.,28.5,40.41
-1.,3.,24.61
PG: LEFT WING
4,T
-1.,-3.,24.61
-1.,-28.5,40.41
-1.,-28.5,36.41
-1.,-3.,12.31
PG: VERTICAL STABILIZER
4,T
2.946,0.5,55.672
14.076,0.5,64.205
14.076,0.,58.025
2.946,0.,49.492
PG: VERTICAL STABILIZER
4,T
2.946,0.,49.492
14.076,0.,58.025
14.076,-0.5,64.205
2.946,-0.5,55.672
SG: MONOPOLE
0.,8.34
1
0.,0.
.140,.280,90.,.0845,3
1.,0.
PD: ROLL PLANE PATTERN
0.,90.,90.
0,360,1
T,1000.
PP: PEN PLOT
T
1,1.25,3
EX: EXECUTE
PD: AZIMUTH PLANE PATTERN
90.,0.,90.
0,360,1
T,1000.
PP: PEN PLOT
T
2,1.25,3
EX:
PG:NOSE
4,T
.89,-1.36,-7.35
.775,-1.36,-9.0
.87,0.,-9.0
.985,0.,-7.35
PG:NOSE
4,T
.985,0.,-7.35
.87,0.,-9.
.775,1.36,-9.0
.89,1.36,-7.35
PD: ELEVATION PLANE PATTERN
90.,90.,89.
0,360,1
T,1000.
PP: PEN PLOT
T
1,1.25,3
EX:
```

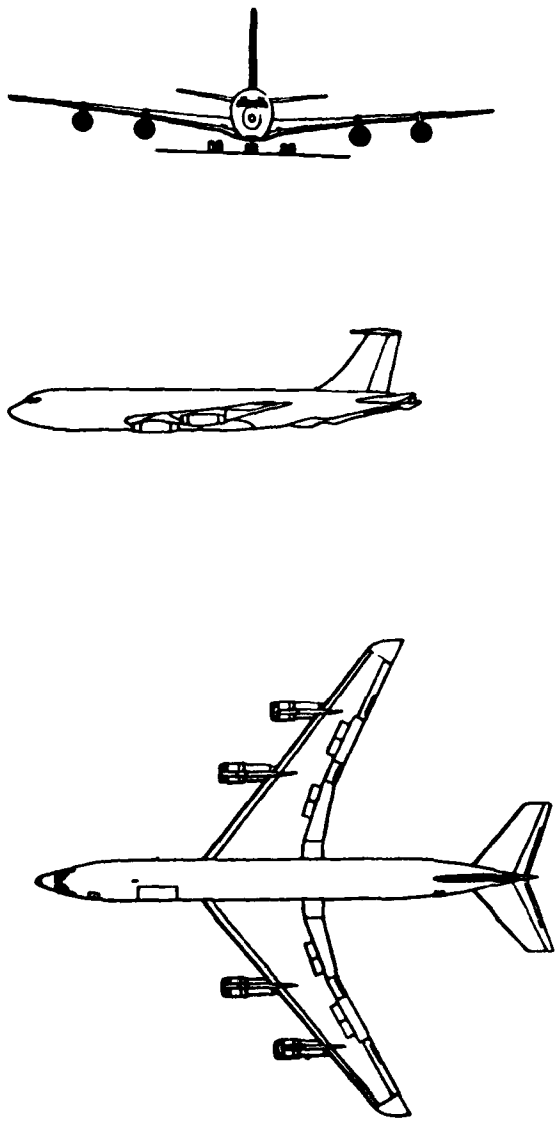

Figure 31. Line drawing model of KC-135.

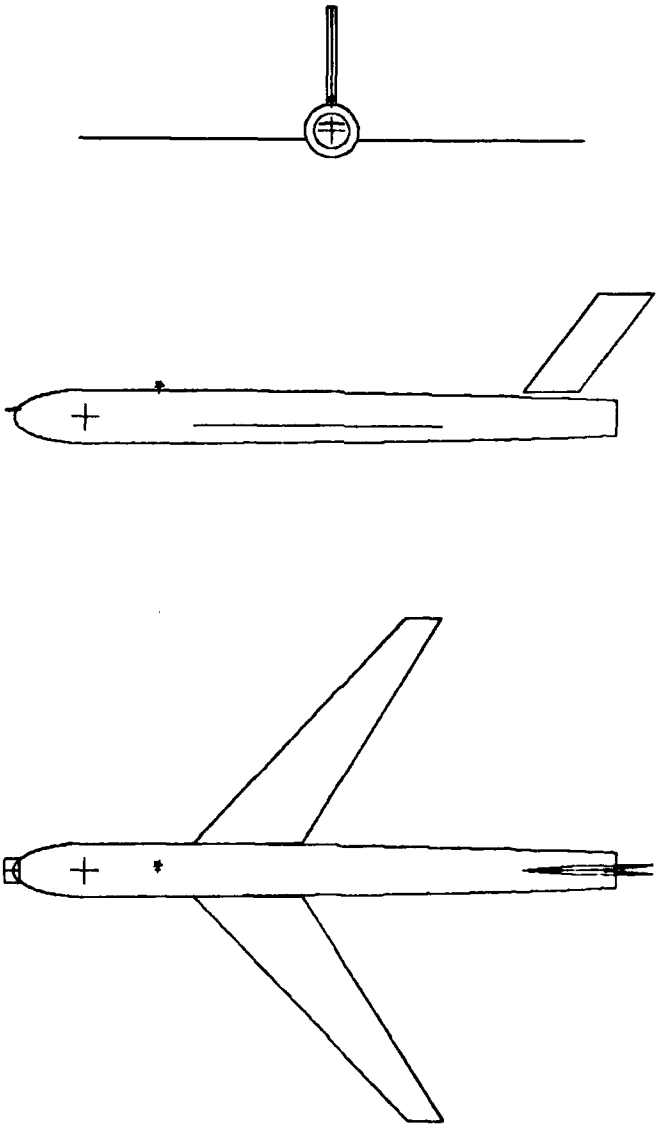

Figure 32. Computer simulated model of KC-135.
(Antenna mounted forward of wings)

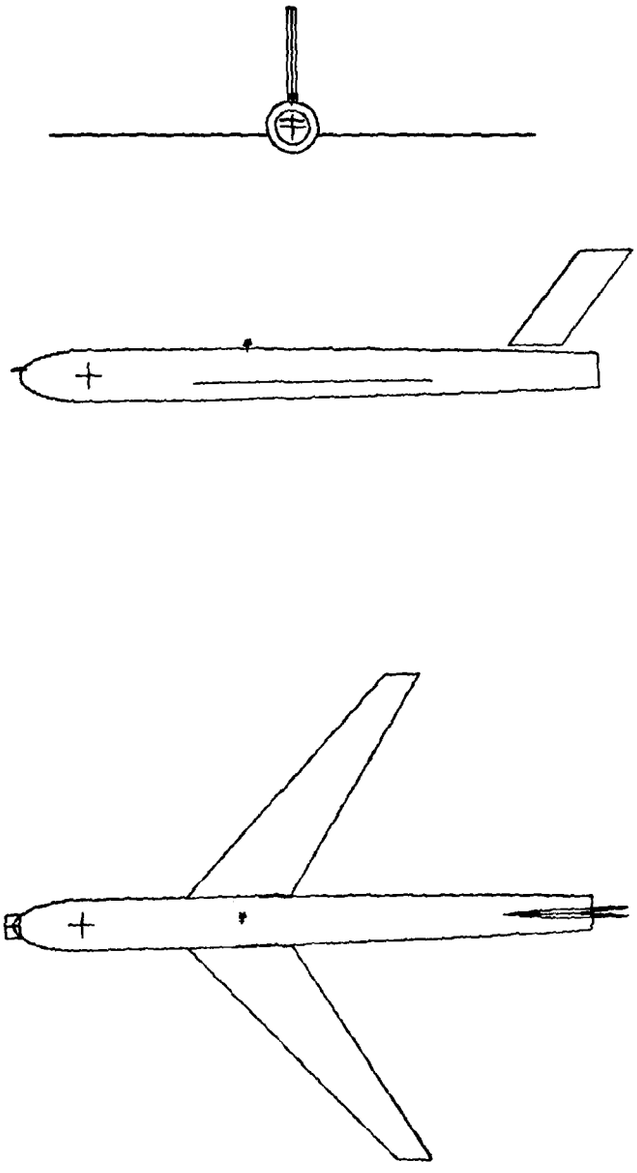

Figure 33. Computer simulated model of KC-135.

(Antenna mounted over wings)

The computed results are shown from Figure 34 to Figure 42 and found to be in very good agreement with the measurements in the roll plane and elevation planes. Measurements were not available in the azimuth plane. The experimental results were obtained in an anechoic chamber using a 1/25 scale model KC-135 aircraft at NASA (Langley, Virginia).

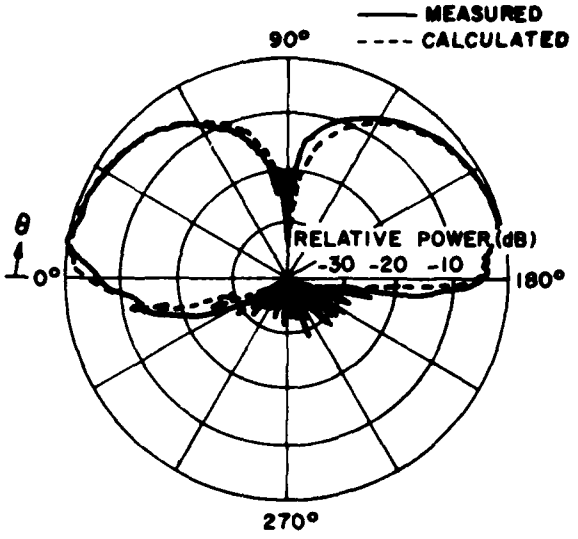

(a)

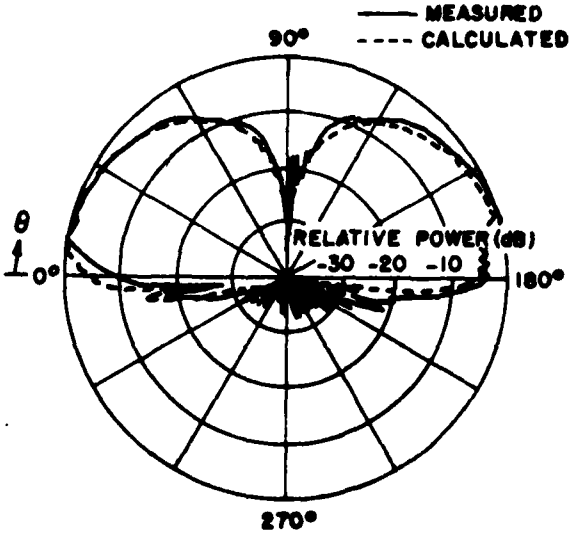

(b)

Figure 34. (a) Roll plane pattern (E_ϕ) for 1/25 scale model of KC-135 with $\lambda/4$ monopole on fuselage forward of wings at frequency of 34.92 GHz (model frequency). (b) Roll plane pattern (E_ϕ) for $\lambda/4$ monopole over wing.

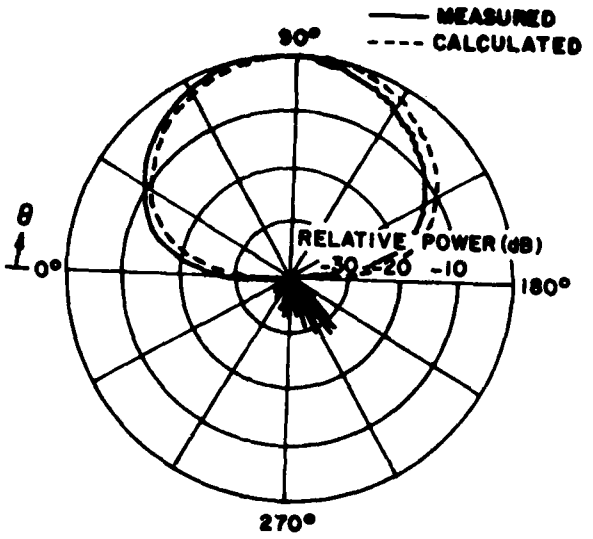

(a)

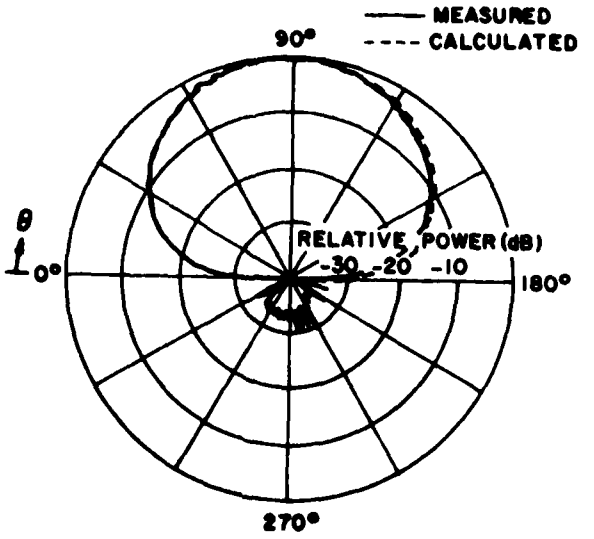

(b)

Figure 35. (a) Roll plane pattern (E_ϕ) for KA band axial waveguide forward of wings. (b) Roll plane pattern (E_ϕ) for KA band axial waveguide over wings.

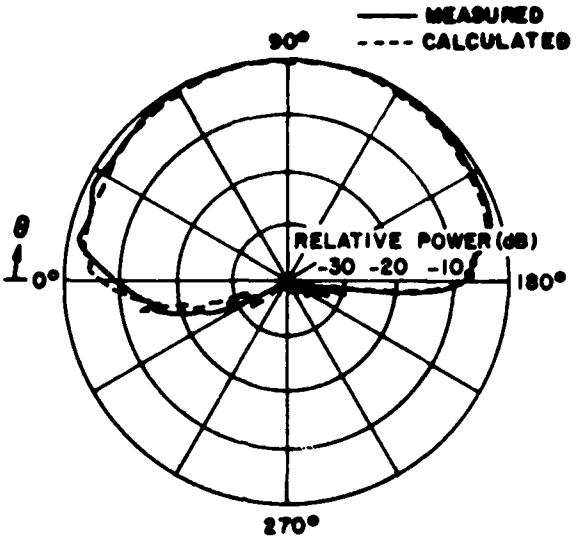

(a)

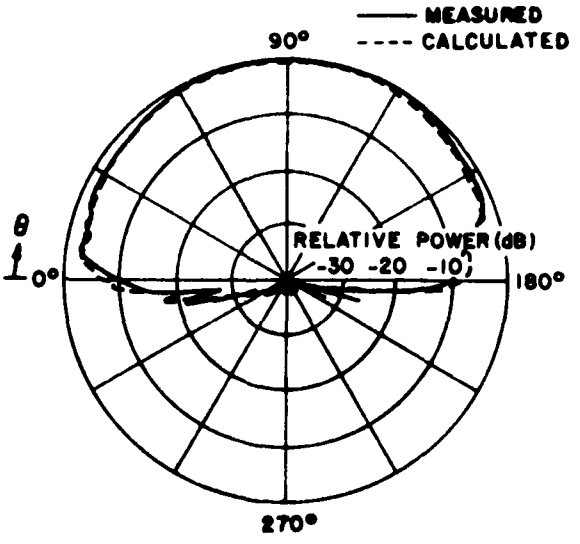

(b)

Figure 36. (a) Roll plane pattern (E_θ) for KA band circumferential waveguide forward of wings. (b) Roll plane pattern (E_θ) for KA band circumferential waveguide over wings.

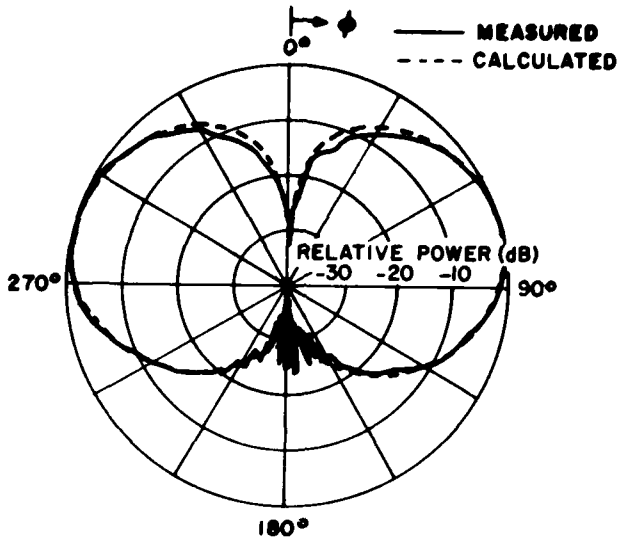

(a)

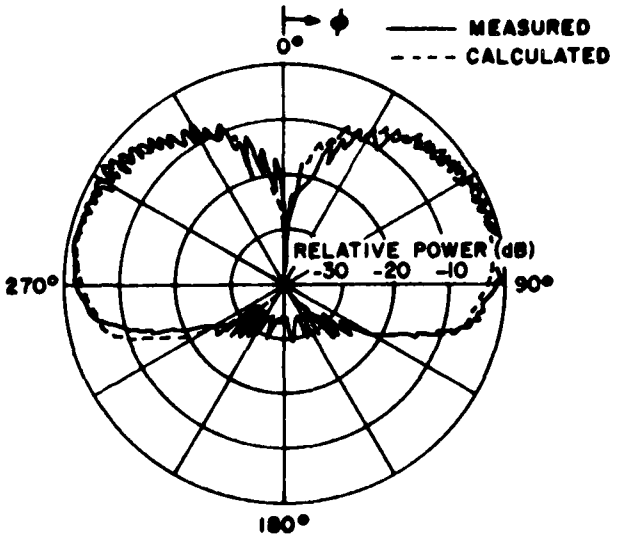

(b)

Figure 37. (a) Elevation plane pattern for λ/4 monopole mounted forward of wings on KC-135 aircraft. (b) Elevation plane pattern for λ/4 monopole mounted over wings on KC-135 aircraft.

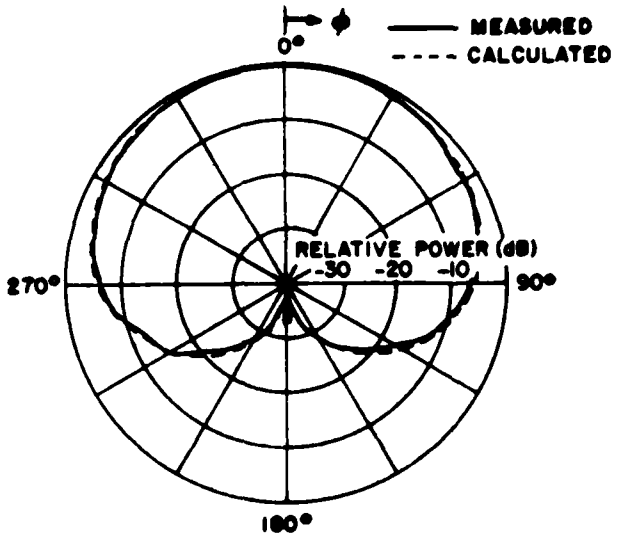

(a)

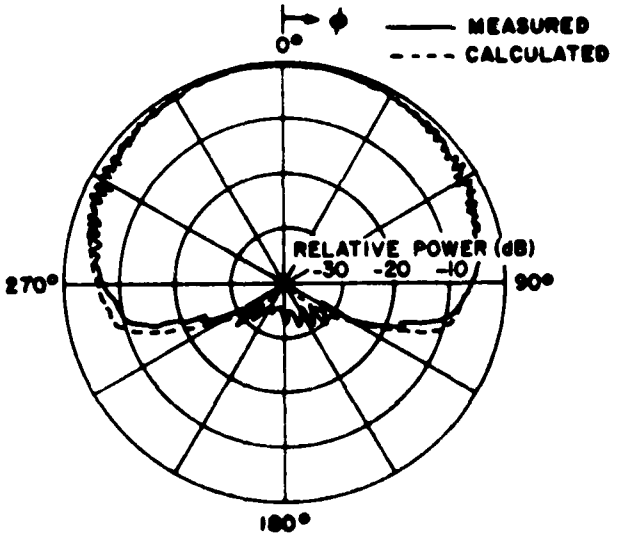

(b)

Figure 38. (a) Elevation plane pattern for axial KA band waveguide mounted forward of wings on KC-135 aircraft. (b) Elevation plane pattern for axial KA band waveguide mounted over wings on KC-135 aircraft.

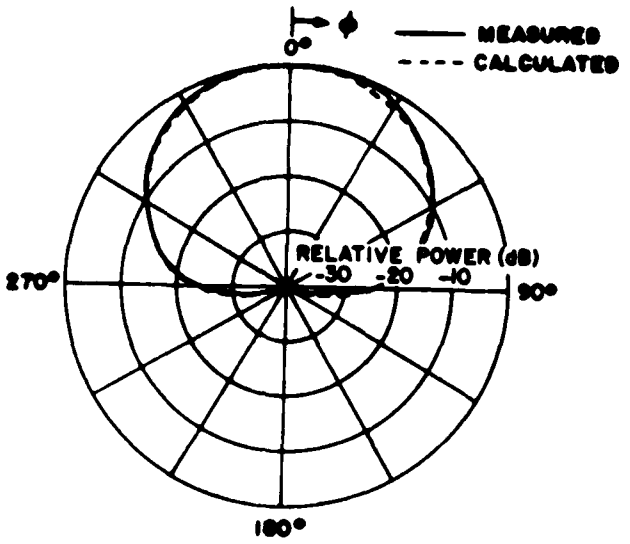

(a)

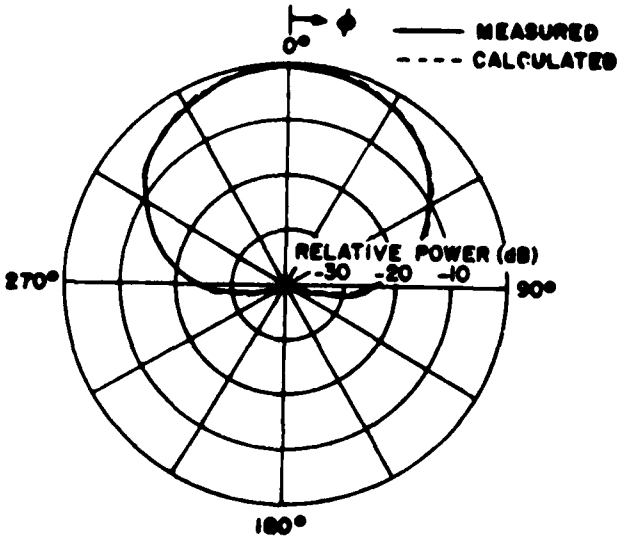

(b)

Figure 39. (a) Elevation plane pattern for circumferential KA band waveguide mounted forward of wings on KC-135 aircraft. (b) Elevation plane pattern for circumferential KA band waveguide mounted over wings on KC-135 aircraft.

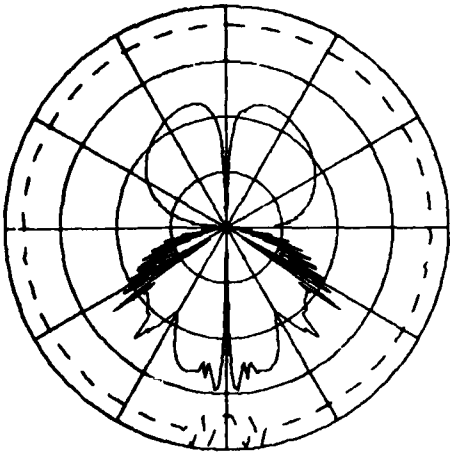

(a)

——— E_ϕ

----- E_θ

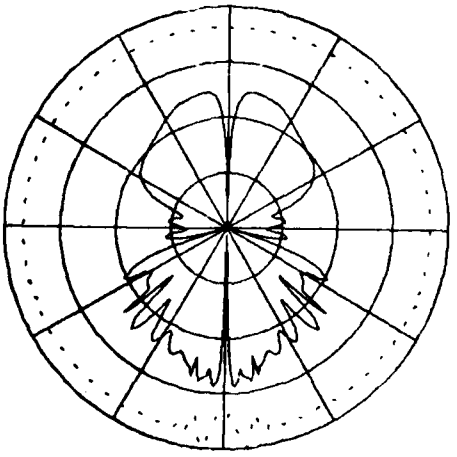

(b)

Figure 40. Azimuth plane pattern for λ/4 monopole mounted (a) forward of wings (b) over wings.

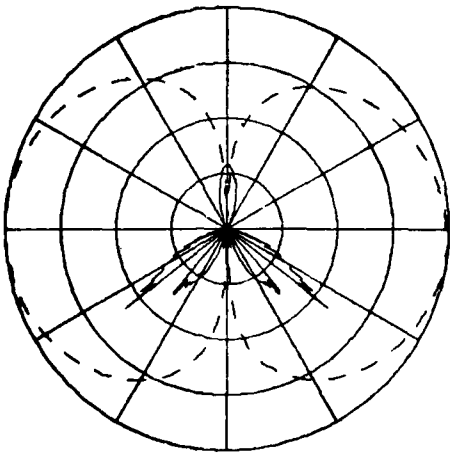

——— E_ϕ

(a)

----- E_θ

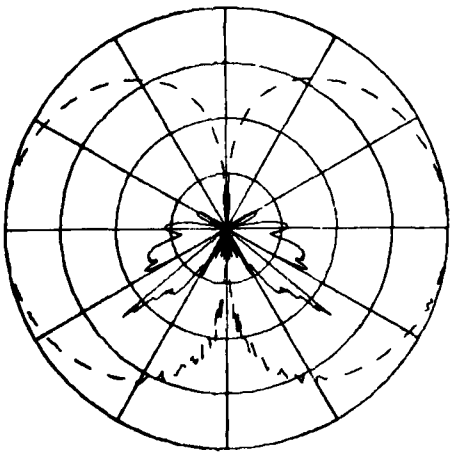

(b)

Figure 41. Azimuth plane pattern for KA band axial slot mounted (a) forward of wings (b) over wings.

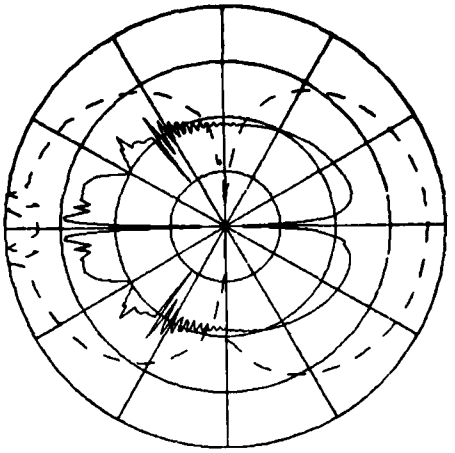

——— E_ϕ

(a)

----- E_θ

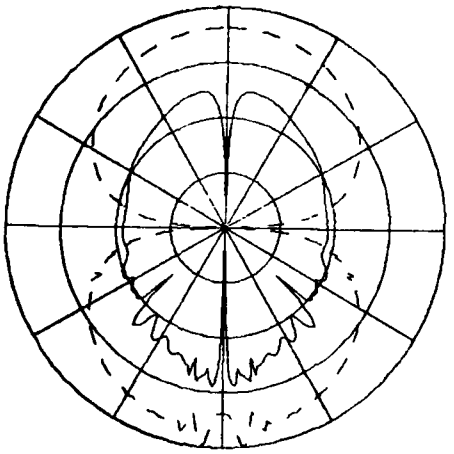

(b)

Figure 42. Azimuth plane pattern for KA band circumferential slot mounted (a) forward of wings (b) over wings.

Example 5: Simulation of Lindberg Antenna mounted on KC-135

Consider a Lindberg Antenna (cross slot, 90° phase difference between two slots) mounted on the fuselage of a KC-135. The slot size is $.39^{\lambda}$ x $.78^{\lambda}$ and operating at a frequency of 6.25 GHz. The line drawing is shown in Figure 43, and the computer simulated model is shown in Figure 44. The input data is as follows:

```
UN: CONVERT TO INCHES
3
FQ: 6.25 GHZ
1,6.25,1.
FG: KC135 AIRCRAFT
3.,80.,8.
0.,0.,0.
PG: RIGHT WING
4,T
-1.,3.,12.31
-1.,28.5,36.41
-1.,28.5,40.41
-1.,3.,24.61
PG: LEFT WING
4,T
-1.,-3.,24.61
-1.,-28.5,40.41
-1.,-28.5,36.41
-1.,-3.,12.31
PG: VERTICAL STABILIZER
4,T
2.946,0.5,55.672
14.076,0.5,64.205
14.076,0.,58.025
2.946,0.,49.492
PG: VERTICAL STABILIZER
4,T
2.946,0.,49.492
14.076,0.,58.025
14.076,-0.5,64.205
2.946,-0.5,55.672
PG:NOSE
4,T
.89,-1.36,-7.35
.775,-1.36,-9.0
.87,0.,-9.0
.985,0.,-7.35
PG:NOSE
4,T
.985,0.,-7.35
.87,0.,-9.
.775,1.36,-9.0
.89,1.36,-7.35
SG: CROSS SLOT
0.,2.25
2
0.,0.
.7375,1.475,0.,.0845,1
1.,0.
0.,0.
.7375,1.475,90.,.0845,1
1.,90.
PD: ROLL PLANE PATTERN
0.,90.,90.

0,360,1
T,1000.
PP: PEN PLOT
T
1,1.5,3
EX:
PD: AZIMUTH PLANE PATTERN
90.,0.,90.
0,360,1
T,1000.
EX:
PD: ELEVATION PLANE PATTERN
90.,90.,89.
0,360,1
T,1000.
EX:
```

```
PD: AZIMUTH PLANE PATTERN
90.,0.,70.
0,360,1
T,1000.
EX:
PD: AZIMUTH PLANE PATTERN
90.,0.,80.
0,360,1

T,1000.
EX:
PD: AZIMUTH PLANE PATTERN
90.,0.,100.
0,360,1
T,1000.
EX:
PD: AZIMUTH PLANE PATTERN
90.,0.,110.
0,360,1
T,1000.
EX:
PD: AZIMUTH PLANE PATTERN
90.,0.,120.
0,360,1
T,1000.
EX:
```

The computation results are show from Figure 45 to Figure 52. There are no measurement data available.

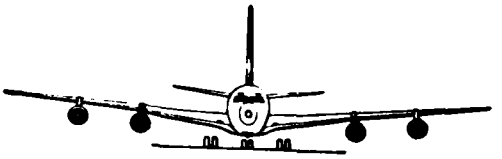

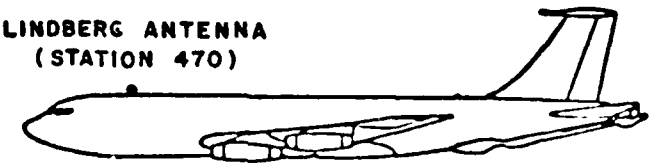

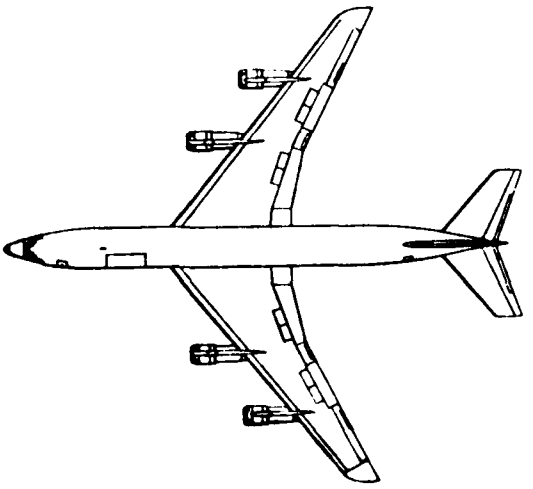

Figure 43. Line drawing for Lindberg Antenna mounted on KC-135.

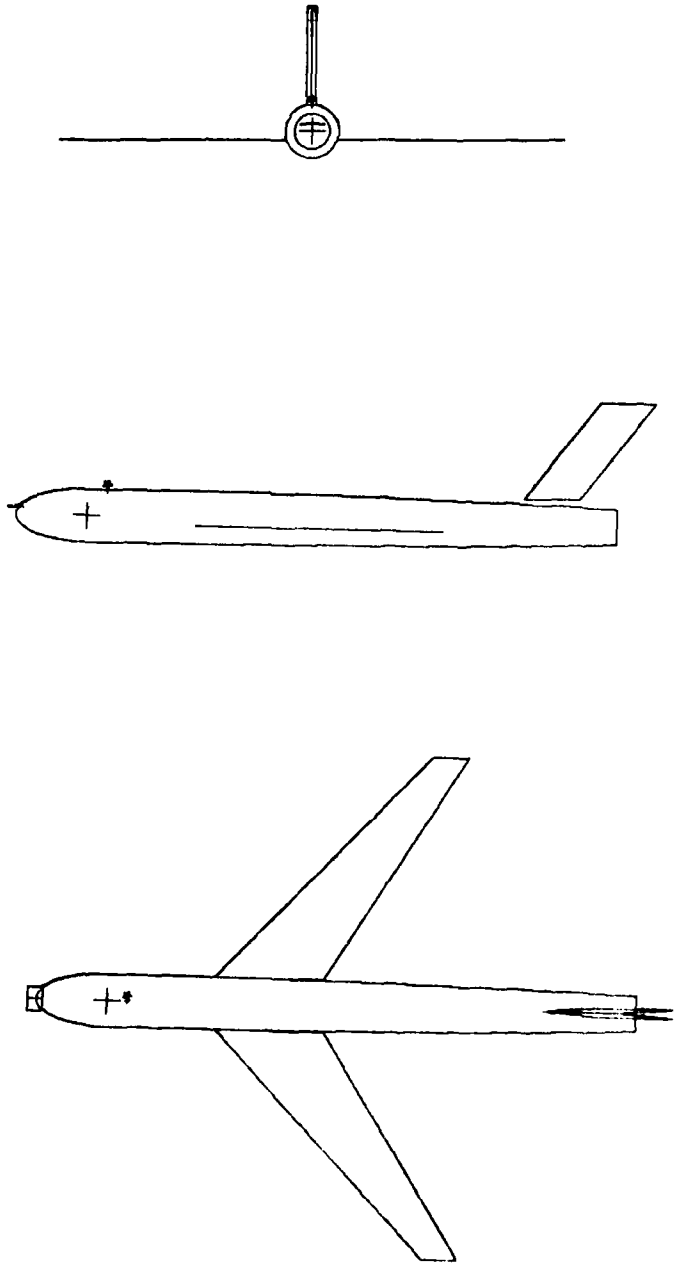

Figure 44. Computer simulated model for Lindberg Antenna mounted on KC-135.

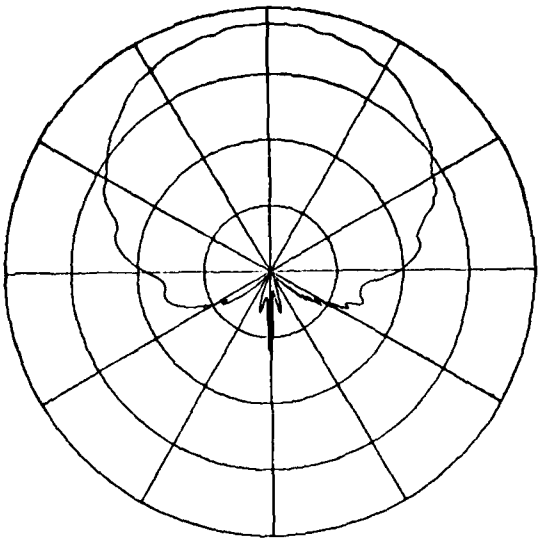

(a)

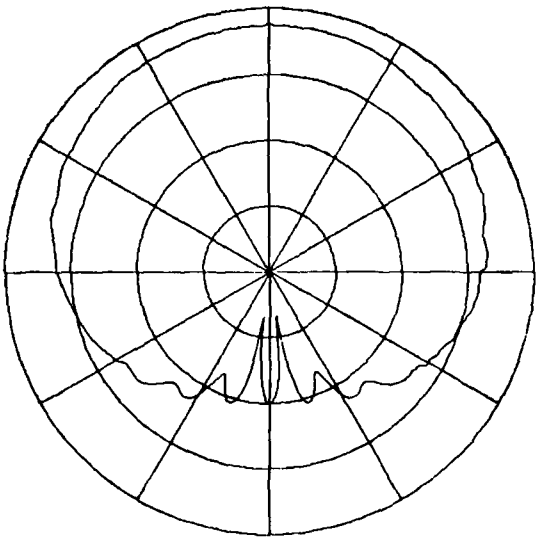

(b)

Figure 45. Roll plane pattern for Lindberg Antenna mounted on KC-135 (a) E_θ (b) E_ϕ

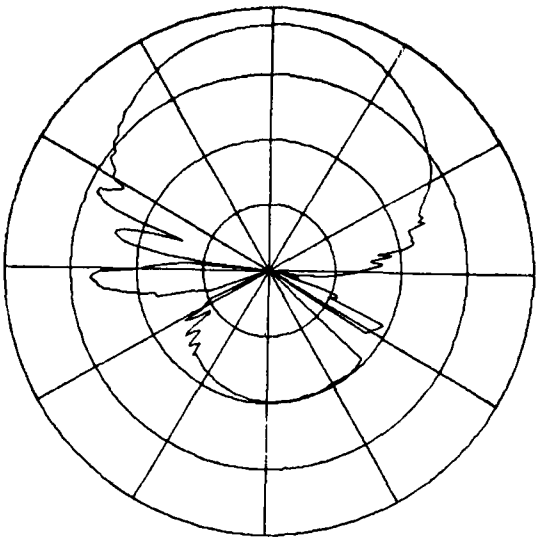

(a)

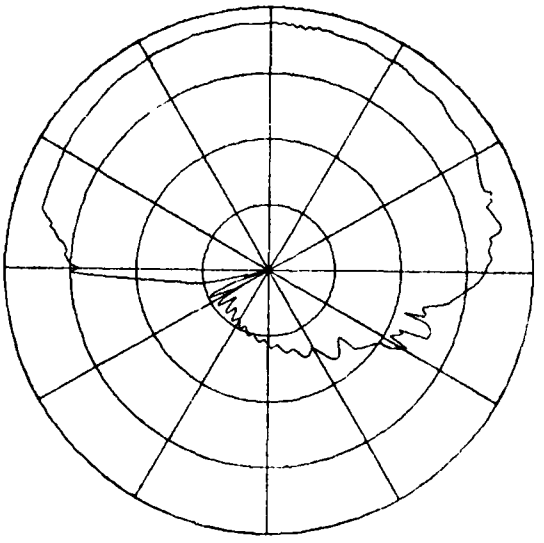

(b)

Figure 46. Elevation plane pattern for Lindberg Antenna mounted on KC-135 (a) E_θ (b) E_ϕ

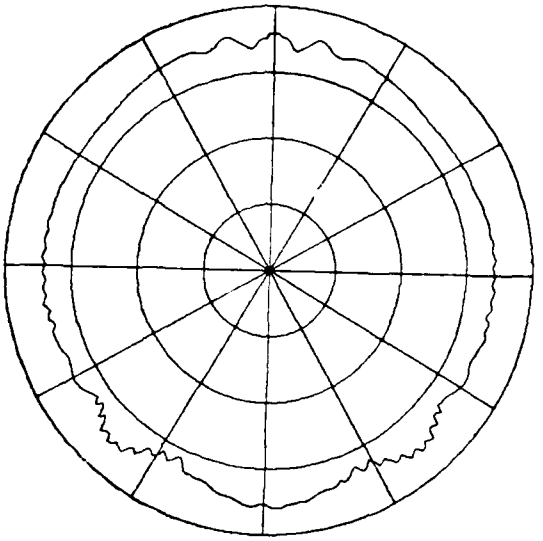

(a)

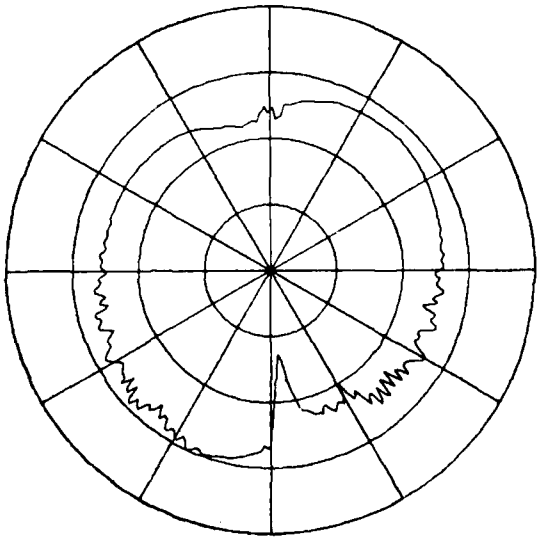

(b)

Figure 47. Azimuth plane (θ_p=70°) pattern for Lindberg Antenna mounted on KC-135 (a) E_θ (b) E_ϕ

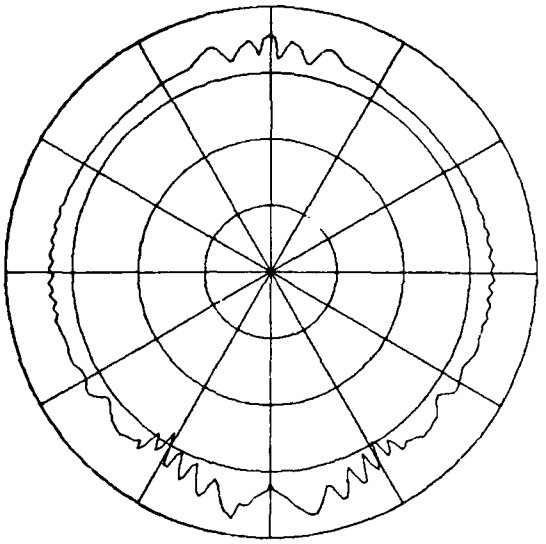

(a)

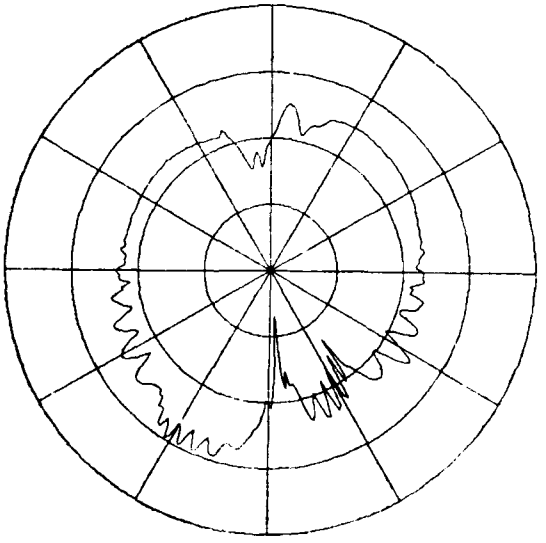

(b)

Figure 48. Azimuth plane (θ_p=80°) pattern for Lindberg Antenna mounted on KC-135 (a) E_θ (b) E_ϕ

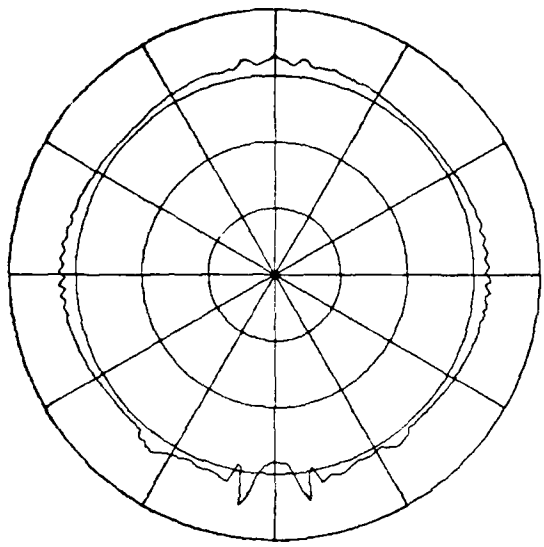

(a)

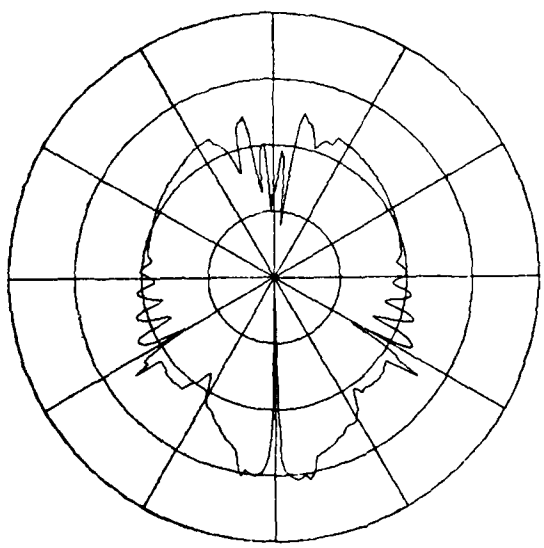

(b)

Figure 49. Azimuth plane (θ_p=90°) pattern for Lindberg Antenna mounted on KC-135 (a) E_θ (b) E_ϕ

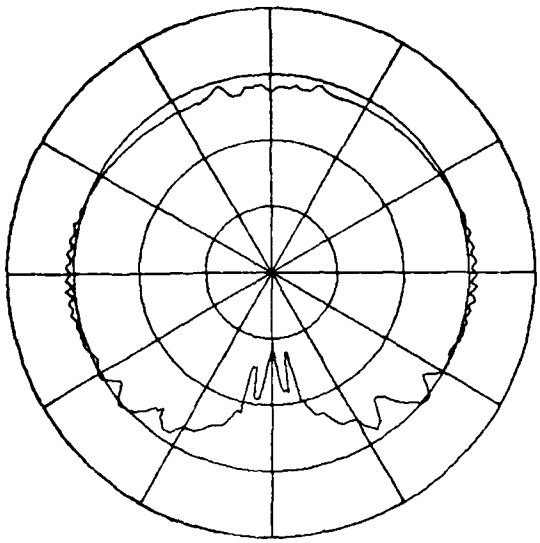

(a)

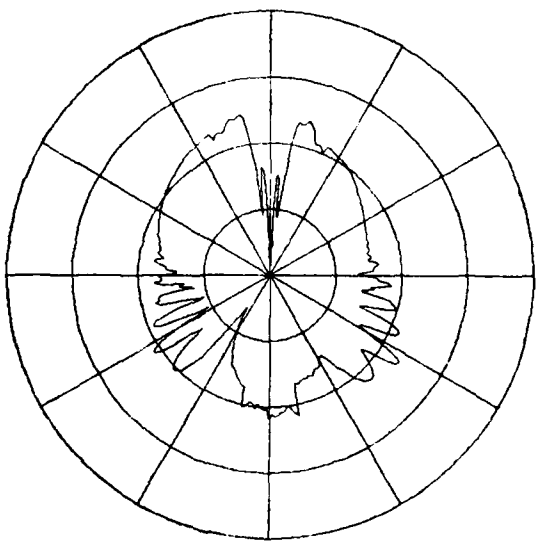

(b)

Figure 50. Azimuth plane (θ_p=100°) pattern for Lindberg Antenna mounted on KC-135 (a) E_θ (b) E_ϕ

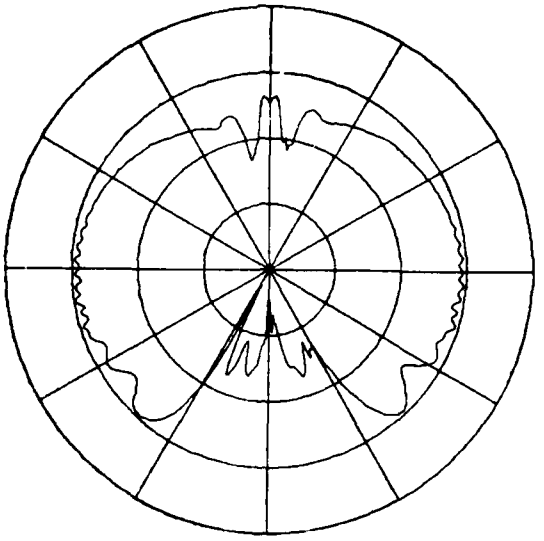

(a)

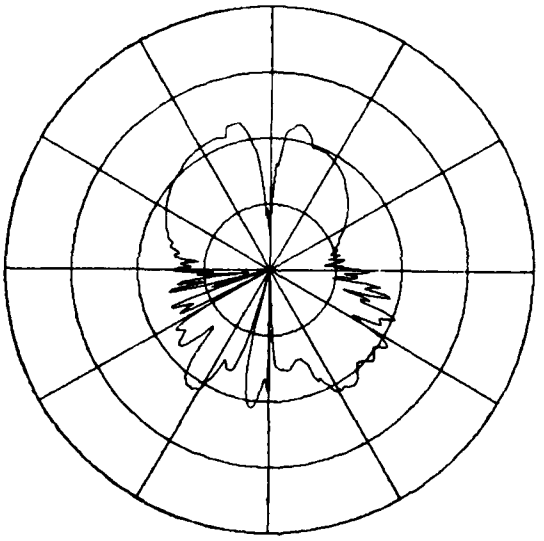

(b)

Figure 51. Azimuth plane (θ_p=110°) pattern for Lindberg Antenna mounted on KC-135 (a) E_θ (b) E_ϕ

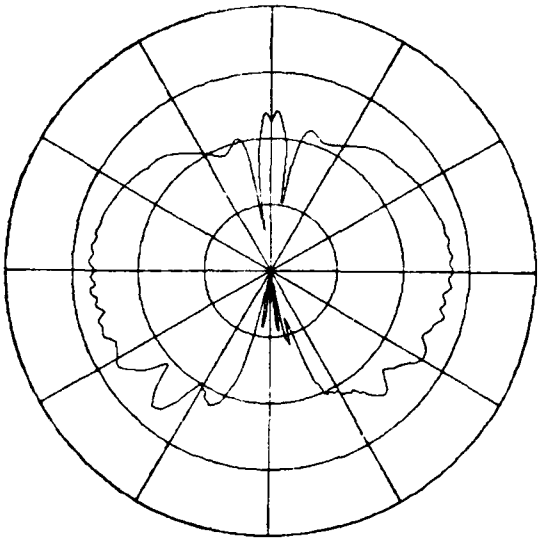

(a)

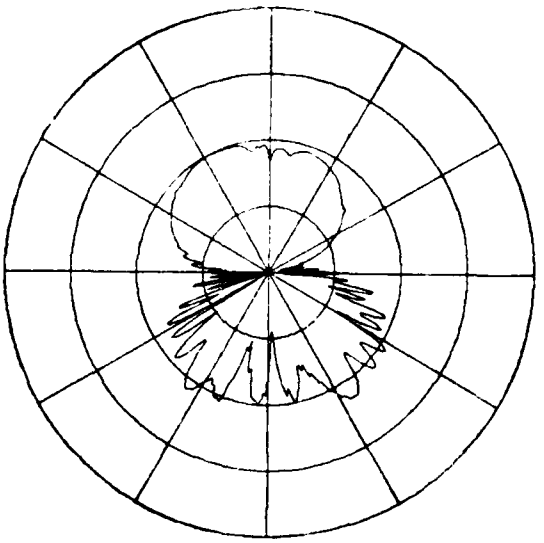

(b)

Figure 52. Azimuth plane (θ_p=120°) pattern for Lindberg Antenna mounted on KC-135 (a) E_θ (b) E_ϕ

Example 6: Simulation of F-16 Fighter Aircraft

Consider a quarter-wavelength monopole mounted on the fuselage and operating at a frequency of 0.96 GHz. A photograph of the F-16 aircraft is shown in Figure 53; whereas, the line drawings are shown in Figure 54. Our computer simulated model of the F-16 is shown in Figure 55. Note that a composite prolate spheroid is used to represent the fuselage, and a total of fourteen plates are used to model the rest of the structure. The input data is as follows:

```
UN:IN INCHES
3
FG:F16A FUSELAGE GEOMETRY AT STATION 250
24.,400.,250.
0.,0.,0.
FQ:FREQUENCY
1,0.96,1.
SG:SOURCE GEOMETRY
0.,13.25
1
0.,0.
0.,0.,0.,3.0758,3
1.,0.
PG:CURVATURE SIMULATED PLATE #1 ON POS. SIDE
6,T
8.2046,22.4421,-61.
2.1418,36.5,-61.
-4.0866,50.942,-8.6
-5.4054,54.,8.743
-5.4054,54.,158.95
8.2046,22.4421,158.95
PG:CURVATURE SIMULATED PLATE #2 ON POS. SIDE
5,T
8.2046,22.4421,158.95
-5.4054,54.,158.95
-6.2805,54.,209.084
-7.6944,54.,290.084
5.9156,22.4421,290.084
```

```
PG:CURVATURE SIMULATE PLATE #3 ON POS. SIDE
3,T
0.5,19.2,-150.
2.1418,36.5,-61.
8.2046,22.4421,-61.
PG:WING ON POS. SIDE
4,F
-5.4054,54.,8.743
-5.4054,180.,114.47
-5.4054,180.,158.95
-5.4054,54.,158.95
PG:HORIZONTAL STABILIZER ON POS. SIDE
4,F
-5.4054,54.,219.7958
-5.4054,109.101,266.031
-5.4054,109.101,290.084
-5.4054,54.,290.084
PG:VERTICAL STABILIZER ON NEG. SIDE
4,T
20.,0.,160.
120.,0.,261.
120.,-3.6,300.
18.2,-6.94,234.
PG:VERTICAL STABILIZER ON POS. SIDE
4,T
18.2,6.94,234.
120.,3.6,300.
120.,0.,261.
20.,0.,160.
PG:COCKPIT SIMULATED PLATE
3,T
16.955,-15.3846,-75.
27.8846,0.,-25.
24.,0.,0.
PG:COCKPIT SIMULATED PLATE
3,T
24.,0.,0.
27.8846,0.,-25.
16.955,15.3846,-75.
PG:CURVATURE SIMULATED PLATE #1 ON NEGATIVE SIDE
6,T
8.2046,-22.4421,158.95
-5.4054,-54.,158.95
-5.4054,-54.,8.743
-4.0866,-50.942,-8.6
2.1418,-36.5,-61.
8.2046,-22.4421,-61.
```

```
PG:CURVATURE SIMULATED PLATE #2 ON NEG. SIDE
5,T
5.9156,-22.4421,290.084
-7.6944,-54.,290.084
-6.2805,-54.,209.084
-5.4054,-54.,158.95
8.2046,-22.4421,158.95
PG:CURVATURE SIMULATED PLATE #3 ON NEG. SIDE
3,T
8.2046,-22.4421,-61.
2.1418,-36.5,-61.
0.5,-19.2,-150.
PG:WING ON NEG. SIDE
4,F
-5.4054,-54.,158.95
-5.4054,-180.,158.95
-5.4054,-180.,114.47
-5.4054,-54.,8.743
PG:HORIZONTAL STABILIZER ON NEG. SIDE
4,F
-5.4054,-54.,290.084
-5.4054,-109.101,290.084
-5.4054,-109.101,266.031
-5.4054,-54.,219.7958
PP:POLAR PLOT IN DB
T
1,3.5,3
PD:ELEVATION PLANE CUT
90.,90.,89.8
0,360,1
T,50000.
PI:
9
EX:
PD:ROLL PLANE CUT
0.,0.,90.
0,180,1
T,50000.
TO:
F,F,F
T,T
T,T,T,F,T,T,T,T
1,9,1
2,6,1
1,5,1
1,3,2
1,4,1
1,4,1
1,4,1
1,4,1
2,3,1
1,3,2
DD:
5
1,6,1,3
1,6,4,1
1,6,4,4
4,1,1,6
4,4,1,6
RD:
1
1,4
EX:EXECUTE
PD:AZIMUTH PLANE CUT
90.,0.,89.8
0,180,1
T,50000.
EX:
```

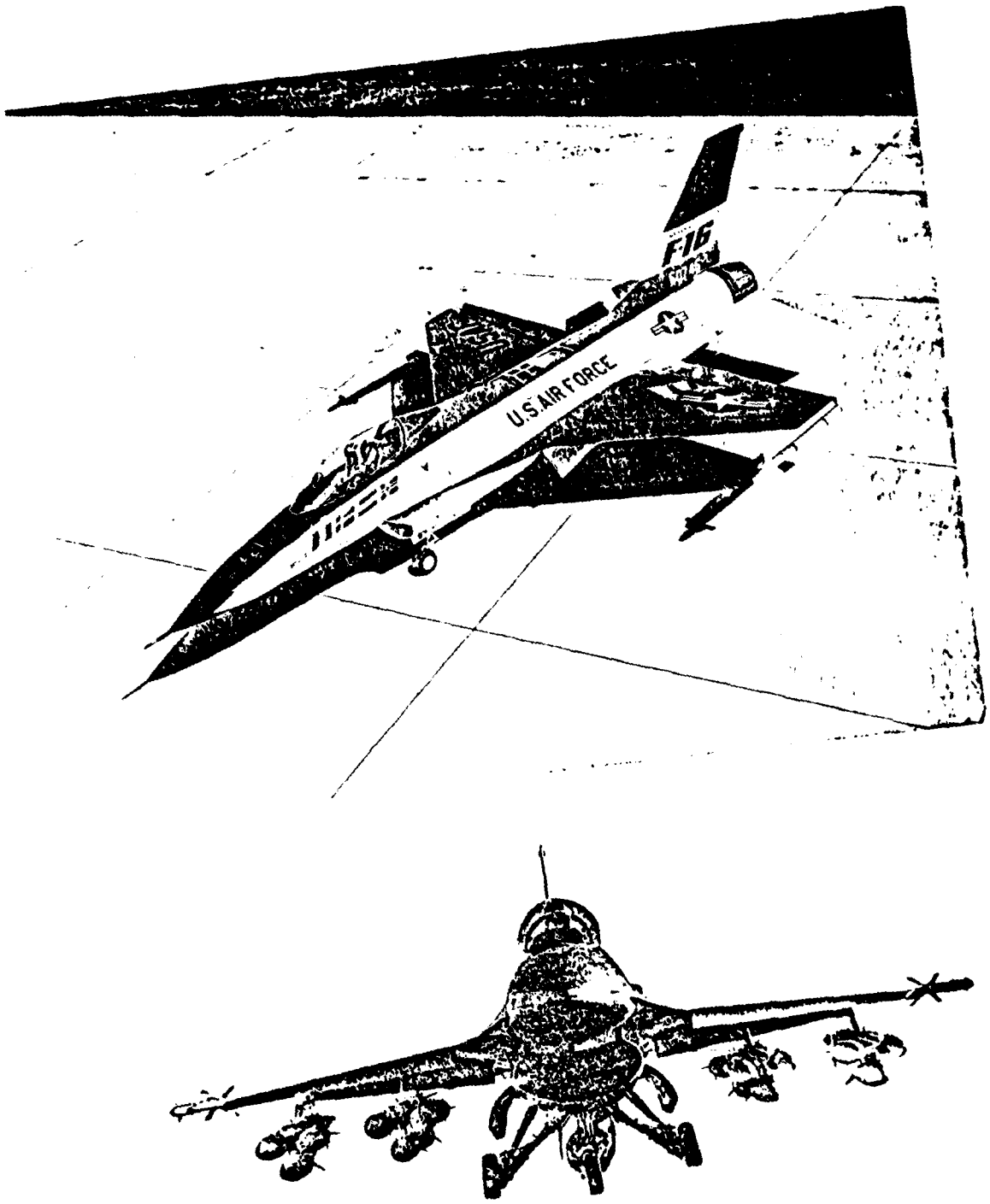

Figure 53. F-16 Fighter.

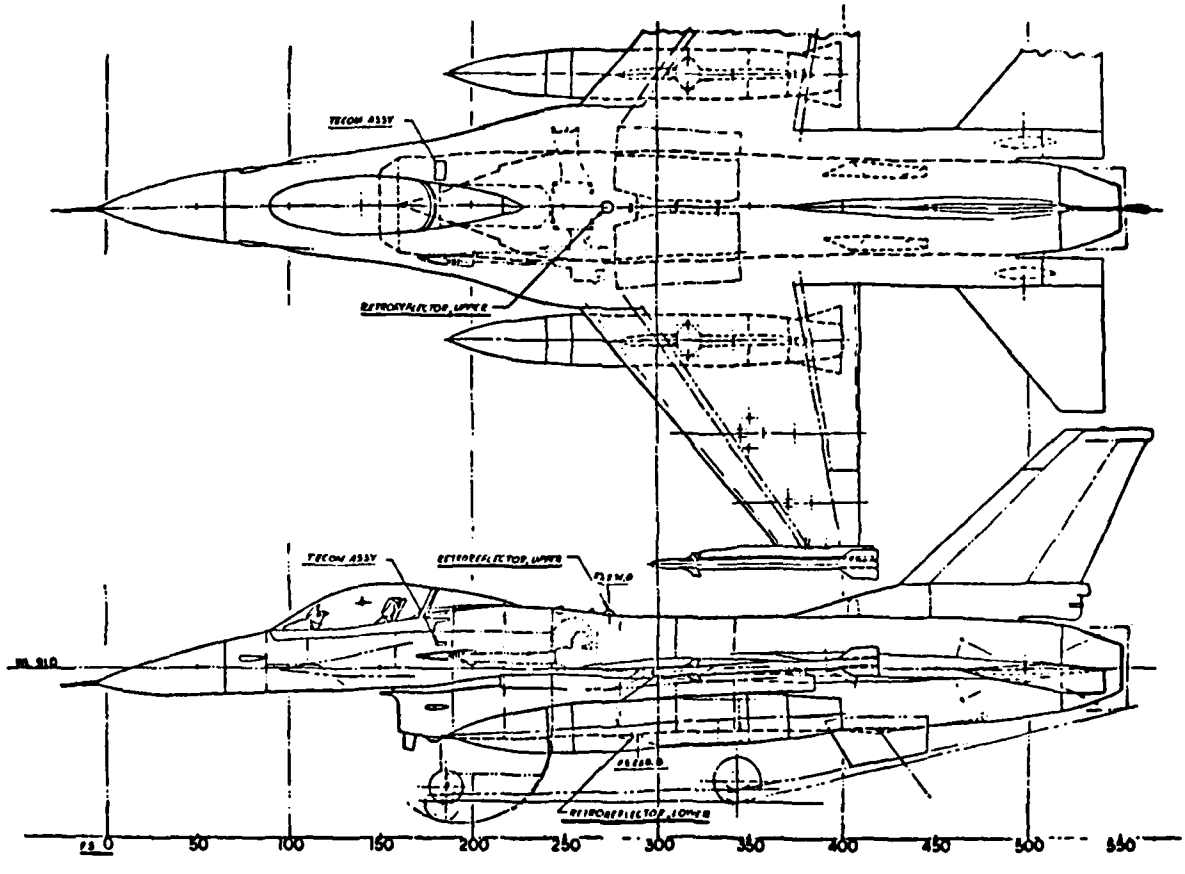

Figure 54. F-16 Line Drawing.

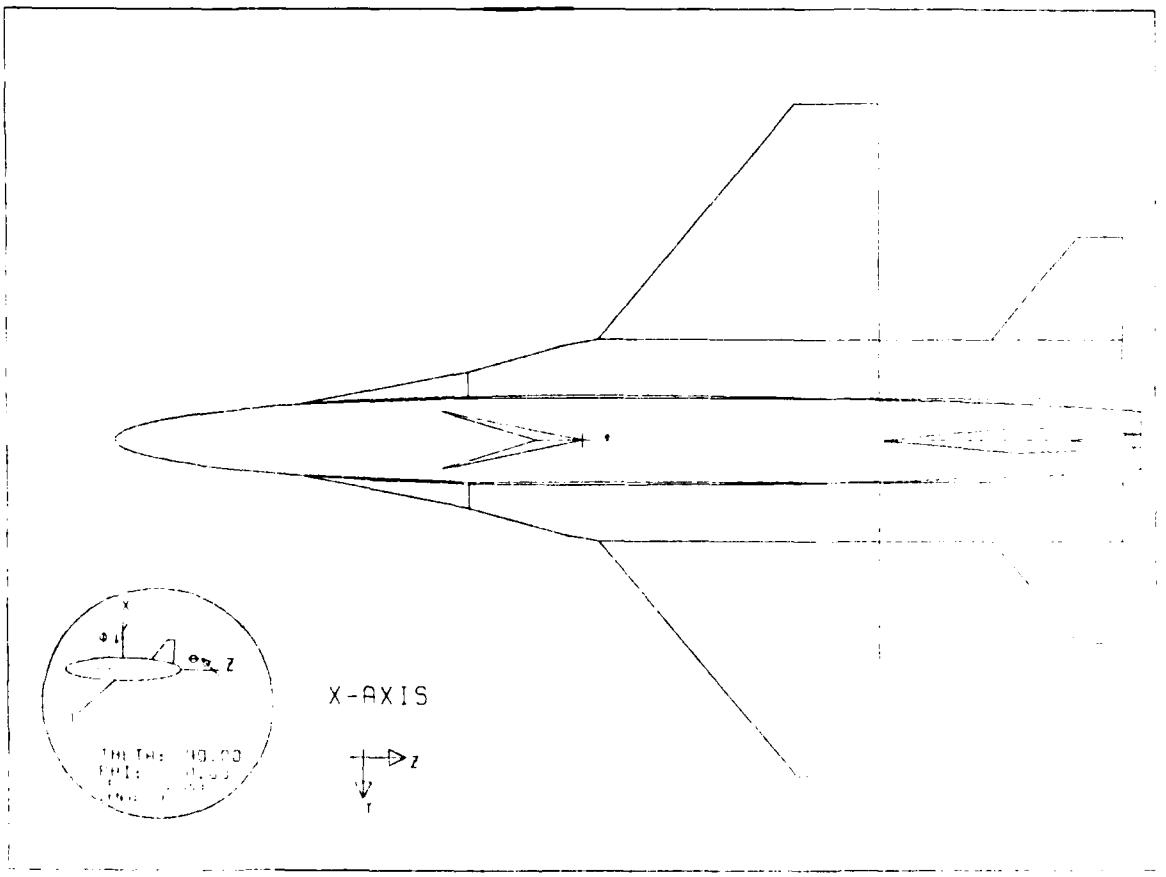

(a) Top View

Figure 55. F-16 Computer Simulated Model.

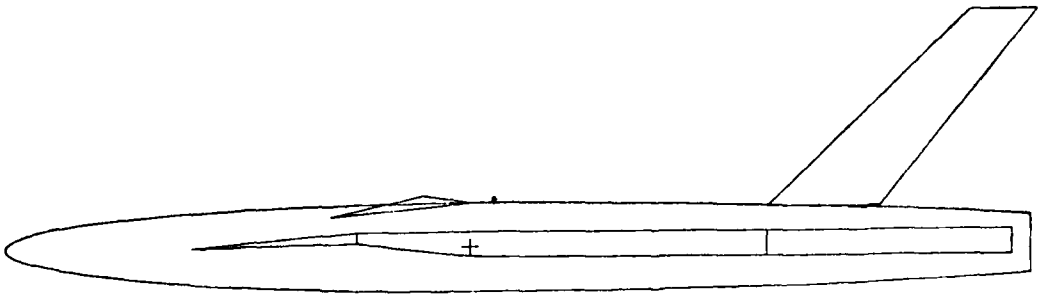

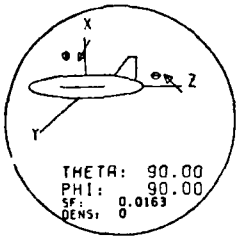

Y-AXIS

Figure 55. (b) Side View.

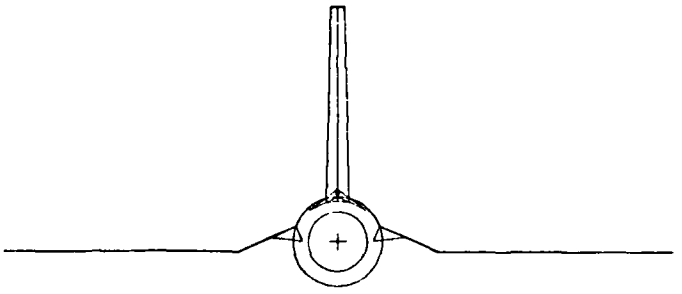

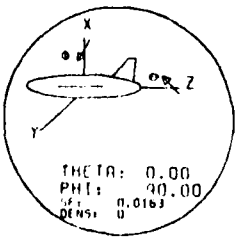

Z-AXIS

Figure 55. (c) Front View.

The computational results are shown from Figure 56 to Figure 58. It was found that the cockpit and tail section simulations could not be completed without further information about the structure and materials actually used by the original manufacturer. However, the computed results are still satisfactory as compared with the measured data taken by General Dynamics. Further study is needed, and the final results will be shown in a future report.

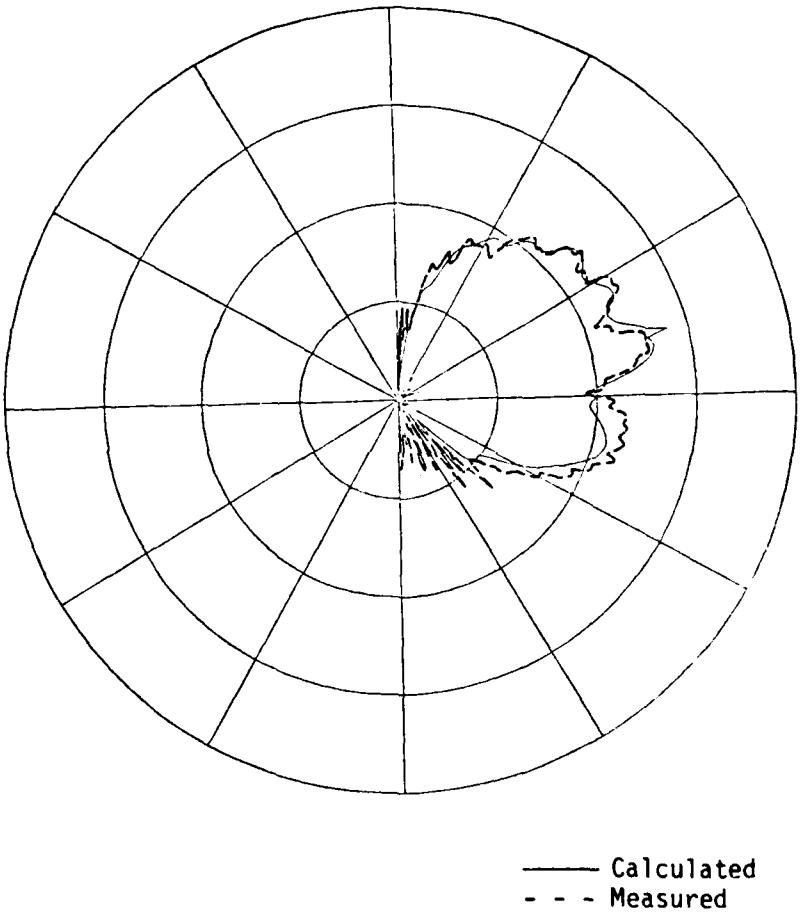

Figure 56. Roll plane ($E\phi$) radiation pattern of a $\lambda/4$ monopole mounted on top of an F-16 aircraft.

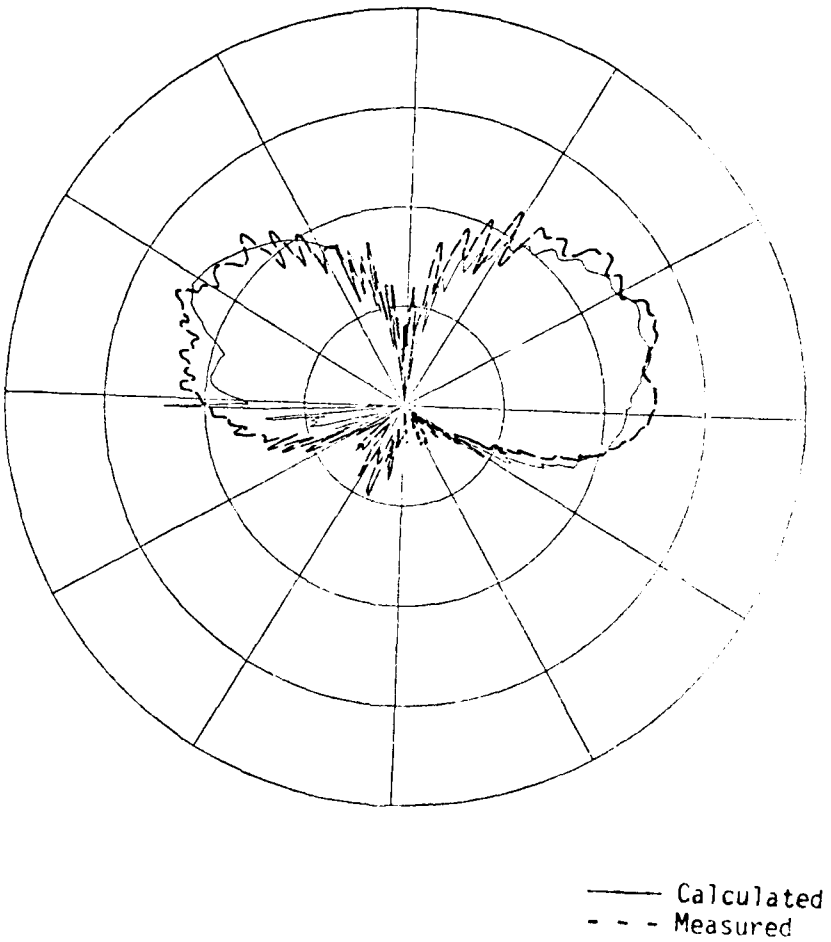

Figure 57. Elevation plane ($E\phi$) radiation pattern of a $\lambda/4$ monopole mounted on top of an F-16 aircraft.

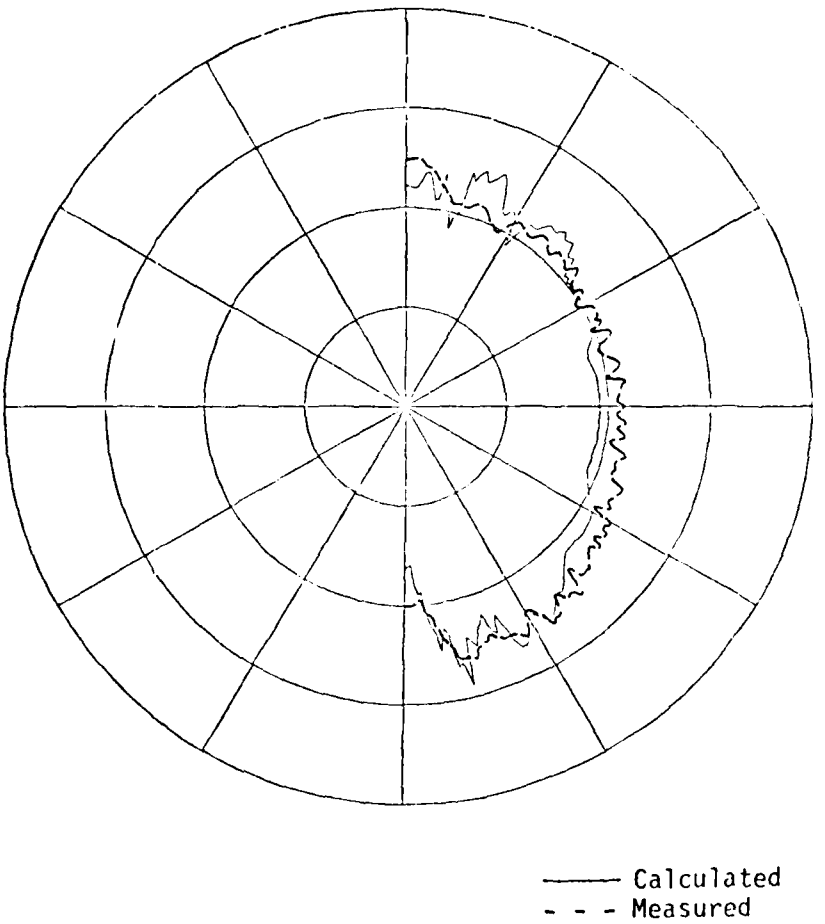

Figure 58. Azimuth plane (Eθ) radiation pattern of a λ/4 monopole mounted on top of an F-16 aircraft.

REFERENCES

1. R.G. Kouyoumjian and P.H. Pathak, "A Uniform Geometrical Theory of Diffraction for an Edge in a Perfectly-Conducting Surface," Proc. IEEE, Vol. 62, November 1974, pp. 1448-1461.

2. R.G. Kouyoumjian, P.J. Pathak and W.D. Burnside, "A Uniform GTD for the Diffraction by Edges, Vertices and Convex Surfaces," Theoretical Methods for Determining the Interaction of Electromagnetic Waves with Structures, edited by J.K,. Skwirynski, Sijthoff and Noordhoff, Netherlands, 1979.

3. P.H. Pathak, N. Wang, W.D. Burnside and R.G. Kouyoumjian, "A Uniform GTD Solution for the Radiation from Sources on a Convex Surface," IEEE Trans. on Antenna and Propagation, Vol. AP-29, No. 4, July 1981, p. 609-622.

4. J.H. Richmond, "Radiation and Scattering by Thin-Wire Structures in the Complex Frequency Domain," Report 2902-10, July 1973, The Ohio State University ElectroScience Laboratory, Department of Electrical Engineering; prepared under Grant No. NGL 36-008-138 for National Aeronautics and Space Administration.

5. W.D. Burnside, M.C. Gilreath, R.J. Marhefka, and C.L. Yu, "A Study of KC-135 Aircraft Antenna Patterns," IEEE Trans. on Antennas and Propagation, Vol. AP-23, No. 3, May 1975, pp. 309-316.

6. R.J. Marhefka, "Analysis of Aircraft Wing-Mounted Antenna Patterns," Report 2902-25, June 1976, The Ohio State University ElectroScience Laboratory, Department of Electrical Engineering; prepared under

Grant No. NGL 36-008-138 for National Aeronautics and Space Administration.

7. W.D. Burnside, E.L. Pelton, N. Wang, "Analysis of Aircraft Simulations Using an Elliptic Cylinder and Multiple Plate," Report 711305-1, April 1979, The Ohio State University ElectroScience Laboratory, Department of Electrical Engineering; prepared under Contract N00019-78-C-0524 for Naval Air Systems Command.

8. W.D. Burnside, N. Wang, and E.L. Pelton, "Near Field Analysis of Airborne Antennas," IEEE Trans. on Antenna and Propagation, Vol. AP-28, No. 3, May 1980, p. 318-327.

9. W.D. Burnside and T. Chu, "Airborne Antenna Pattern Code User's Manual," Report 711588-2, March 1980, The Ohio State University ElectroScience Laboratory, Department of Electrical Engineering; prepared under Contract N62269-78-C-0379 for Naval Air Development Center.

10. W.D. Burnside, R.G. Kouyoumjian, R.J. Marhefka, R.C. Rudduck, and C.H. Walter, "Asymptotic High Frequency Techniques for UHF and Above Antennas," Annual Report 4508-6, August 1977, The Ohio State University ElectroScience Laboratory, Department of Electrical Engineering; prepared under Contract N000123-76-C-1371 for Naval Regional Procurement Office.

11. W.D. Burnside, "User's Manual Flat Plate Program," Report 4508-4, May 1977, The Ohio State University ElectroScience Laboratory, Department of Electrical Engineering; prepared under Contract N00123-76-C-1371 for Naval Regional Procurement Office, Long Beach, California.

12. R.J. Marhefka, "User's Manual for Plates and Cylinder Computer Code," Report 4508-8, March 1978, The Ohio State University ElectroScience Laboratory, Department of Electrical Engineering; prepared under Contract N00123-76-C-1371 for Naval Regional Procurement Office, Long Beach, California.

13. C.C. Huang, N. Wang and W.D. Burnside, "The High-Frequency Radiation Patterns of a Spheroid-Mounted Antenna," Report 712527-1, March 1980, The Ohio State University ElectroScience Laboratory, Department of Electrical Engineering; prepared under Contract N00019-80-C-0050 for Naval Air Systems Command.

14. H. Chung, W.D. Burnside and N. Wang, "The Near Field Radiation Patterns of a Spheroid-Mounted Antenna," Report 712527-2, November 1980, The Ohio State University ElectroScience Laboratory, Departmetn of Electrical Engineering; prepared under Contract N00019-80-C-0050 for Department of the Navy.

15. H. Chung, W.D. Burnside, and N. Wang, "Analysis of the Curved Junction Edge between a Flat Plate and A Prolate Spheroid," Report 713321-1, May 1981, The Ohio State University ElectroScience Laboratory, Department of Electrical Engineering; prepared under Contract No. N00019-80-C-0593 for Department of the Navy.

MISSION
of
Rome Air Development Center

RADC plans and executes research, development, test and selected acquisition programs in support of Command, Control Communications and Intelligence (C^3I) activities. Technical and engineering support within areas of technical competence is provided to ESD Program Offices (POs) and other ESD elements. The principal technical mission areas are communications, electromagnetic guidance and control, surveillance of ground and aerospace objects, intelligence data collection and handling, information system technology, ionospheric propagation, solid state sciences, microwave physics and electronic reliability, maintainability and compatibility.